SCUOLA DI DOTTORATO

UNIVERSITÀ DEGLI STUDI DI MILANO-BICOCCA

School of Medicine and Surgery

PhD program in Molecular and Translational Medicine

XXX Cycle

STUDY OF MULTIPOTENT RENAL PKH^{HIGH} STEM-LIKE CELLS, ISOLATED FROM HUMAN NEPHROSPHERES: REGENERATIVE ABILITIES AND TRANSCRIPTOMIC PROFILE

Dott.ssa Chiara Meregalli

Matr. No. 718179

Tutor: Prof. Roberto Perego

Co-tutor: Dott.ssa Silvia Bombelli

Coordinator: Prof. Andrea Biondi

ACADEMIC YEAR 2016/2017

To my family

Table of contents

Table of abbreviations

(alphabetical order)

AKI: Acute kidney injury

ASC: Adult stem cell(s)

DEG: Differentially expressed gene(s)

ECM: Extracellular matrix

ESC: Embryonic stem cell(s)

ICM: Innel cell mass

iPSC: Iduced-pluriponet stem cell(s)

IRI: Ischemia-riperfusion injury

LN: Low/neg *i.e*. $PKH^{low/neg}$ cells

NS: Nephrosphere(s)

PCC: Primary cell culture(s)

RSC: Renal stem-like cell(s) *i.e.* $PKH^{high}/CD133^{+}/CD24^{-}$ cells

SC: Stem cell(s)

Chapter 1

General Introduction

STEM CELLS

GENERAL DEFINITION AND PROPERTIES

Every cell in the human body can be traced back to a fertilized egg and the body is made up of different cell types which come from a pool of stem cells (SC) present in the early embryo. During early development, as well as later in life, SC give rise to all the differentiated cells.

SC are generally defined as undifferentiated cells that have the capacity both to self-renew and to generate differentiated progeny. In SC both tasks can be accomplished in a single step since they are able to undergo not only symmetric but also asymmetric division. Upon asymmetric cell division, SC originate one more differentiated daughter cell (progenitor) and another cell that is still a stem cell (Fig. 1, in the middle). Instead, upon symmetric division two identical SC or two progenitor daughter cells are generated (Fig. 1, on the sides). In the first case of symmetric division, daughter cells are both stem cells while in the second one they have no more stem properties and lies in a more differentiated step respect to the mother cell.

SC number remains constant if only asymmetric division occurs. Instead, given that symmetric division provides a mechanism that can increase SC population in case of SC loss, it should be balanced to prevent a dangerous escalation of SC number leading to tumor-like lesions. In fact, symmetric

and asymmetric division coexist both in normal and in cancer SC, but in a different ratio. While normal SC mostly divide asymmetrically, except totipotent ones, cancer SC prefer symmetric division (Cicalese, 2009). To the same extent, the symmetric division that generates two progenitor cells has to be controlled to avoid SC exhaustion (Fig.1).

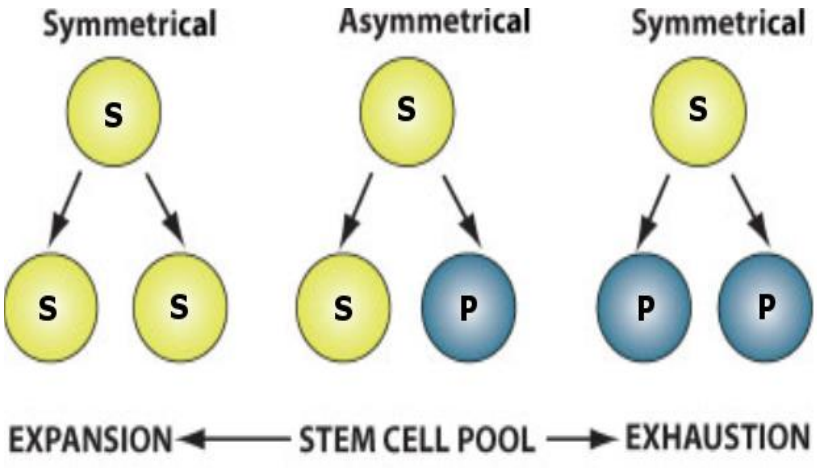

Figure 1: Schematic representation of two different types of stem cell (S) divisions. Asymmetric division (in the middle) gives rise to a more differentiated cell, called progenitor (P), and an identical stem cell. Symmetric division generates alternatively two identical stem cells or two more differentiated progenitor cells. Modified from Alison and Islam *J Pathol. 2009 Jan; 217(2):144-60.*

Two main mechanisms seem to regulate asymmetric cell division: asymmetric partition of intracellular components that

determine cell fate, termed ‘intrinsic’ mechanism, and asymmetric separation of cell components due to external signals from the SC niche, termed ‘extrinsic’ mechanism (Alison and Islam, 2009). In fact, all SC are thought to be placed in specialized microenvironment called “niche”, which regulate SC behavior through direct physical cell-cell contact and paracrine signalling. In example, specialized junctions between SC and the niche cells can determine the orientation of the centrosome during cell division regulating the direction of the mitotic spindle, and thus the location of daughter cells (Morrison and Kimble, 2006).

Other features typical of SC are quiescence and clonality. Quiescence consists in the slow or rare division that is thought to avoid the differentiation and the risk to introduce mutations during the error-prone process of DNA synthesis. To avoid this risk, cells remain in a semi-permanent G0 phase of cell cycle, reducing their metabolic activity to the minimum (Trumpp, 2010). Instead, clonality deals with the ability of SC to regenerate all cell types from a single cell.

Moreover, SC have the ability to resist to cytotoxic insults through enzyme-based detoxification systems or through the ability to rapidly efflux xenobiotics. Some membrane transporters belonging to the ABC superfamily, but also the aldehyde dehydrogenase (ALDH) gene superfamily and certain cytochrome P450 enzymes are involved in these processes.

Finally, levels of condensation of chromatin together with epigenetic mechanisms modulate the accessibility to DNA and allow maintaining the unique properties associated with stemness of SC and the subsequent fate of their progeny (Alison and Islam, 2009).

CLASSIFICATION

Depending on the potential to differentiate into particular lineages, SC could also be classified into five groups with a progressive inverse ratio between self renewal capacity and differentiation step (Fig.2):

1. Totipotent cells are cells that are able to differentiate in all three germ layers but also in extraembryonic tissues such as placenta. Only these cells are able to generate an entire organism and to support the growth in uterus. Totipotent cells are all the cells that by symmetrical division are present in the steps from fertilized eggs until 8-cell stage embryos (morula).
2. Pluripotent cells are embryonic stem cells (ESC) derived from the inner cell mass of blastocyst and have the ability to differentiate in all three germ layers, but, respect to totipotent cells, they are characterized by the inability to form extraembryonic tissues.

   The three germ layers generated by ESC will differentiate into endoderm derivetives (gut, stomach, lung, liver and pancreas), mesoderm derivatives (cardiovascular,

musculoskeletal and urinary systems) and ectoderm derivatives (central nervous system, eye lens, epidermis, hair and mammary glands).

The inner cell mass of the blastocyst is composed of 30-34 cells that are defined as pluripotent because they give rise to all three germ layers (ectoderm, mesoderm and endoderm) and through these, they can differentiate into all the cell types of the body.

ESC express pluripotency markers (transcription factors: Oct4, Sox2, Nanog; surface antigens: SSEA-4, SSEA-3; proteoglycans: TRA-1-60, TRA-1-81).

The unique potential of human ESC to differentiate into three germ layers and subsequently to any cell type of human body make them an attractive tool for biomedical research. As an important limit, it has to be considered the foundamental ethic problem that the usage of these cells poses. Moreover, as a side effect they often form teratoma *in vivo* during differentiation (Singh, 2014).

3. Multipotent cells, called also adult stem cells (ASC), demonstrate a restrict pattern of differentiation towards many related cell types. The lineage-restriction of differentiation is determined by the tissue of origin. ASC could be found in all tissues along the body during lifespan after development. These cells have the characteristic of multipotency and the ability to differentiate in all cell types

that compose the tissue of their origin (in example hematopoietic stem cells give rise only to blood cells).

4. Oligopotent cells are progenitor cells able to differentiate into few cell types of specific lineages such as myeloid progenitor cells, which give rise only to basophils, eosinophils, neutrophils, monocytes, thrombocytes and erythrocytes.
5. Unipotent cells are progenitor cells that can only differentiate into one particular cell type such as hepatoblasts forming hepatocytes.

In addition, induced pluripotent stem cells (iPSc) were obtained for the first time in 2006 by Takahashi and Yamanaka by reprogramming somatic cells through viral overexpression of four embryonic transcription factors: Oct 3/4, Sox2, c-Myc and Klf4 (Takahashi and Yamanaka, 2006). As well as ESC, iPSc are pluripotent cells with the ability to give rise to various tissues in developing embryos when injected into blastocysts. Morever, iPSc can also generate teratomas in immunocompromised mice.

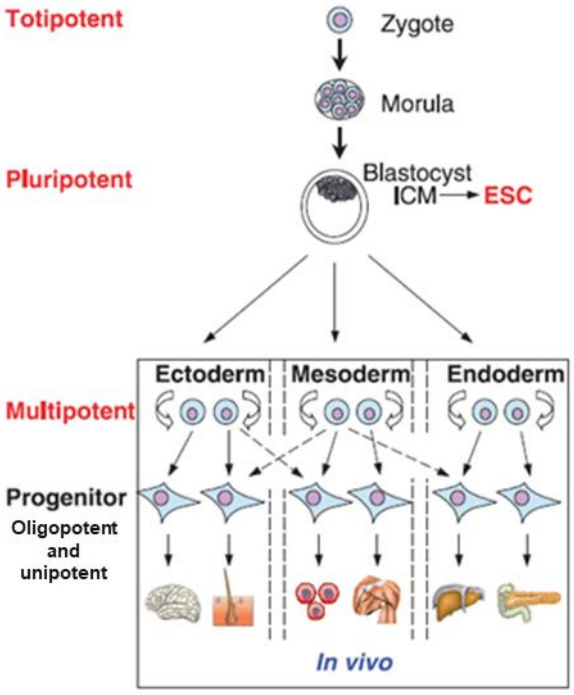

Figure 2: Stem cell hierarchy. Zygote to morula are defined as totipotent. At the blastocyst stage, only the inner cell mass (ICM) retains the capacity to build up all three germ layers. In adult tissues, multipotent stem and progenitor cells exist in tissues and organs to replace lost or injured cells. Modified from Wobus and Boheler *Physiol Rev 85: 635– 678, 2005.*

Adult stem cells

As aforementioned, it is thought that also adult tissues contain SC, known as adult stem cells (ASC), which retain the capability to control tissue damage and cell death by differentiating new cells (Snippert and Clevers, 2011). Some

ASC, such as bone marrow-derived ones, are able to migrate out of their natural side to reach the damaged area, thanks to signals of injury, and to participate to tissue repair (Mimeault and Batra, 2006). All ASC are described as rare, quiescent, with the ability of self renew, maintaining the SC pool, and differentiate all lifespan long (Axelson and Johansson, 2013). But it should be kept in mind that different ASC are characterized by different time of quiescence:replication ratio. In example, epidermal, blood and intestinal stem cells undergo daily turnover as part of their physiological differentiation process (Hsu and Fuchs, 2012), while in the hair follicle ASC are needed only periodically to fuel cyclical hair growth. Furthermore, ASC often remain quiescent for extended periods of time. However, even within relatively non-regenerative tissues, such as adult skeletal muscle and brain, cell-type specific ASC exist. Such ASC undergo extremely low or no division during homeostasis steady state, but can respond efficiently to stimuli.

Since ASC do not pose a risk for developing teratoma, they have represented till now and continue to represent the preferable cell source in regenerative medicine respect to ESC. However, also the use of allogenic ASC rises the problem of immune rejections.

STEM CELLS IN KIDNEY

Historically, the kidney is counted among organs thought to lack regenerative abilities. Study of kidney development and of very low cellular turnover rate in adult tissue have supported the idea that mammalian kidney lacks regenerative properties. For example, in humans nephrogenesis ceases during gestation period (at approximately week 36), whereas in mouse it continues until birth and then rapidly attenuates (Hartman, 2007). The identification of a renal ASC is made very difficult, due to the kidney complexity, in terms of cell type number and embryonic origin (McCampbell and Wingert, 2012).

Kidney ontogeny

Each kidney derives from the mesodermal germ layer and is comprised of nephrons. Mammal kidney develops from a pronephros, then a mesonephros and finally a metanephros that becomes the adult kidney, as described in Figure 3.

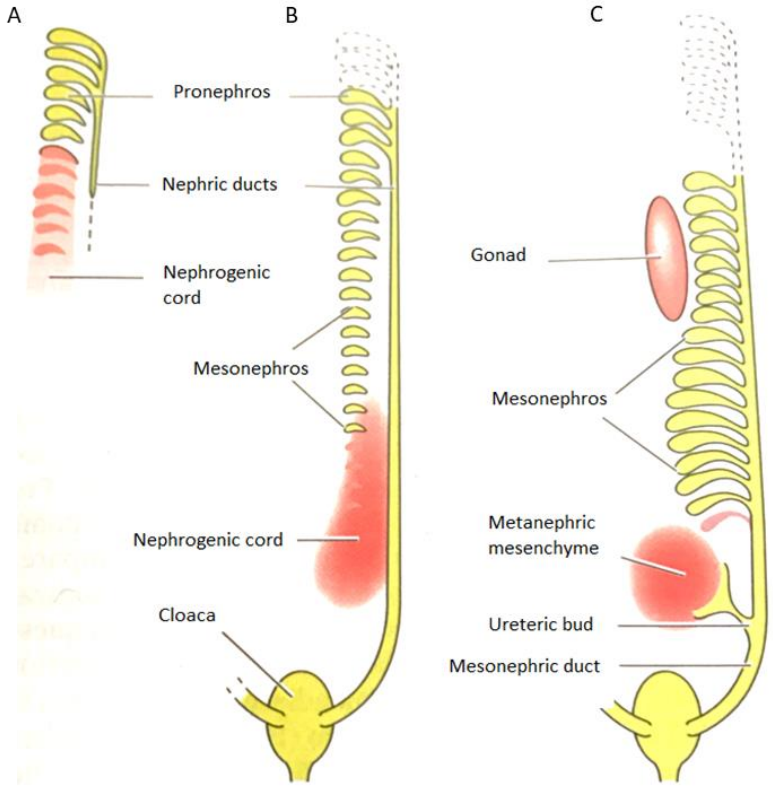

Figure 3: Schematic representation of kidney ontogeny in vertebrates. A. Pronephros formation is stimulated by nephric ducts which induce the nephrogenic cord during their posterior progression. B. When pronephros regresses, mesonephric ducts are formed. C. The definitive mammal metanephric kidney. It is induced from the ureteric bud.
Modified from Gilbert *Developmental Biology, third Italian version, 2005*

Many questions remain about the genetic signalling pathways that direct pro- and mesonephros specification, and the molecular relationships between renal progenitors of these structures and the metanephric kidneys. What is largely known is that the metanephric mesenchyme could generate nephrons, whereas the ureteric bud epithelium could give rise to collecting ducts.

As the metanephric mesenchyme and the ureteric bud interact, the first one is subdivided into the cap mesenchyme and the stromal mesenchyme, suggesting a first specification in kidney lineages. The cap mesenchyme is condensed and characterized by the expression of the Six2 transcription factor since it undergoes an epithelial transition, forming a renal vesicle in which finally Six2 expression is lost. Instead, the stromal mesenchyme is defined by expression of FoxD1 and these cells will contribute to the interstitial population. Previous studies have demonstrated that the cap mesenchyme contains a self-renewing group of nephrogenic SC. Cap mesenchyme specification probably involves the signalling of BMP growth factors and transcriptional activities mediated by Osr1 and Pax2 transcription factors. It also expresses the transcription factors Cited1, Eya1, Sall1 and Wt1 (Fig.4).

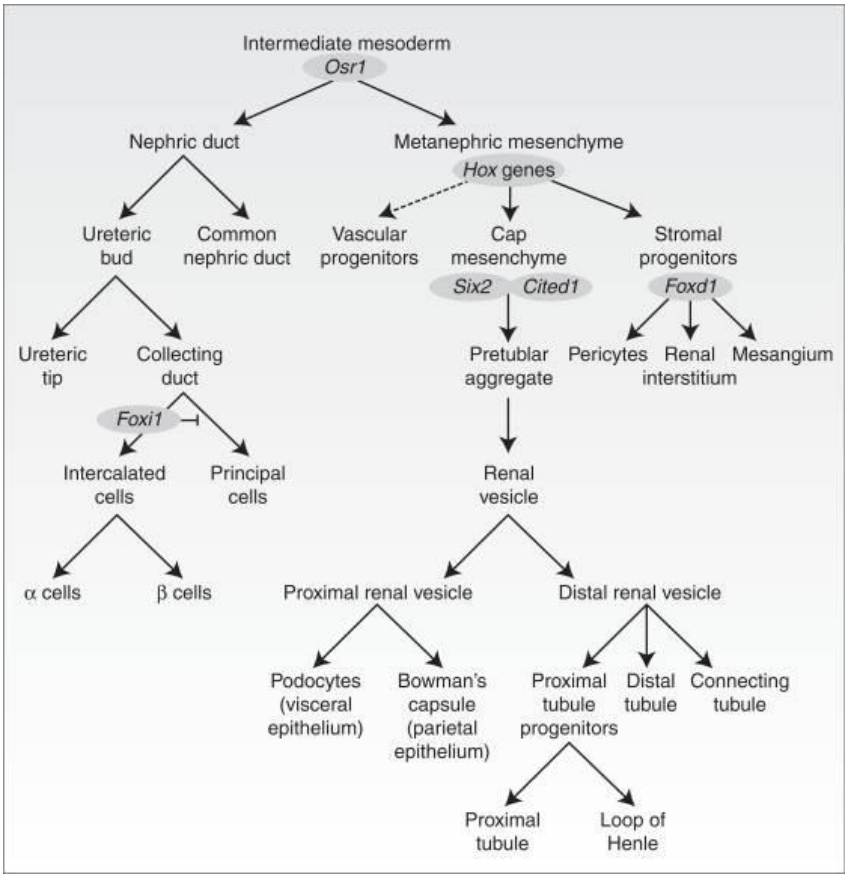

Figure 4: Lineage relationships within the developing mammalian metanephros.

Key marker genes expressed at specific stages of differentiation are evidenced in gray ovals. From Little and McMahon *Cold Spring Harb Perspect Biol*., *2012.*

In particular, among genes associated with cap mesenchyme identity, Six2 is essential to maintain the SC population. In the absence of Six2, nephrogenesis terminates. It can be concluded that the phenomenon of cap mesenchyme self-

renewal is transient, and the cessation of nephrogenesis is associated with cap mesenchyme resolution. It is unclear whether the cap mesenchyme termination is due to the terminal commitment of cells and/or an exhaustion of self-renewal properties.

The debate about adult renal stem cells

Due to the lack of markers for adult cells which could retain stem properties in adult renal tissue, the demonstration of the existence of a renal ASC is very hard. Moreover, the mechanism underlying the recovery of renal cell injury is still a matter of debate that concerns the involvement of fully differentiated cells, or the existence of quiescent scattered progenitors (Lombardi, 2016).

Traditionally, tubular cells were considered as cells with a high regenerative potential, based on the quick functional recovery in animal models and on the robust proliferative activity observed in tubular tissue after injury (Basile, 2012).

But what truly happens after tubular injury, and how, and to what extent, does tubular regeneration occur is still unclear. There are evidences suggesting that tubular regeneration is orchestrated within the tubule itself, but the responsible cell source is uncertain.

Two main hypotheses have been proposed about the source of the newly formed proximal epithelial cells responsible for recovery after injury.

The first one is based on the fact that at the steady state fully differentiated epithelial cells of the proximal tubule are in the G1 phase of the cell cycle, ready to progress at once into the cycle in the case of injury (Vogetseder, 2008). In such a scenario, fully differentiated tubular cells would transiently undergo dedifferentiation, proliferation and, ultimately, re-differentiation (Fig. 5A).

Instead, the second hypothesis argues the existence of an intratubular scattered progenitor population in a quiescent state, which is ready to re-enter the cell cycle for replacing cell loss for tubular damage (Fig 5B).

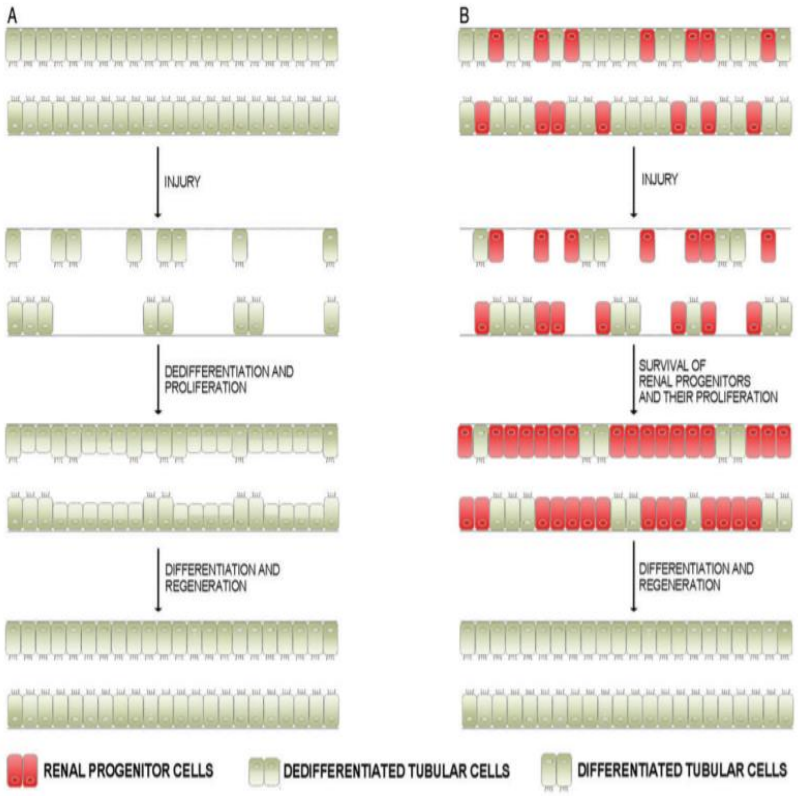

Figure 5. Schematic representation of the two opposite hypotheses, which explain tubular regeneration. (A) Differentiated tubular cells surviving the injury undergo a step of dedifferentiation, proliferate, migrate in correspondence of the damaged tubular base membrane and then differentiate, replacing the lost tubular cells. (B) Tubular progenitors are scattered among differentiated tubular cells. They are highly resistant to injury, so that they are able to survive, proliferate, migrate and then differentiate to replace lost tubular cells.

Lombardi et al. *Nephrol Dial Transplant (2016) 31: 1243–1250.*

What we actually know about adult renal stem cells

In mouse

Examination of adult mouse kidneys suggested the possibility of some cell proliferation, but at a first analysis these findings were interpreted to represent a negligible contribution to organ homoeostasis (Messier and Leblond, 1960). The long-standing dogma has been that kidneys are endowed with a set amount of nephrons that can only decline in activity and number from injury or disease and cannot be repaired during the lifespan of an individual.

Early cell division studies using a pulse–chase of tritiated thymidine reported incorporation of the label throughout the proximal, distal and collecting tubules of healthy male rats. Later, proliferation was documented using BrdU pulse–chase experiments and cell-cycle markers in juvenile rat kidneys and the rate of cell division was noted to range between 2% and 4%, higher than the 0.4% seen in adults. These investigations found that mitotic cells in the

proximal tubule had differentiated traits, as they co-expressed markers of the brush border and showed proper distribution of several polarity proteins, suggesting that dividing cells were differentiated epithelia (Suzuki, 2016).

In 2006 stem cell antigen 1 (Sca1)-positive cells were isolated from the adult mouse kidney (Dekel, 2006). The $Sca1^+$ cells were localized mainly in the papilla. When these cells were administered to an ischemia-induced acute kidney injury (AKI) model, some of them were integrated into renal tubules, suggesting their multipotency.

In glomeruli the regenerative activity is more limited than in tubules; in fact, progenitors were identified in Bowman's capsule during infancy but not in adulthood.

Moreover, intratubular slow-cycling cells where demonstrated to exist all along the nephron. Progenitor cells where localized in proximal tubules, exploiting their expression of the SC marker NFATc1 (Langworthy, 2009), and in the loop of Henle and distal tubules, revealing Lgr5 (Barker, 2012) or c-Kit (Rangel, 2013) expression.

In 2008 it was demonstrated for the first time a role for resident cells in renal repair after acute injury by fate mapping (Humphreys, 2008). They ruled out that there is no implication of murine extratubular cells in re-epithelialization following AKI. The group used a transgenic model in which epithelial precursors in the embryonic kidney as well as adult tubular epithelial cells rising from these progenitors are traced. The authors showed that following an ischemia–reperfusion injury (IRI), all reparative epithelial cells derived from within the tubule, excluding a direct contribution of bone marrow-derived cells. However, it has to be observed that

this system does not discriminate between terminally differentiated tubular cells and intratubular scattered progenitors.

Instead, by lineage tracing in rainbow mice, a more recent paper proved the existence of a population of fate-restricted unipotent progenitor population with specific clonogenic and proliferative potential which can sustain renal epithelial renewal during lifespan (Rinkevich, 2014).

In human

In 2005 Bussolati et al., using CD133 that is considered as a universal marker for SC in other tissues, isolated a $CD133^+$ population from the human interstitium of renal cortex (Bussolati, 2005). These cells expressed Pax2, but not CD34 or CD45 endothelial or hematopoietic stem cell markers. They could also be induced to differentiate into tubular epithelial cells and endothelial cells *in vitro* and, when intravenously administered to a glycerol-induced AKI model of severe combined immune deficiency (SCID) mice, they were incorporated predominantly into the proximal and distal tubules.

$CD133^+$ cells, also expressing CD24, were described among the parietal cells of Bowman's capsule (Sagrinati, 2006). These cells can be differentiated into tubular epithelial cells, osteogenic cells, adipocytes, and neuronal cells and were

integrated predominantly into renal tubules when injected intravenously in glycerol-treated SCID mice.

Ronconi et al. identified $CD133^+CD24^+$ populations as arranged in a precise sequence within the Bowman's capsule (Ronconi, 2009). In fact, these cells do not express the podocytic marker of differentiation podocalexin (PDX^-) at the urinary pole, in contrast with those localized between the urinary and the vascular poles (PDX^+). On the contrary, cells at the vascular pole did not exhibit CD133 and CD24 progenitor markers, but displayed the typical feature of differentiated podocytes, expressing PDX. Only the first population ($CD133^+/CD24^+/PDX^-$) was able to regenerate both tubular cells and podocytes after adriamycin-induced renal injury, while the second one could repair only podocytic injury. Moreover, Angelotti et al. demonstrated the presence of small clusters of $CD133^+/CD24^+/CD106^+$ cells that were localized at the urinary pole of Bowman's capsule, while a distinct population of scattered $CD133^+/CD24^+/CD106^-$ cells was localized in the proximal tubule as well as in the distal convoluted tubule (Angelotti, 2012).

$CD133^+/CD24^+/CD106^+$ cells showed a high proliferative rate and could differentiate toward both podocytes and tubules. By contrast, $CD133^+/CD24^+/CD106^-$ were less proliferative and suggested a commitment toward the tubular lineage.

Injected in SCID mice affected by acute tubular injury, both these populations could engraft the kidney and improve renal

function. Finally, $CD133^+/CD24^+/CD106^-$ cells proliferated upon tubular injury and became the predominant in regeneration in patients with acute or chronic tubular damage (Angelotti, 2012).

Other markers can be found coexpressed with $CD133^+$ and their localization differs based on the position along the nephron (Fig. 6).

It has to be underlined that in Bowman's capsule and in the proximal tubules some $CD133^+$ cells coexpress the mesenchymal marker vimentin, which is not normally expressed in epithelial cells.

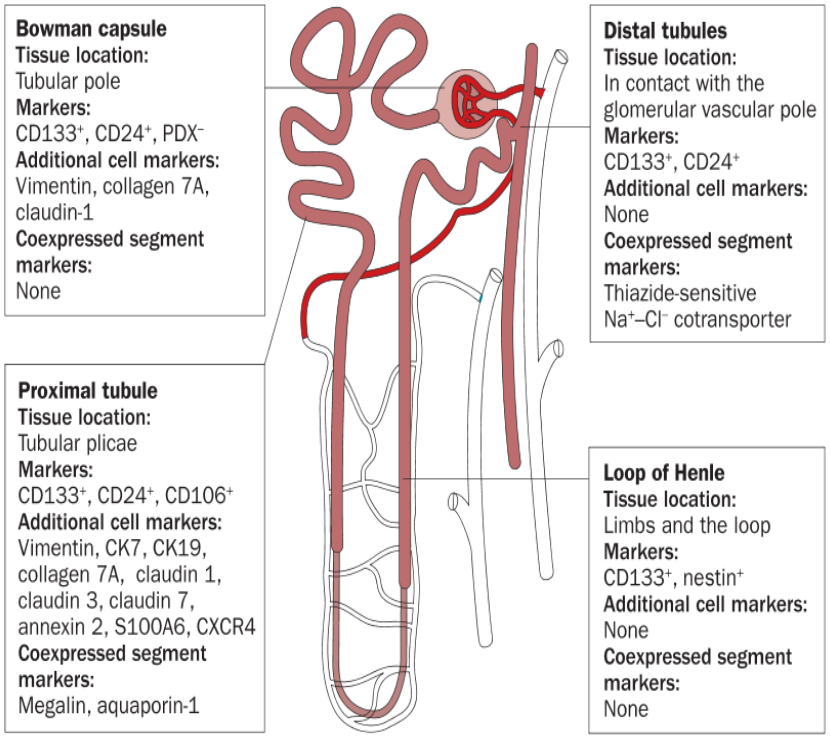

Figure 6: Localization of the marker CD133 along the nephron and its coexpression with additional markers. $CD133^+$ cells are localized in all nephron segment: Bowman's capsule, proximal tubule, distal tubule and loop of Henle.
From Bussolati and Camussi *Nat. Rev. Nephrol. 2015 Dec;11(12):695-706*

Sallustio et al. obtained the genomic characterization of multipotent $CD133^+$ adult renal cells from human glomeruli and tubules (Sallustio, 2010). These cells were demonstrated to express the renal embryonic transcription factor Pax2 and

CD24 surface marker and lacked CD34, CD105 and CD45 expression. Of interest, they described a role of TRL2, a pattern-recognition receptor involved in innate immunity, in stimulating their isolated cells to undergo branching and to form tubular-like structures.

Lindgren et al. sorted a SC population exploiting the activity of ALDH, thought to play a role in SC maintenance by converting retinal into retinoic acid (Lindgren, 2011). They also demonstrated that cells with high ALDH activity also expressed CD133, CD24, vimentin markers and key suppressors of apoptosis, resambling progenitor cells.

Instead, Smeets et al. described within proximal tubules a population of $CD133^+$ and $CD24^+$ cells involved in regeneration of injured tubules (Smeets, 2013).

More recently, Bussolati et al. and Ward et al. found $CD133^+$ cells also in the inner medulla (Bussolati, 2012; Ward, 2011).

All these populations showed the expression of Pax2 and Wt1 renal fetal markers, CD24 and some mesenchymal SC markers like CD29, CD73 and CD90. Instead, the expression of CD106 marker differed among the various isolated populations. In general, $CD133^+$ cells were characterized by clonogenicity and the ability to differentiate into proximal and distal tubules and into glomerular podocytes. Moreover, these cells generated tubular structures expressing renal markers when injected into immunodeficient mice.

Of note, Buzhor et al. demonstrated that human kidney epithelial cells displayed the ability to form non-clonal kidney spheroids when grown in suspension culture in nonadherent conditions (Buzhor, 2011). They hypothesized that growth conditions may influence the phenotype and the function of these cells. In this case, the characterization of spheroid cells showed an $EpCAM^{+}/CD24^{+}/CD133^{+}/CD44^{+}$ phenotype and upregulation of cell matrix/cell contact molecules.

Subsequently, the same group searched for adult human cells re-expressing the fetal marker NCAM-1 when placed in culture (Buzhor, 2013). It is well known that NCAM-1 is not present in the adult renal tissue but it can be reactivated after AKI. Revealed $NCAM\text{-}1^{+}$ cells were similar to mesenchymal ones in terms of transcription factors (Six2, Sal1, Pax2, Wt1 and Oct-4). Moreover, they showed clonogenicity, tubulogenic differentiation and sphere forming abilities but did not succeed in obtaining any significant difference respect to $NCAM\text{-}1^{-}$ cells when injected in an AKI mouse model.

In conclusion, our knowledge about adult renal stem cell existence in mouse and human is not conclusive and many controversial points remain open.

PKH^{high} cells within clonal human nephrospheres provide a purified adult renal stem-like cell population

In this scenario, our group contributed to the debate for the definition of a renal SC, isolating a pure population of multipotent stem-like cells by a functional approach (Bombelli, 2013). Taking advantage from the ability of SC to grow as spheres, Bombelli et al. obtained nephrospheres containing cells at different level of maturation, i.e. both adult stem like cells and progenitors.

Spheres showed a clonal growth and sphere number was maintained along passages, so that the authors concluded that there is only a sphere initiating cell per nephrosphere. Of note, sphere cells injected in nude mice were able to give rise to human epithelial tubular structures with characteristics of both proximal and distal tubules.

For the isolation of cells with stem properties within the nephrospheres, a lipophilic dye (PKH26) retained in quiescent stem cells after asymmetric division and diluted in progenitors along proliferation, was used.

Having stained cells before nephrosphere formation, the most fluorescent cells would be self renewing quiescent cells with stem abilities. Based on PKH26 epifluorescence three different populations were separated by cell sorting: PKH^{high}, PKH^{low} and PKH^{neg} cells. Among these, only PKH^{high} cells showed self renewal ability, in terms of reforming new secondary nephrospheres and multipotency, differentiating

through three different renal lineages: epithelial, endothelial and podocytic. Instead, PKH^{low} and PKH^{neg} cells failed to differentiate both in podocytic and in endothelial lineages. PKH^{high} cells were then considered as cells with stem-like properties.

Investigating the expression of renal progenitor markers described in literature, (CD133 and CD24) an enrichment in $CD133^{+}/CD24^{-}$ phenotype in the PKH^{high} population was observed. In addition, only $PKH^{high}/CD133^{+}/CD24^{-}$ and $PKH^{high}/CD133^{+}/CD24^{+}$ showed the ability to self renew, but only the first subpopulation could differentiate into epithelial, endothelial and podocytic renal lineages, while the second one failed the endothelial and podocytic differentiation.

It was finally concluded that $PKH^{high}/CD133^{+}/CD24^{-}$ cells are those with stem-like properties within nephrospheres.

HUMAN CELL SURFACE MARKERS FOR ASC ISOLATION

CD133

Since CD133 was identified as a pentaspan transmembrane protein for human hematopoietic SC, it represents one of the key biomarkers for isolation and characterization of SC in general (Li, 2013). CD133 is considered a marker for SC in several tissues, but it is also expressed in more differentiated or committed cells. For this reason, it is important to understand the role of CD133 protein. The idea that CD133 deals with stemness derived from the fact that stemness

genes, OCT4 and SOX2, have been found to bind to the promoter region of CD133 gene locus as also confirmed by the ectopic OCT4 or SOX2 expression (Iida, 2012).

Human CD133, also called prominin 1, is a transmembrane glycoprotein of 865 amino acids with a total molecular weight of 120 kDa. It is selectively localized in microvilli and other membrane protrusions. In general, $CD133^+$ and $CD133^-$ cells display different characteristics. For example, $CD133^+$ and $CD133^-$ glioma cells belong to independent cancer stem cell populations. CD133 expression is regulated by many extracellular or intracellular factors. In particular, hypoxia, mitochondrial dysfunction or depletion of mitochondrial DNA induces a reversible up-regulation of CD133 expression. Increased expression of hypoxia inducible factors (HIF1alpha and HIF2 alpha) induces the expansion of the $CD133^+$ cells. In fact, it was demonstrated that one binding site in CD133 promoter is essential for promoter activity induced by both HIF-1alpha and HIF-2alpha through direct interaction (Ohnishi, 2013).

Also transforming growth factor β1 (TGFβ1) is described to be capable of upregulating CD133 expression by modulating its epigenetic regulation and, finally, the expression of some toll like receptors (TLR) are shown to increase in $CD133^+$ cells (You, 2010). Therefore, CD133 expression may play an important role in communication through membrane receptors.

Also microRNA (miRNA) profiling has revealed that several miRNA are involved in regulation of CD133 expression in a variety of cells among which adult renal progenitors (Sallustio, 2013), but most of these miRNAs exhibit indirect regulation of CD133 expression, whereas a specific miRNA targeting CD133 expression has not been identified yet.

In epithelial cells, CD133 is a membrane protein found to be released as a whole or in part, into the extracellular space, in CD133-enriched membrane particles. Interestingly, the release of these particles is described as implicated in (neuro)epithelial cell differentiation (Corbeil, 2010).

CD133 is also a cholesterol-interacting membrane protein responsible for the generation of plasma membrane protrusions, their lipid composition and organization as well as the membrane-to-membrane interactions. Moreover, CD133 inhibits transferrin indicating the involvement of CD133 in cell metabolism. This is also confirmed by the fact that gene expression and enzymatic activity of hexokinase II, a key enzyme in the glycolytic pathway, are lower in $CD133^+$ than in $CD133^-$.

CD133 has eight N-glycosylation sites on its extracellular loops and N-glycosylation of CD133 is thought to be associated with cell differentiation and promoted by hypoxia. In addition, silencing CD133 reduces the glucose uptake, indicating that CD133 expression may be responsible for energetic metabolism and the survival of $CD133^+$ cells.

Further analysis in $CD133^+$ and $CD133^-$ cells has found that freshly isolated $CD133^+$ cells from benign prostate tissue express transcripts associated with cell development, ion homeostasis and cell communication. Instead, $CD133^-$ cells revealed transcripts related to cell proliferation and metabolism (Shepherd, 2008). Observation of CD133 expression in several neuroblastoma cell lines/tumor samples has shown that CD133 represses the expression of differentiation markers but accelerates cell proliferation, anchorage-independent colony formation and in vivo tumor formation of neuroblastoma cells (Takenobu, 2011).

It was also demonstrated that downregulation of endogenous CD133 inhibits the stem-like properties and enhances chemoradiotherapeutic response in liver cancer stem cells, supporting that stem-targeted therapy via CD133 silencing could be an effective way for treatment of CD133-expressing cancer types (Lan, 2013).

CD24

CD24 has been extensively used as a marker of hematopoietic and neuronal cell differentiation, in addition to stem cell characterization. Corresponding to its wide distribution and variable glycosylation, a wide range of functions has been attributed to CD24 (Fang,2010).

CD24 gene was cloned and found to encode a small protein whose mature form consists of only 27 amino acids.

Interestingly CD24 protein isolated from different tissues or cell types has different molecular weights due to its glycosylation, highly variable and cell-type dependent. CD24 is localized in the membranes of developing cells including pre-B cells, keratinocytes, and renal tubular epithelium. CD24 functions as an alternative ligand of P-selectin, while several cell context-specifc ligands of CD24 itself have been identified. In general, CD24 tends to be expressed at higher levels in progenitor cells and metabolically active cells and to a lesser extent in terminally differentiated cells. CD24 function is unclear for most cell types, however, diverse immunological functions have been reported.

For example, CD24 is expressed at high levels on B-cell progenitors and remains expressed on mature resting B cells but not on terminally differentiated plasma cells (Hunte, 1998). To the same extent, CD24 is highly expressed on immature T cells and weakly expressed on peripheral T cells (Crispe and Bevan, 1987) but it is upregulated in activated T cells (Hubbe, 1994). It is well known that CD24 has apoptotic activity, and its cross-linking induces the sustained activation of p38 MAPK (mitogen-activated protein kinases).

REGENERATIVE APPROACHES FOR KIDNEY DISEASE

The only therapeutic options for patients with end-stage renal disease are lifelong dialysis treatment or organ transplantation. Advances in the understanding of the mechanisms of rejection, as well as the development of new immunosuppressant therapies have led to an increase of the number of patients eligible for renal transplantation, although the availability of donors has remained stable. Consequently, in renal diseases, the need for kidneys is urgent and the hope is that this need can be fulfilled by stem cell and regenerative medicine approaches. Kidney regeneration is particularly difficult because of the described anatomical complexity of the organ. The combination of stem cell research, regenerative medicine and tissue engineering seems a promising approach to generate new nephrons to compensate their loss in chronic kidney diseases.

The different possibilities potentially applicable in kidney regenerative medicine are here summarized (Yamanaka and Yokoo, 2015 and Poornejad, 2016a). It has to be underlined that in our group the scaffold decellularization and recellularization strategy has been exploited for regenerative attempts.

DIRECTED DIFFERENTIATION OF IPSC AND ESC INTO KIDNEY CELLS

Pluripotent stem cells have been successfully differentiated into various types of cells and tissues, including intestine, hepatic, neural, hematologic, pancreatic and cardiac lineages. The approach through which iPSC or ESC are differentiated into renal cells is accomplished by the sequential application of chemicals or growth factors. Recent progress in SC knowledge has permitted to generate human nephron progenitor cells, including intermediate mesoderm and metanephric mesenchyme cells. The understanding of the molecular mechanisms of kidney development is important for the induction of appropriate cells to generate nephrons. For example, a Wnt agonist is commonly used to promote mesoderm differentiation and it has been found to be important to determine the mesodermal anterior-posterior axis.

Renal progenitor cells are essential for the *de novo* development of a whole kidney and the differentiation of induced intermediate mesoderm into appropriate renal progenitor cells would allow to regenerate a complete 3D kidney structure from pluripotent SC. However, the possibility of successful regeneration of a functional vascular system remain a matter of debate. It has been suggested that the interaction between podocytic progenitors and endothelial cells may play an important role for glomerular

microvasculature assembly (Pavenstädt, 2003). When the glomerular vasculature is established, endothelial cells appear responsible of a pool of signals, inducing the final maturation of podocytes. However, these issues should be addressed.

BLASTOCYST COMPLEMENTATION

Injection of pluripotent SC into blastocysts generates a chimeric body. This “blastocyst complementation” system was applied to the reconstruction of several tissues and organs, including thymic epithelium, heart, germ cells, hepatocytes, pancreas and kidney. These studies indicated that cells derived from pluripotent SC could develop in a vacant developmental niche. Furthermore, these results also demonstrated that blastocyst complementation could be used to generate organs derived from donor pluripotent SC in vivo exploiting a xenogeneic environment. This blastocyst complementation system has already been applied to whole kidney reconstruction (Usui, 2012). Nondeficient-kidney murine iPSC were injected into blastocysts from kidney-deficient mice lacking Sall1 that is essential for kidney development. In this way, the two generated kidneys derived almost entirely from injected iPSC. Instead, the vascular and nervous systems were not constituted by cells of iPSC origin. The kidney was therefore not completely complemented, since the renal vascular system was a chimeric structure

originating from both host cells and donor iPSC. The generation of xenogenic organs using interspecific blastocysts thus requires a host animal strain lacking all renal lineages. However, one of the most important problem associated with the traslability in humans of blastocyst complementation is rapresented by the ethical issue.

3-D KIDNEYS

The first evidence of potential 3-D self-organizing kidneys was described in 1960 (Weiss and Taylor, 1960). Mesonephric chick embryonic kidney cells were demonstrated to be able to reform a well-organized renal structure. Recently, it was also shown that stem cell-derived kidney cells were able to form renal structures by small organoid formation without any scaffold. Morizane et al. differentiated mouse ESC into kidney progenitor cells that were able to form tubule-like structures when cultured on Matrigel (Morizane, 2013). The authors also suggested that this self-organization would be improved by the coculture with NIH3T3-Wnt4 cells that increases branched tubular structures. Moreover, Taguchi et al. reported differentiation of mouse ESC and human iPSC to renal cells capable of reconstructing 3D embryoid bodies, including podocytes and renal proximal and distal tubules, which could be vascularized upon transplantation (Taguchi, 2014). In any case the self-vascularization of 3-D kidney organoids has not

been obtained yet. In this sense, an effort was made subcapsularly implanting embryonic metanephroi in rat and mice models to obtain partially functional renal tissue.

More recently, it has been demonstrated that rat renal stem/progenitor cells are able to reconstitute a 3D kidney-like structure in vitro (Kitamura., 2014). Kidney-like structures are formed when a pellet of kidney stem/progenitor cells is suspended in an extracellular matrix gel and cultured in the presence of several growth factors. The reconstructed kidney-like structures included all the kidney substructures (glomeruli, proximal tubules, the loop of Henle, distal tubules, and the collecting ducts), but not the vasculature. Thus, it was suggested that an aggregation of tissue stem/progenitor cells may have the ability to reconstitute the nephron unit and that these cells showed similar functions respect to metanephric mesenchymal cells.

Only Takasato et al. generated kidney organoids by direct differentiation of human pluripotent stem cells into progenitors for both collecting duct and nephrons. Within these organoids, they found distal and proximal tubules, early loops of Henle, and glomeruli containing podocytes elaborating foot processes but also $CD31^{+}$ vascular cells (Takasato, 2015). When transcription profiles of these kidney organoids were compared to human fetal tissues, they showed a high congruence.

However, despite significant improvements in renal organoid formation, these structures remain immature and limited to 5–7 mm in diameter, making their use as a tool for regeneration very far to become (Little, 2016).

Summarizing the attempts to obtain 3D organoids from renal cells, it has to be underlined that vascularized organids were obtained only exploiting iPSc. This rises the question about the most appropriate cell type to use for these attempts.

USE OF NEPHROGENIC NICHE GROWING XENOEMBRYOS

The developing xenoembryo was exploited as a niche for organogenesis using mesenchymal SC. Briefly, a metanephros was generated in organ culture by microinjecting transfected human mesenchymal SC, which express the growth factor, ureteric bud inducer, GDNF into the site of budding, and the recipient embryo was then allowed to grow. Donor human mesenchymal SC were integrated into the rudimentary metanephros and differentiated into interstitial cells, and glomerular epithelial cells. The developed metanephros was then transplanted into the omentum to allow vascular integration from the recipient to form a functional nephron. As a result, a human mesenchymal SC-derived “neokidney” was generated, which contained a human nephron integrated with host vasculature (Yokoo, 2006). Moreover, the neokidney was able to produce urine and to secrete human Epo in response to the induction

of anemia in the host animal (Yokoo, 2008). However, the limit of this technique was the inability of the neokidney to reconstruct a ureter or collecting tubules derived from the ureteric bud. In genereal, these results indicate that it might be potentially possible to reconstruct a whole kidney by transplanting renal lineage-committed SC at a suitable time and location to regenerate derivatives of the metanephric mesenchyme and ureteric bud.

SCAFFOLD DECELLULARIZATION/ RECELLULARIZATION

Promising results on the reconstruction of whole rat hearts, kidneys, livers and lungs have been reported, but there are still major challenges that need to be solved. Native kidney extracellular matrix (ECM) has been reported to provide a scaffold for cell seeding of SC to differentiate into whole organs. Efficient cell removal during decellularization is crucial to avoid the induction of an immune response at the time of transplantation; however, enough care should be taken to keep the composition and structure of ECM intact. In fact, the ECM plays a crucial role in kidney development and repair by providing a scaffold for the spatial organization of cells, by secreting and storing growth factors and cytokines. ECM scaffolds from whole human-cadaveric and animal organs can be obtained by detergent-based decellularization. This strategy was used by Ott et al. to regenerate a functional rat heart (Ott, 2008). A whole-heart scaffold with intact 3D

scaffold and vasculature was prepared by coronary perfusion with detergents. The rat heart was then seeded with neonatal cardiac cells or rat aortic endothelial cells, which induced the formation of contractile myocardium. Decellularized cadaveric scaffolds have then been used in many other organ, such as liver (Baptista, 2011), respiratory tract (Song, 2011), nerves (Crapo, 2012), tendons (Martinello, 2014), valves (Honge, 2011), bladder (Loai, 2010) and mammary glands (Wicha, 1982). Furthermore, this approach has been applied also to the kidney regeneration in many animal models, including rats (Ross, 2009), rhesus monkeys (Nakayama, 2010) and pigs (Sullivan, 2012).

In 2009, Ross et al. pioneered the decellularization of whole rat kidneys with Triton X-100, 5 mM $MgSO_4$, 1 M NaCl solutions, and 0.0025%-deoxyribonuclease perfusion under constant pressure (Ross, 2009). They also showed partial preservation of laminin and collagen IV after complete cell removal. In 2012, they also described the decellularization of whole rat kidneys using a combination of SDS and Triton X-100 perfusion (Ross, 2012). Bonandrini et al. perfused rat kidneys with 1% SDS solution for 17 h to achieve acellular scaffolds with partially preserved collagen IV, fibronectin, and laminin, as well as an intact vascular network. They also repopulated matrix with murine ESC and kidney-specific markers were expressed after 3 days of cell culture (Bonandrini, 2014). In 2013, Song et al. reduced the

decellularization time to 12 h using 1% SDS under constant pressure (Song, 2013). In 2014, Yu et al. decellularized rat kidneys in 7 h with a combination of 0.1% Triton X-100 and 0.8% SDS (Yu, 2014). Moreover, Peloso et al. improved the protocol exploiting a combination of 1% Triton X-100 and 1% SDS to decellularize rat kidneys under constant perfusion rate (Peloso, 2015). Caralt et al. found that Triton X-100 combined with SDS was the optimum method for both cell removal and preservation of matrix integrity (Caralt, 2015).

In 2012, decellularization of whole porcine kidneys have been reported (Sullivan, 2012). Sullivan et al. injected whole porcine kidneys with 0.25% SDS, 0.5% SDS, and 1% Triton X-100 for 36 h. In the same year, also Orlando et al. decellularized porcine kidneys with 0.5% SDS in 48 h (Orlando, 2012). Of interest, Poornejad et al. demonstrated that exploiting one freezing/thawing cycle and incremental administering SDS under constant pressure allowed to reduce decellularization time to less than 7 h (Poornejad, 2016b). This is an important step forward since long SDS exposure caused enormous damage to collagen and reduced the amount of intrinsic growth factors in the scaffolds.

The obtained scaffolds are then exploited as a support for various attempts of recellularization but the cell source able to sustain this process is still debated and searched.

In 2009, Ross et al. repopulated whole rat kidneys with murine ESC for the first time (Ross, 2009). Instead Song et al. seeded rat kidney matrix with human umbilical vein endothelial cells (HUVEC) through the artery to repopulate the vasculature and rat neonatal cells through the ureter (Song et al., 2013). Moreover, Caralt et al. perfused rat kidney only with human renal cortical tubular epithelial cells through the renal artery (Caralt, 2015). In general, to date the only approach to obtain reepithelialization concomitant to reendothelization of the scaffolds is the use of the two different specific cell types. In fact, perfusing the matrix with endothelial cells through the vasculature is a common method to obtain endothelial repopulated structures. Of note, our previous data demonstrated the ability of $PKH^{high}/CD133^{+}/CD24^{-}$ human renal stem-like cells to differentiate in 2D culture in von Willebrand factor-positive (vWf^{+}) cells, typical feature of endothelial cells (Bombelli, 2013). Based on these results, with our recent work we surprisingly demonstrated that human nephrosphere cells, a mixture of stem-like cells and progenitor cells, are able to give rise to structures that resembles to vasculature as well as tubules on renal decellularized scaffolds (Bombelli, 2017). We could also demonstrate that SC-like cells alone are able to give rise to vWF^{+} vascular structures, as we will discuss along the thesis work. Actually, all these data demonstrated

that our SC-like cells could differentiate beyond linage restrictions.

However, it has to be noticed that the sites of recellularization strictly depends on the way of cell inoculum. In fact, Remuzzi et al. suggest the existence of physical barriers, which oppose to a uniform cell distribution in decellularized scaffolds (Remuzzi, 2017).

Of note, as a limit to the use of decellularized scaffolds for regenerative attempts there are many parameters still requiring optimization: cell type and number, seeding method, perfusion rate, way of infusion to reach homogenous cell distribution and the problem of massive thrombi, despite strong anticoagulation prophylaxis.

In conclusion, despite significant recent advances, the reconstruction of a complete functional kidney remains difficult, and many problems are still unsolved. Research in SC field will hopefully solve some problems. This will pave the way to the issue of new therapeutic strategies for kidney regeneration aimed at repairing damage and restoring kidney function.

Our attempts of renal acellular scaffold repopulation are mainly addressed to evaluate the regenerative and differentiative potential of our SC-like cells and have to be intended as a contribution to this issue.

AIM OF THE THESIS

Today kidney diseases affect approximately 11% to 13% of adult population worldwide (Hill, 2016) and it is therefore considered a global public health problem. In chronic renal failure dialysis and organ transplantation are the only successful treatments. However, the Italian Transplant Information System reports that 6527 individuals are on the wait-list for a kidney transplant, with only 1931 kidney transplants taking place during 2016 (https://trapianti.sanita.it/statistiche/home.asp).

It has also to be taken into account that the average of waiting time for transplant is 3,1 years and the patient mortality during waiting time is 1,8% (http://www.aido.it/dati_statistici/liste.htm). The evident shortage of transplantable kidneys has driven researches towards bioengineering strategies for renal tissue regeneration.

Chronic kidney diseases are characterized by the loss of nephrons, thus a possible therapeutic approach, based on the combination of stem cell research, regenerative medicine and tissue engineering, has to take into account the necessity to generate and replace new nephrons. To date one of the valuable alternatives for renal reconstitution is the recellularization of decellularized scaffolds (Poornejad, 2016a), even if the cell type usable for this purpose is not so

well defined yet. The most attractive one could be represented by adult renal stem cells, which could play a direct role in the regeneration. However, the existence of quiescent scattered stem cells as responsible for kidney injury repair is still debated. Besides, the definition of a univocal population of adult renal stem like cells is not so easy, basically due to the lack of unique markers.

Our group previously adapted the sphere forming assay to the adult human kidney cells to obtain nephrospheres composed by cells with stem abilities and their progeny (Bombelli, 2013).

Among the nephrospheres cells, our group identified and isolated a subpopulation of PKH26 most fluorescent cells, with characteristics of adult renal stem-like cells (PKH^{high} cells), and able to differentiate *in vitro* along tubular epithelial, podocytic and endothelial lineages.

It has also been demonstrated that PKH^{high} subpopulation is heterogeneous and the only cells able to self-renew and to differentiate along the three different lineages had $PKH^{high}/CD133^{+}/CD24^{-}$ (RSC) phenotype (Bombelli, 2013).

Given these premises, **the work performed during this PhD course was:**

1. to participate in the research aimed to set up the method to efficiently decellularize slices of human renal scaffolds and, taking advantage of our previous data, to exploit the whole nephrosphere cells to repopulate these scaffolds.

The achievement of these aims is described in chapter 2 and a relative paper has just been published *(Bombelli S, Meregalli C, Scalia C, Bovo G, Torsello B, De Marco S, Cadamuro M, Viganò P, Strada G, Cattoretti G, Bianchi C, Perego RA: "Nephrosphere-Derived Cells Are Induced to Multilineage Differentiation when Cultured on Human Decellularized Kidney Scaffolds" Am J Pathol. 2017 Oct 14. doi: 10.1016/j.ajpath.2017.09.012).*

2. As shown in chapter 3, to deepen our previous data and those described in chapter 2. The specific aims pursued are:
I). to prove the regenerative capability of PKH^{high} stem-like cell subpopulation.
II). to find the molecular signature of $PKH^{high}/CD133^{+}/CD24^{-}$ rnal stem-like cell (RSC).

- To reach the <u>first aim</u>, PKH^{high} cells were seeded on decellularized scaffolds and the repopulated structures were characterized by sequential immunofluorescence staining, revealing their potential by themselves to differentiate along proximal and distal tubule as well as along endothelium. It has been defined for the first time an adult human cell population with stem-like properties able to give rise to an epithelial and endothelial lineage of differentiation.
- Concerning the <u>second aim</u>, a transcriptomic analysis of our RSC ($PKH^{high}/CD133^{+}/CD24^{-}$), of their $PKH^{low/neg}$ progeny and of terminally differentiated primary cell cultures (PCC) was performed obtaining the signature of RSC, the only able to differentiate along tubular, podocytic and endothelial

lineages. It was also possible to select and validate few potential markers able to identify and possibly isolate from adult human renal tissue cells that hopefully can match the stem-like characteristics of our RSC.

REFERENCES

https://trapianti.sanita.it/statistiche/home.asp

http://www.aido.it/dati_statistici/liste.htm

Alison MR, Islam S: “Attributes of adult stem cells.” *J Pathol. 2009 Jan; 217(2):144-60.*

Angelotti ML, Ronconi E, Ballerini L, Peired A, Mazzinghi B, Sagrinati C, Parente E, Gacci M, Carini M, Rotondi M, Fogo AB, Lazzeri E, Lasagni L, Romagnani P: “Characterization of renal progenitors committed toward tubular lineage and their regenerative potential in renal tubular injury*.” Stem Cells. 2012 Aug;30(8):1714-25.*

Axelson H, Johansson ME: “Renal stem cells and their implications for kidney cancer.” *Semin Cancer Biol. 2013 Feb; 23(1):56-61.*

Baptista PM, Siddiqui MM, Lozier G, Rodriguez SR, Atala A, Soker S: “The use of whole organ decellularization for the generation of a vascularized liver organoid.” *Hepatology. 2011, Feb; 53(2):604-17.*

Barker N1, Rookmaaker MB, Kujala P, Ng A, Leushacke M, Snippert H, van de Wetering M, Tan S, Van Es JH, Huch M, Poulsom R, Verhaar MC, Peters PJ, Clevers H:
"Lgr5(+ve) stem/progenitor cells contribute to nephron formation during kidney development." *Cell Rep. 2012 Sep 27;2(3):540-52*

Basile DP, Anderson MD, Sutton TA: "Pathophysiology of acute kidney injury." *Compr Physiol 2012; 2: 1303–1353*

Bombelli S, Zipeto MA, Torsello B, Bovo G, Di Stefano V, Bugarin C, Zordan P, Viganò P, Cattoretti G, Strada G, Bianchi C, Perego RA: "PKH^{high} cells within clonal human nephrospheres provide a purified adult renal stem cell population." *Stem Cell Res 2013, 11: 1163-1177.*

Bombelli S, Meregalli C, Scalia C, Bovo G, Torsello B, De Marco S, Cadamuro M, Viganò P, Strada G, Cattoretti G, Bianchi C, Perego RA: "Nephrosphere-Derived Cells are Induced to Multilineage Differentiation when Cultured on Human Decellularized Kidney Scaffolds." *Am J Pathol. 2017 Oct 14. doi: 10.1016/j.ajpath.2017.09.012.*

Bonandrini B, Figliuzzi M, Papadimou E, Morigi M, Perico N, Casiraghi F, Sangalli F, Conti S, Benigni A, Remuzzi A, Remuzzi G: “Recellularization of well-preserved acellular kidney scaffold using embryonic stem cells.” *Tissue Eng Part A 2014, 20: 1486-1498.*

Bussolati B, Bruno S, Grange C, Buttiglieri S, Deregibus MC, Cantino D, Camussi G: “Isolation of renal progenitor cells from adult human kidney.” *Am J Pathol. 2005 Feb;166(2):545-55.*

Bussolati B, Collino F, Camussi G: “CD133+ cells as a therapeutic target for kidney diseases.” *Expert Opin Ther Targets. 2012 Feb;16(2):157-65.*

Bussolati B, Camussi G: “Therapeutic use of human renal progenitor cells for kidney regeneration*.” Nat Rev Nephrol. 2015 Dec;11(12):695-706.*

Buzhor E, Harari-Steinberg O, Omer D, Metsuyanim S, Jacob-Hirsch J, Noiman T, Dotan Z, Goldstein RS, Dekel B: “Kidney spheroids recapitulate tubular organoids leading to enhanced tubulogenic potency of human kidney-derived cells.” *Tissue Eng Part A. 2011 Sep;17(17-18):2305-19.*

Buzhor E, Omer D, Harari-Steinberg O, Dotan Z, Vax E, Pri-Chen S, Metsuyanim S, Pleniceanu O, Goldstein RS, Dekel B: “Reactivation of NCAM1 defines a subpopulation of human adult kidney epithelial cells with clonogenic and stem/progenitor properties.” *Am J Pathol. 2013 Nov;183(5):1621-33.*

Caralt M, Uzarski JS, Iacob S, Obergfell KP, Berg N, Bijonowski BM, Kiefer KM, Ward HH, Wandinger-Ness A, Miller WM, Zhang ZJ, Abecassis MM, Wertheim JA: “Optimization and critical evaluation of decellularization strategies to develop renal extracellular matrix scaffolds as biological templates for organ engineering and transplantation.” *Am J Transplant 2015, 15: 64-75.*

Cicalese A, Bonizzi G, Pasi CE, Faretta M, Ronzoni S, Giulini B, Brisken C, Minucci S, Di Fiore PP, Pelicci PG: “The tumor suppressor p53 regulates polarity of self-renewing divisions in mammary stem cells.” *Cell. 2009 Sep 18;138(6):1083-95.*

Corbeil D, Marzesco AM, Wilsch-Brauninger M, Huttner WB: “The intriguing links between prominin-1 (CD133), cholesterol-based membrane microdomains, remodeling of apical plasma membrane protrusions, extracellular membrane particles, and (neuro)epithelial cell differentiation.” *FEBS Lett 2010, 584(9):1659–1664.*

Crapo PM, Medberry CJ, Reing JE, Tottey S, van der Merwe Y, Jones KE, Badylak SF: “Biologic scaffolds composed of central nervous system extracellular matrix.” *Biomaterials. 2012 May;33(13):3539-47.*

Crispe IN, Bevan MJ: “Expression and functional significance of the J11d marker on mouse thymocytes.” *J Immunol 1987; 138: 2013–2018*.

Dekel B, Zangi L, Shezen E, Reich-Zeliger S, Eventov-Friedman S, Katchman H, Jacob-Hirsch J, Amariglio N, Rechavi G, Margalit R, Reisner Y: “Isolation and characterization of nontubular sca-1+lin- multipotent stem/progenitor cells from adult mouse kidney.” *J Am Soc Nephrol. 2006 Dec;17(12):3300-14.*

Fang X, Zheng P, Tang J, Liu Y: “CD24: from A to Z.” *Cell Mol Immunol. 2010 Mar;7(2):100-3.*

Gilbert: “Developmental Biology*.” Zanichelli ed. Third Italian version based on seventh America edition, 2005.*

Hartman HA, Lai HL, Patterson LT: “Cessation of renal morphogenesis in mice.” *Dev Biol. 2007 Oct 15;310(2):379-87.*

Hill NR, Fatoba ST, Oke JL, Hirst JA, O'Callaghan CA, Lasserson DS, Hobbs FD: “Global Prevalence of Chronic Kidney Disease - A Systematic Review and Meta-Analysis.” *PLoS One. 2016; 11(7): e0158765.*

Honge JL, Funder J, Hansen E, Dohmen PM, Konertz W, Hasenkam JM: “Recellularization of aortic valves in pigs.” *Eur J Cardiothorac Surg. 2011 Jun;39(6):829-34.*

Hsu YC, Fuchs E: “A family business: stem cell progeny join the niche to regulate homeostasis.” *Nat Rev Mol Cell Biol. 2012 Jan 23;13(2):103-14.*

Hubbe M, Altevogt P: “Heat-stable antigen/CD24 on mouse T lymphocytes: evidence for a costimulatory function.*” Eur J Immunol 1994; 24: 731–737.*

Humphreys BD, Valerius MT, Kobayashi A, Mugford JW, Soeung S, Duffield JS, McMahon AP, Bonventre JV: “Intrinsic epithelial cells repair the kidney after injury.” *Cell Stem Cell. 2008 Mar 6;2(3):284-91.*

Hunte BE, Capone M, Zlotnik A, Rennick D, Moore TA: “Acquisition of CD24 expression by Lin-CD43+B220l^{ow}ckit^{hi} cells coincides with commitment to the B cell lineage.” *Eur J Immunol 1998; 28: 3850–3856.*

Iida H, Suzuki M, Goitsuka R, Ueno H: “Hypoxia induces CD133 expression in human lung cancer cells by up-regulation of OCT3/4 and SOX2.” *Int J Oncol 2012, 40(1):71–79.*

Lan X, Wu YZ, Wang Y, Wu FR, Zang CB, Tang C, Cao S, Li SL: *“*CD133 silencing inhibits stemness properties and enhances chemoradiosensitivity in CD133-positive liver cancer stem cells.” *Int J Mol Med. 2013 Feb;31(2):315-24.*

Langworthy M, Zhou B, de Caestecker M, Moeckel G, Baldwin HS: “NFATc1 identifies a population of proximal tubule cell progenitors.” *J Am Soc Nephrol. 2009 Feb;20(2):311-21.*

Li Z: “CD133: a stem cell biomarker and beyond*.” Exp Hematol Oncol. 2013 Jul 1;2(1):17.*

Lindgren D, Boström AK, Nilsson K, Hansson J, Sjölund J, Möller C, Jirström K, Nilsson E, Landberg G, Axelson H, Johansson ME: “Isolation and characterization of progenitor-like cells from human renal proximal tubules”. *Am J Pathol. 2011 Feb;178(2):828-37.*

Little MH, McMahon AP: “Mammalian kidney development: principles, progress, and projections.” *Cold Spring Harb Perspect Biol. 2012 May 1;4(5).*

Little MH: “Growing Kidney Tissue from Stem Cells: How Far from "Party Trick" to Medical Application?” *Cell Stem Cell. 2016 Jun 2;18(6):695-8.*

Loai Y, Yeger H, Coz C, Antoon R, Islam SS, Moore K, Farhat WA: “Bladder tissue engineering: tissue regeneration and neovascularization of HA-VEGF-incorporated bladder acellular constructs in mouse and porcine animal models.” *J Biomed Mater Res A. 2010 Sep 15;94(4):1205-15.*

Lombardi D, Becherucci F, Romagnani P: “How much can the tubule regenerate and who does it? An open question.” *Nephrol Dial Transplant. 2016 Aug;31(8):1243-50.*

Martinello T, Bronzini I, Volpin A, Vindigni V, Maccatrozzo L, Caporale G, Bassetto F, Patruno M: “Successful recellularization of human tendon scaffolds using adipose-derived mesenchymal stem cells and collagen gel*.” J Tissue Eng Regen Med. 2014 Aug;8(8):612-9.*

McCampbell KK, Wingert RA: “Renal stem cells: fact or science fiction?” *Biochem J. 2012 Jun 1;444(2):153-68.*

Messier B, Leblond CP: “Cell proliferation and migration as revealed by radioautography after injection of thymidine-H3 into male rats and mice.” *Am J Anat. 1960 May;106:247-85.*

Mimeault M, Batra SK: “Concise review: recent advances on the significance of stem cells in tissue regeneration and cancer therapies*.” Stem Cells. 2006 Nov;24(11):2319-45.*

Morizane, R., Monkawa, T., Fujii, S., Yamaguchi, S., Homma, K., Matsuzaki, Y., Okano, H., and Itoh, H: “Kidney specific protein-positive cells derived from embryonic stem cells reproduce tubular structures in vitro and differentiate into renal tubular cells.” *PLoS One 8, e64843, 2013.*

Morrison SJ, Kimble J: “Asymmetric and symmetric stem-cell divisions in development and cancer.” *Nature. 2006 Jun 29;441(7097):1068-74.*

Nakayama KH, Batchelder CA, Lee CI, Tarantal AF: “Decellularized rhesus monkey kidney as a three-dimensional scaffold for renal tissue engineering.” *Tissue Eng Part A 2010, 16: 2207-2216.*

Ohnishi S, Maehara O, Nakagawa K, Kameya A, Otaki K, Fujita H, Higashi R, Takagi K, Asaka M, Sakamoto N, Kobayashi M, Takeda H: “Hypoxia-inducible factors activate CD133 promoter through ETS family transcription factors.” *PLoS One. 2013 Jun 20;8(6):e66255.*

Orlando G, Farney AC, Iskandar SS, Mirmalek-Sani SH, Sullivan DC, Moran E, AbouShwareb T, De Coppi P, Wood KJ, Stratta RJ, Atala A, Yoo JJ, Soker S: “Production and implantation of renal extracellular matrix scaffolds from porcine kidneys as a platform for renal bioengineering investigations.” *Ann Surg. 2012 Aug;256(2):363-70.*

Ott HC, Matthiesen TS, Goh SK, Black LD, Kren SM, Netoff TI, Taylor DA: “Perfusion-decellularized matrix: using nature's platform to engineer a bioartificial heart.” *Nat Med. 2008 Feb;14(2):213-21.*

Pavenstädt H, Kriz W, Kretzler M: Cell biology of the glomerular podocyte. *Physiol Rev. 2003 Jan;83(1):253-307.*

Peloso A, Ferrario J, Maiga B, Benzoni I, Bianco C, Citro A, Currao M, Malara A, Gaspari A, Balduini A, Abelli M, Piemonti L, Dionigi P, Orlando G, Maestri M: “Creation and implantation of acellular rat renal ECM-based scaffolds.” *Organogenesis 2015, 11: 58-74.*

Poornejad N, Schaumann LB, Buckmiller EM, Roeder BL, Cook AD: “Current Cell-Based Strategies for Whole Kidney Regeneration.” *Tissue Eng Part B Rev. 2016a Oct;22(5):358-370.*

Poornejad N, Nielsen JJ, Morris RJ, Gassman JR, Reynolds PR, Roeder BL, Cook AD: “Comparison of four decontamination treatments on porcine renal decellularized extracellular matrix structure, composition, and support of human renal cortical tubular epithelium cells.” *J Biomater Appl. 2016b Mar;30(8):1154-67.*

Rangel EB1, Gomes SA, Dulce RA, Premer C, Rodrigues CO, Kanashiro-Takeuchi RM, Oskouei B, Carvalho DA, Ruiz P, Reiser J, Hare JM: “C-kit(+) cells isolated from developing kidneys are a novel population of stem cells with regenerative potential.” *Stem Cells. 2013 Aug;31(8):1644-56.*

Remuzzi A, Figliuzzi M, Bonandrini B, Silvani S, Azzollini N, Nossa R, Benigni A, Remuzzi G: “Experimental Evaluation of Kidney Regeneration by Organ Scaffold Recellularization*.” Sci Rep. 2017 Mar 7;7:43502.*

Rinkevich Y, Montoro DT, Contreras-Trujillo H, Harari-Steinberg O, Newman AM, Tsai JM, Lim X, Van-Amerongen R, Bowman A, Januszyk M, Pleniceanu O, Nusse R, Longaker MT, Weissman IL, Dekel B: “In vivo clonal analysis reveals lineage-restricted progenitor characteristics in mammalian kidney development, maintenance, and regeneration.” *Cell Rep. 2014 May 22;7(4):1270-83.*

Ronconi E, Sagrinati C, Angelotti ML, Lazzeri E, Mazzinghi B, Ballerini L, Parente E, Becherucci F, Gacci M, Carini M, Maggi E, Serio M, Vannelli GB, Lasagni L, Romagnani S, Romagnani P: “Regeneration of glomerular podocytes by human renal progenitors*.” J Am Soc Nephrol. 2009 Feb;20(2):322-32.*

Ross EA, Williams MJ, Hamazaki T, Terada N, Clapp WL, Adin C, Ellison GW, Jorgensen M, Batich CD: “Embryonic stem cells proliferate and differentiate when seeded into kidney scaffolds.” *J Am Soc Nephrol 2009, 20: 2338-2347.*

Ross EA, Abrahamson DR, St John P, Clapp WL, Williams MJ, Terada N, Hamazaki T, Ellison GW, Batich CD: “Mouse stem cells seeded into decellularized rat kidney scaffolds endothelialize and remodel basement membranes.” *Organogenesis 2012, 8: 49-55.*

Sallustio F, De Benedictis L, Castellano G, Zaza G, Loverre A, Costantino V, Grandaliano G, Schena FP: “TLR2 plays a role in the activation of human resident renal stem/progenitor cells.” *FASEB J. 2010 Feb;24(2):514-25.*

Sallustio F, Serino G, Costantino V, Curci C, Cox SN, De Palma G, Schena FP: “miR-1915 and miR-1225-5p regulate the expression of CD133, PAX2 and TLR2 in adult renal progenitor cells.” *PLoS One. 2013 Jul 8;8(7):e68296.*

Sagrinati C, Netti GS, Mazzinghi B, Lazzeri E, Liotta F, Frosali F, Ronconi E, Meini C, Gacci M, Squecco R, Carini M, Gesualdo L, Francini F, Maggi E, Annunziato F, Lasagni L, Serio M, Romagnani S, Romagnani P: “Isolation and characterization of multipotent progenitor cells from the Bowman's capsule of adult human kidneys*.” J Am Soc Nephrol. 2006 Sep;17(9):2443-56.*

Shepherd CJ, Rizzo S, Ledaki I, Davies M, Brewer D, Attard G, de Bono J, Hudson DL: “Expression profiling of CD133+ and CD133- epithelial cells from human prostate.” *Prostate 2008, 68(9):1007–1024.*

Singh RK, Gaikwad SM, Chatterjee S and Ray P: *"*Chapter 2-Stem Cells: The Holy Grail of Regenerative Medicine." *W. Cai (ed.), Engineering in Translational Medicine*, *Springer-Verlag London 2014.*

Smeets B, Boor P, Dijkman H, Sharma SV, Jirak P, Mooren F, Berger K, Bornemann J, Gelman IH, Floege J, van der Vlag J, Wetzels JF, Moeller MJ: "Proximal tubular cells contain a phenotypically distinct, scattered cell population involved in tubular regeneration." *J Pathol. 2013 Apr;229(5):645-59.*

Snippert HJ, Clevers H: "Tracking adult stem cells." *EMBO Rep. 2011 Feb;12(2):113-22.*

Song JJ, Kim SS, Liu Z, Madsen JC, Mathisen DJ, Vacanti JP, Ott HC: "Enhanced in vivo function of bioartificial lungs in rats." *Ann Thorac Surg. 2011 Sep;92(3):998-1006.*

Song JJ, Guyette JP, Gilpin SE, Gonzalez G, Vacanti JP, Ott HC: "Regeneration and experimental orthotopic transplantation of a bioengineered kidney*." Nat Med 2013, 19: 646-651.*

Sullivan DC, Mirmalek-Sani SH, Deegan DB, Baptista PM, Aboushwareb T, Atala A, Yoo JJ: “Decellularization methods of porcine kidneys for whole organ engineering using a high-throughput system.” *Biomaterials 2012, 33: 7756-7764.*

Suzuki E, Fujita D, Takahashi M, Oba S, Nishimatsu H: “Adult stem cells as a tool for kidney regeneration.” *World J Nephrol. 2016 Jan 6;5(1):43-52.*

Taguchi A, Kaku Y, Ohmori T, Sharmin S, Ogawa M, Sasaki H, Nishinakamura R: “Redefining the in vivo origin of metanephric nephron progenitors enables generation of complex kidney structures from pluripotent stem cells*.” Cell Stem Cell. 2014 Jan 2;14(1):53-67.*

Takahashi K, Yamanaka S: “Induction of pluripotent stem cells from mouse embryonic and adult fibroblast cultures by defined factors.” *Cell. 2006 Aug 25;126(4):663-76.*

Takasato M, Er PX, Chiu HS, Maier B, Baillie GJ, Ferguson C, Parton RG, Wolvetang EJ, Roost MS, Chuva de Sousa Lopes SM, Little MH: “Kidney organoids from human iPS cells contain multiple lineages and model human nephrogenesis.” *Nature. 2015 Oct 22;526(7574):564-8.*

Takenobu H, Shimozato O, Nakamura T, Ochiai H, Yamaguchi Y, Ohira M, Nakagawara A, Kamijo T: “CD133 suppresses neuroblastoma cell differentiation via signal pathway modification.” *Oncogene 2011, 30(1):97–105*.

Trumpp A, Essers M, Wilson A: “Awakening dormant haematopoietic stem cells.” *Nat Rev Immunol. 2010 Mar;10(3):201-9.*

Usui J, Kobayashi T, Yamaguchi T, Knisely AS, Nishinakamura R, Nakauchi H: “Generation of kidney from pluripotent stem cells via blastocyst complementation.” *Am J Pathol. 2012 Jun;180(6):2417-26.*

Vogetseder A, Picard N, Gaspert A, Walch M, Kaissling B, Le Hir M: “Proliferation capacity of the renal proximal tubule involves the bulk of differentiated epithelial cells.” *Am J Physiol Cell Physiol 2008; 294: C22–C28*

Ward HH, Romero E, Welford A, Pickett G, Bacallao R, Gattone VH 2nd, Ness SA, Wandinger-Ness A, Roitbak T: “Adult human CD133/1(+) kidney cells isolated from papilla integrate into developing kidney tubules*.” Biochim Biophys Acta. 2011 Oct;1812(10):1344-57.*

Weiss P, Taylor AC: “Reconstitution of complete organs from single-cell suspensions of chick embryos in advanced stages of differentiation.” *Proc Natl Acad Sci U S A. 1960 Sep;46(9):1177-85.*

Wicha MS, Lowrie G, Kohn E, Bagavandoss P, Mahn T: “Extracellular matrix promotes mammary epithelial growth and differentiation in vitro.” *Proc Natl Acad Sci U S A. 1982 May;79(10):3213-7.*

Wobus AM, Boheler KR: “Embryonic stem cells: prospects for developmental biology and cell therapy.” *Physiol Rev. 2005 Apr;85(2):635-78.*

Yamanaka S, Yokoo T: “Current Bioengineering Methods for Whole Kidney Regeneration*.” Stem Cells Int. 2015;2015:724047.*

Yokoo T, Fukui A, Ohashi T, Miyazaki Y, Utsunomiya Y, Kawamura T, Hosoya T, Okabe M, Kobayashi E: “Xenobiotic kidney organogenesis from human mesenchymal stem cells using a growing rodent embryo.” *J Am Soc Nephrol. 2006 Apr;17(4):1026-34.*

Yokoo T, Fukui A, Matsumoto K, Ohashi T, Sado Y, Suzuki H, Kawamura T, Okabe M, Hosoya T, Kobayashi E: “Generation of a transplantable erythropoietin-producer derived from human mesenchymal stem cells.” *Transplantation. 2008 Jun 15;85(11):1654-8.*

You H, Ding W, Rountree CB: “Epigenetic regulation of cancer stem cell marker CD133 by transforming growth factor-beta.” *Hepatology 2010,51(5):1635–1644.*

Yu YL, Shao YK, Ding YQ, Lin KZ, Chen B, Zhang HZ, Zhao LN, Wang ZB, Zhang JS, Tang ML, Mei J: “Decellularized kidney scaffold-mediated renal regeneration.” *Biomaterials 2014, 35: 6822-6828.*

Chapter 2

Nephrosphere-derived cells are induced to multilineage differentiation when cultured on human decellularized kidney scaffolds

Silvia Bombelli, PhD[1], Chiara Meregalli, MSc[1], Carla Scalia, BSc[1], Giorgio Bovo, MD[2], Barbara Torsello, PhD[1], Sofia De Marco, MSc[1], Massimiliano Cadamuro, PhD[1], Paolo Viganò, MD[3], Guido Strada, MD[3], Giorgio Cattoretti, MD[1,2], Cristina Bianchi, PhD[1], Roberto A Perego, MD[1]*.

[1]School of Medicine and Surgery, Milano-Bicocca University, Via Cadore 48, 20900 Monza, Italy
[2]Anatomo-Pathology Unit, ASST Monza, San Gerardo Hospital, Via G. B. Pergolesi 33, 20900 Monza, Italy
[3]Urology Unit, ASST North Milan, Bassini Hospital, Via Massimo Gorki 50, 20092 Cinisello Balsamo, Italy

Am J Pathol. 2017 Oct 14.
https://doi.org/10.1016/j.ajpath.2017.09.012

Abstract

In end-stage chronic kidney disease, the option of organ transplantation is limited due to the scarce availability of kidneys. The combination of stem cell research, regenerative medicine and tissue engineering seems a promising approach to produce new transplantable kidneys. Currently, the possibility to repopulate naturally obtained scaffolds with cells of different sources is advancing. The aim of this paper was to test, for the first time, whether the nephrosphere (NS) cells, composed by renal stem/progenitor-like cells, were able to repopulate different nephron portions of renal extracellular matrix (ECM) scaffolds obtained after decellularization of human renal tissue slices. Our decellularization protocol enabled us to obtain a completely acellular renal scaffold while maintaining the ECM structure and composition in terms of Collagen IV, Laminin and Fibronectin. NS cells, cultured on decellularized renal scaffolds with basal medium, differentiated into proximal and distal tubules as well as endothelium, as highlighted by histology and by the specific expression of epithelial CK 8.18, proximal tubular CD10, distal tubular CK7 and endothelial vWf markers. Endothelial medium promoted the differentiation towards the endothelium, while epithelial medium towards epithelium. NS cells seem to be a good tool for scaffold repopulation, paving the way for experimental investigations focused on whole-kidney reconstruction.

Introduction

Kidney diseases are considered a global public health issue given their worldwide incidence and associated morbidity and mortality, affecting approximately 8% to 16% of the adult population[1]. The only therapeutic options for patients with end-stage renal disease are lifelong dialysis treatment or organ transplantation. Advances in the understanding of the mechanisms of rejection, as well as the development of new immunosuppressant therapies have led to an increase of the number of patients eligible for renal transplantation, although the availability of donors has remained stable. Consequently, in renal diseases, the need for kidneys is urgent and the hope is that this need can be fulfilled by stem cell and regenerative medicine approaches. For this purpose, the interactions between the study of renal stem cells for regenerative medicine and tissue engineering is fundamental to produce new transplantable organs. Bussolati and Camussi[2] recently reviewed different types of renal progenitor cells that were successfully engrafted into the renal tissue in animal models of acute injury. Nevertheless, the action of these progenitor cells in models of chronic renal diseases, in which new nephrons have to be generated to compensate their loss, has still to be disclosed.

In recent years, tissue engineering research focused its attention on scaffolds of natural extracellular matrix (ECM), obtained by removing cellular components from the native

organs by a decellularization process. Decellularized kidney scaffolds have been obtained from rats[3-6], pigs[3,6-10], non-human primates[11,12] and from cadaveric human kidneys[3] lacking the transplantation criteria[13-15]. Attempts of cellular repopulation have been performed both in perfusion and in static cultures using different cell types such as rat neonatal kidney cells and human umbilical vein endothelial cells (HUVEC)[3], mouse kidney stem cells[6], mouse embryonic stem cells[4,16-18], human embryonic stem cells[19], human iPS-derived renal progenitor cells[20] and human iPS-derived endothelial cells[6]. Although the decellularized ECM scaffolds could also be useful for assessing the capability of the adult renal stem/progenitor cells to regenerate whole nephrons, no attempts of repopulation of decellularized natural human kidney ECM scaffold with adult human renal stem/progenitor cells have been performed until now.

We have previously identified a population of renal stem-like cells in clonal human nephropsheres (NS)[21], and with these NS cells it is possible to generate three-dimensional tubular-like structures in 3D cultures and in vivo under the renal capsule of nude mice[21]. In the present paper, we wanted to investigate the differentiation abilities of NS cells and their capability to repopulate different nephron portions when cultured on renal ECM scaffolds obtained by decellularization of human renal tissue slices.

Material and methods

Tissues

Normal kidney tissue was obtained from 18 patients (11 male, 7 females; age range 48-84) following nephrectomy due to the presence of renal tumors. The normal tissue was taken from a healthy region of the kidney, without any indication of cancer, opposite to the tumor and exceeding the diagnostic needs. All procedures were performed after written patient consent and approved by the Local Ethical Committee. NS cultures were established from all fresh renal tissue samples. The remaining part of all tissue samples were formalin-fixed paraffin-embedded (FFPE). Frozen pieces of renal tissue, comprising cortex, medulla and papilla, were stored at -80°C until use.

Nephrosphere cultures

The single cell suspension from renal tissue[22] and the NS cultures[21] were obtained from 12 different tissue samples as described. The suspension obtained after mechanical dissociation and enzymatic digestion was sieved through a 250 µm cell strainer and then passed through a pipette syringe to obtain a single cell suspension[21]. Red blood cells were removed by hemolysis with 0.8% NH_4Cl solution for 5 minutes. After a 24-48 hours adhesion step, the trypsinized bulk epithelial cells were plated (10,000 cells/ml) in Stem Cell medium on poly-Hema (Sigma Aldrich, St. Louis, MO), or 1%

Agarose, coated dishes in non-adherent conditions for the formation of floating NS. After 10-12 days NS were collected for use[21]. When necessary, NS cells were dissociated enzymatically for 5 minutes in TrypLE Express (Life Technologies, Waltham, MA) and then mechanically by repetitive pipette syringing to generate a single cell suspension.

Immunofluorescence and FACS analysis

Immunofluorescence on floating NS obtained from 3 different tissue samples was performed by fixing the spheres in 4% paraformaldehyde for 20 minutes, blocking for 20 minutes with PBS containing 0.1% BSA (Sigma Aldrich) and 0.3% Triton X-100 and then by incubation with the specific primary antibody overnight at 4°C. The primary antibodies used are the following: rabbit anti-von Willebrand factor (DAKO, Copenhagen, Denmark; 1:2000), rabbit monoclonal anti-Cytokeratin 7 (clone EPR1619Y, Abcam, Cambridge, United Kingdom; 1:200), mouse monoclonal anti-Cytokeratin 8.18 (clone 5D3, Thermo Fisher Scientific, Waltham, MA; 1:50), rabbit anti-PAX2 (Thermo Fisher Scientific; 1:50), mouse monoclonal anti-N-Cadherin (clone 32, Becton Dickinson, San Jose, CA; 1:100), rabbit anti-E-Cadherin (Cell Signaling Technology, Massachusetts, USA; 1:50). For the secondary antibody, spheres were incubated with Alexa Fluor 594 conjugated anti-mouse or Alexa Fluor 488 conjugated anti-

rabbit IgG antibodies (Molecular Probes Invitrogen, Waltham, MA) for 1 hour. The spheres were resuspended with ProLong Gold Antifade with DAPI (Molecular Probes) and the slides mounted. Immunofluorescence of cells obtained after dissociation of NS from 3 tissue samples was performed on cytospinned preparation as described[22]. Immunofluorescence micrographs were obtained at 400x magnification using a Zeiss LSM710 confocal microscope and Zen2009 software (Zeiss, Oberkochen, Germany). FACS staining was performed as described[22-23] on 4 different NS samples and analysis was performed on 20,000 events with a MoFLO Astrios cell sorter and Kaluza 1.3 software (both from Beckman Coulter, Miami, FL). For FACS analysis the following antibodies were used: rabbit monoclonal anti-Cytokeratin 7 (clone EPR1619Y, Abcam; 1:20), mouse monoclonal FITC-conjugated anti-CK (clone CK3-6H5, Miltenyi Biotec, Auburn, CA; 1:10), mouse monoclonal PE-conjugated anti-CD13 (clone WM15, Biolegend, San Diego, CA; 1:10), mouse monoclonal APCH7-conjugated anti-CD10 (clone HI10a, Becton Dickinson; 1:20), mouse anti-Prominin 2 (Neuromics, Edina, MN; 1:10).

Decellularization

A total of 12 different frozen renal tissues were cut into approximately 2 mm thick slices maintaining all kidney regions. Slices were decellularized using a modification of

two published methods[3,7]. The slices were washed with 2x PBS supplemented with Penicillin and Streptomicin (P/S) for 15 minutes, followed by 1 hour of 0.02% Trypsin, 2 hours of 2% Tween-20, 3 hours of 4% sodium deoxycholate and 1% SDS (all from Euroclone, Milan, Italy) overnight treatment. Following each step, the slices were washed with 2x PBS for 15 minutes. Every step and wash was performed under agitation. At the end of decellularization treatments, the slices were subjected to washes with 2x PBS containing P/S for 4 hours and then with 1x PBS containing P/S for other 4 hours.

Decellularized scaffold analysis

Native and decellularized FFPE tissue samples were sectioned at 2 µm thick, deparaffinized and then stained with hematoxylin and eosin (H&E), Trichrome or Alcian Pas (all from Sigma Aldrich). Images were acquired using the ScanScope CS System (Aperio Technologies, Wetzlar, Germany) equipped with Spectrum Plus Digital Pathology Information Management Software. For immunohistochemical analysis, the sections were deparaffinized, subjected to specific antigen retrieval and blocked with human serum for 2 hours at room temperature. Staining was performed overnight at 4°C with the following antibodies: rabbit anti-Type IV Collagen (Thermo Fisher Scientific; 1:100; 0.5% SDS/50mM 2-Mercaptoethanol 10 minutes 95°C, 10 mM EDTA in Tris-buffer pH8; 8 minutes at

800 Watt and 20 minutes at 600 Watt for antigen retrieval); rabbit anti-Laminin (DAKO; 1:50; Proteinase K 5 minutes 37°C for antigen retrieval); rabbit anti-Fibronectin (DAKO; 1:2000; Retrieval 2 (Covance, Princeton, NJ), 20 minutes in the steamer and 20 minutes at room temperature for antigen retrieval). Renal sections were rinsed with 0.05% Tween-20 in PBS and incubated for 30 minutes at room temperature with the appropriate Dako EnVision anti-Rabbit antibody (DAKO). Specimens were developed using 0.04 mg/ml 3,3-diaminobenzedine tetrahydrochloride (DAB, Sigma Aldrich) along with 0.01% H_2O_2 and counterstained with Hematoxylin. All the antibodies were diluted in PBS supplemented with 5% normal human serum type 0 and 0.05% Tween-20 (Euroclone). For the quantitative evaluation of ECM proteins, immunofluorescence was performed by using Alexa Fluor® 594 goat anti rabbit (Molecular Probes). Three different specimens of native kidney and the corresponding decellularized scaffolds were stained and three different fields for each antibody were acquired at 40X magnification and then analyzed for the quantification of ECM protein with ImageJ 1.48v software (NIH) as described[24].

DNA quantification

DNA was extracted from native and decellularized renal slices, obtained from 3 different renal samples with QIamp® DNA Mini Kit (Qiagen, Venlo, Netherlands) according to the

manufacturer instructions and quantified using Nanodrop (Life Technologies).

Nephrosphere culture on decellularized ECM scaffolds

50,000 alive cells obtained by enzymatic and mechanic dissociation from different NS samples[21] were seeded on the decellularized renal scaffolds, obtained from the same patient, and cultured with basal medium or specific cell differentiation media in 24-well poly-Hema coated plates. Ten different experiments were performed with each experiment representing one individual patient. The basal medium was DMEM low glucose (Euroclone) supplemented with 10% FBS (Euroclone). The specific media were: epithelial medium, composed by DMEM-F12 (Lonza, Basel, Switzerland) supplemented with 10% FBS, ITS supplement (5 µg/ml Insulin, 5 µg/ml Transferrin, 5 ng/ml sodium selenite), 36 ng/ml Hydrocortisone, 40 pg/ml Triiodothyronine (all from Sigma Aldrich), 20 ng/ml EGF (Cell Signalling, Danvers, MA) and 50 ng/ml HGF (Cell Signalling); and endothelial medium, composed by Endothelial Basal Medium (EBM) (Lonza) supplemented with 10% FBS and 10 ng/ml VEGF (Miltenyi Biotec). In all differentiating conditions, the cells were allowed to attach to the ECM scaffold for 5 days whilst only adding the medium, without changing.

The cultures were stopped at different time points, formalin fixed for at least 16 hours and paraffin embedded for histological analysis.

3D staining of cultured scaffolds

At 4, 7, 15 and 30 days, a small portion of 3 different cultured scaffolds was cut and fixed in formalin for 1 hour. The scaffolds were then incubated with Alexa Fluor® 680-Falloidin (1:100 in PBS, Molecular Probes) for 15 minutes, with DAPI (Sigma Aldrich) for 10 minutes and then mounted between a glass coverslip and glass slides. Immunofluorescence micrographs were obtained at 400x magnification using the Zeiss LSM710 confocal microscope and Zen2009 software (Zeiss). Z-stack function was used to acquire sequential micrographs every 1.5 or 2 µm, covering the entire thickness of the chosen structures and then 3D reconstructions were performed using the specific ImageJ software plugin.

Histologic characterization

The decellularized scaffolds cultured with NS cells were FFPE, sectioned (2 µm thick) and H&E stained in order to assess the cellular repopulation and to evaluate the morphological features of the formed structures. Images were acquired using the ScanScope CS System (Aperio Technologies) equipped with Spectrum Plus Digital

Pathology Information Management Software. Immunofluorescence staining was performed as described[25,26] on FFPE sections using the following antibodies: rabbit monoclonal anti-Ki-67, marker of cell proliferation (Clone SP6, Thermo Fisher Scientific; 1:100); mouse monoclonal anti-CD10, proximal tubular marker (Clone 56C6, Leica Biosystems, Wetzlar, Germany; 1:100); rabbit monoclonal anti-Cytokeratin 7 (CK7), distal tubular marker (clone EPR1619Y, Abcam; 1:200); mouse monoclonal anti-Calbindin-D28k (CALB), distal tubular marker (clone CB-955, Sigma; 1:1000); mouse monoclonal anti-Cytokeratin 8.18 (CK 8.18), epithelial marker (clone 5D3, Thermo Fisher Scientific; 1:50); rabbit polyclonal anti von Willebrand factor (vWf) endothelial marker (DAKO; 1:2000); mouse monoclonal anti-E Cadherin (ECAD), distal tubular marker (clone NCH-38, DAKO; 1:100); mouse monoclonal anti-N Cadherin (NCAD) proximal tubular marker (Thermo Fisher Scientific; 1:200); mouse monoclonal anti-CD133, marker of parietal cells of the Bowman's capsule (Miltenyi Biotec; 1:100); rabbit polyclonal anti-Cleaved Caspase 3, marker of apoptosis (Cell Signaling Technology; 1:300). Sections were subjected to a pre-conditioning treatment for antigen relaxing[25] by incubation in a 0.5% SDS, 50 mM 2-Mercaptoethanol (MERCK, Darmstadt, Germany) modified Laemmli buffer at 95°C for 10 minutes. After appropriate antigen retrieval (10 mM EDTA in Tris-buffer pH8, 8 minutes

at 800 Watt and 20 minutes at 600 Watt, except for Cleaved Caspase 3 that is 20mM Citrate, 20 minutes in the steamer and 20 minutes at room temperature), the slides were incubated with the specific diluted antibodies overnight in humidity chamber at 4°C followed by Alexa Fluor® 594 goat anti rabbit and Alexa Fluor® 680 goat anti mouse secondary antibodies (Molecular Probes). Primary and secondary antibodies were diluted in TBS containing 2% BSA and 10% lactose[27]. Sections were mounted with ProLong Gold Antifade with DAPI (Molecular Probes) for nuclear counterstaining. Immunofluorescence micrographs were obtained at 400x magnification using a Zeiss LSM710 confocal microscope and Zen2009 software (Zeiss) or using the Hamamatsu Nanozoomer S60 scanner (Nikon, Campi Bisenzio, Italia) equipped with NDP.view2 software to acquire images of the entire slices. FFPE sections (2 µm thick) of renal tissue were processed as described above and used as positive controls. In the case of sequential staining, after the first staining the sections were subjected to antibody elution by incubation in a shaking water bath at 56°C for 30 minutes in a 2% SDS, 114 mM 2-Mercaptoethanol, 60 mM Tris-HCl pH 6.8 solution[26].

Statistical analysis

The unpaired two-tail Student's t-test was used to analyze statistical differences and $p < 0.05$ was considered significant.

Results

Kidney decellularization and scaffold characterization

Decellularization of human kidney slices was performed by a four-step protocol obtaining transparent slices of acellular scaffold (Figure 1A). H&E showed eosinophil staining, typical of collagen, and no basophilic nuclear outlines were detected (Figure 1B). Trichrome (Figure 1C) and Alcian/Pas (Figure 1D) staining showed the preservation of collagen and glycosaminoglycans, respectively. Furthermore, the decellularization treatment resulted in the preservation of the renal architecture, with blood vessels (red arrow), glomeruli (blue arrow) and tubular spaces (green arrow) (Figure 1B). The quantification of DNA extracted from 3 samples of native and decellularized kidney tissue was used to assess the decellularization status. There was a significant ($p<0.001$) reduction of DNA content (98.5%) in decellularized scaffolds (11.63 ± 6.80 ng/mg tissue, mean ± SD) with respect to the native kidney (803.3 ± 128.5 ng/mg tissue) (Figure 1E).

Decellularized scaffold composition

The decellularization did not alter the ECM composition. Type IV Collagen, Laminin, and Fibronectin showed the similar patterns in decellularized slices and native kidneys (Figure 2). In the scaffolds, immunohistochemical staining showed a continuous network of Collagen IV and Fibronectin in the tubular and glomerular basement membrane, whilst the Laminin signal seemed to be more intense in the vascular and glomerular basement membrane (Supplemental figure S1A, bottom right panel). Moreover, immunofluorescent staining of the decellularized scaffold showed that Laminin appeared organized in multiple layer in a ring-like pattern in the vascular basement membrane and more concentrated than in tubular basement membrane (Supplemental figure S1B). Quantitative analysis of ECM proteins with ImageJ software after immunofluorescence staining did not demonstrate any significant difference between the decellularized scaffolds and native kidneys (Figure 2).

Scaffold repopulation with nephrosphere cells

50,000 cells obtained after dissociation of NS[21] were seeded on slices of decellularized scaffolds in 24-well poly-Hema coated plates. Poly-Hema was necessary to avoid the attachment of cells to the plastic. After 5 days, no cells were observed in the free area of the well not covered by the scaffold and at this point the medium was completely

changed for the first time. 3D staining of small scaffold portions cultured with basal medium showed at 4, 7, 15 and 30 days the presence of cells able to proliferate and repopulate the decellularized scaffold, demonstrating the non-toxicity of the decellularized matrix and the capability of the NS cells to attach and proliferate into the scaffolds (Figure 3). The largest parts of the scaffolds were processed for histological characterization. H&E staining confirmed the presence of seeded cells at 30 days of culture (Figure 4 A, B, C) in all three different culture media tested. NS cells cultured in basal medium, without any growth factor stimulating a specific differentiation, could attach in different regions of the nephron, such as the tubular, vascular and glomerular spaces. H&E showed the presence of simple cuboidal epithelial-like cells, typical of the renal tubular portion (Figure 4A, left), as well as simple squamous epithelial-like cells lining the Bowman's capsule and the glomerulus (Figure 4A, right). Flat cells, similar to simple squamous epithelial-like cells can be also observed in other portions of the scaffold, in particular located on the big vessel basement membrane (Figure 4A, middle). NS cells cultured in endothelial medium seemed to preferentially attach to the vascular spaces, with the H&E staining showing the presence of simple squamous endothelial-like cells only (Figure 4B). We could not observe neither any cuboidal epithelium nor repopulation of the Bowman's capsule or the glomerulus. H&E staining of

scaffolds in which NS cells were cultured with epithelial medium showed the presence of simple cuboidal epithelial-like cells (Figure 4C, left) located in the tubular spaces and squamous endothelial-like cells (Figure 4C, right) in the big vessels. Ki-67 staining, performed on sections processed after 15, 23, 30 days of culture, proved the proliferative capacity of these cells and we observed a reduction of their proliferative status during the culture with the three different media (Figure 4D and 4E), in particular, at 30 days the reduction of proliferation was significant compared to 15 and 23 days. Moreover, we do not observe a significant increase of apoptosis, evaluated by Cleaved Caspase 3 expression, at different time points and a decline in cell population over time as a consequence (Supplemental figure S2). NS cells cultured with basal medium seemed to have a better proliferation trend, although not significant, with respect to the other culture conditions.

Of note, though starting from tissue specimens derived from patients of different ages, we did not observe any difference in differentiation plasticity based on age of cell and scaffold donors.

Characterization of repopulated scaffolds

To investigate whether NS cells underwent differentiation to phenotypes of specific nephron compartments when seeded in the decellularized scaffolds, we analyzed the expression of

specific differentiation markers at 30 days, the time point that showed a proliferative behavior similar to tubular cells in renal tissue. We studied the expression of CK8.18, known to be expressed by epithelial cells through the whole nephron[28], the proximal tubular marker CD10, the distal tubular marker CK7 and the endothelial marker von Willebrand Factor (vWf). NS cells cultured on the scaffolds with basal medium for 30 days were able to generate proximal and distal tubular structures as well as endothelial-like structures (Figure 5). Tubular structures expressed CK8.18, and, in a mutually exclusive way, proximal CD10 (Figure 5A) or distal CK7 (Figure 5B) and distal E-Cadherin or proximal N-Cadherin (Supplemental figure S3A). As expected, the structures shown in Figure 5A did not present any Ki-67 signal (Figure 5A, left and middle). Endothelial vWf was not detectable in the structures expressing tubular markers (Figure 5A, left and middle). Instead, some of the structures that presented an endothelial-like morphology expressed endothelial vWf, while lacking the expression of CK8.18, CK7 (Figure 5A, right) and CD10 (data not shown). We also wanted to assess whether the structures expressing endothelial mature markers were correctly located in the correct vascular spaces. Exploiting the typical Laminin pattern observed in the vascular basement membrane, which is different respect tubular ECM (Supplemental figures S1A, bottom right panel and S1B), we evidenced that in the repopulated ECM scaffold all the vWf

positive structures were localized in places where the Laminin pattern was concentrated and organized like in the vessels (Supplemental figure S1C).

NS cells cultured in basal medium also attached and proliferated into the glomerular space. These cells expressed the epithelial marker CK8.18 and they also had a weak expression of CD133, known to be expressed on the parietal cells of Bowman's capsule[29] and, though highly debated, indicated as a marker of renal progenitors (Supplemental figure S3B). Of note, CD133 was not expressed by the newly repopulated tubular structures of decellularized renal scaffold (data not shown). The cells that repopulated the glomerular space did not express the endothelial vWf and the podocyte Synaptopodin and Nephrin markers (Supplemental figure S3B). Therefore, NS cells cultured on the scaffold without specific factors added to the medium differentiated towards epithelial lineage, proximal and distal tubular cells, as well as endothelial lineage.

Most of the structures generated by NS cells cultured on the scaffold with endothelial medium did not express epithelial CK8.18 but they did express endothelial vWf (Figure 5B right, top middle, top left). Additionally, we could not observe the co-expression of CK7 or CD10 and vWf on the same structure (Figure 5B, bottom middle, bottom left). This data indicated that endothelial medium could induce NS differentiation mainly towards endothelial lineage, generating

endothelial-like structures (Figure 5B, left, arrowheads), though a few epithelial structures ($CK8.18^{+}/vWf^{-}$) were present (Figure 5B, left, arrows). NS cells cultured on the scaffolds with epithelial medium only generated structures expressing epithelial markers. No expression of vWf was detected while all the structures expressed CK8.18 (Figure 5C, top), even when the cells were localized in a vascular space presenting a squamous endothelial-like morphology (Figure 5C, top right). Moreover, in our studied cases the structures expressed distal CK7 (Figure 5C, bottom), indicating a differentiation towards distal tubular lineage.

We also studied, at different time points, the expression of differentiation markers in presence of basal medium, the culture condition able to induce the different phenotypes. At 15 days all the studied markers were already expressed; interestingly, at 15 and 23 days we observed that in some structures, expressing Ki-67, the cells coexpressed epithelial (CK8.18), endothelial (vWf) and distal tubular markers (CK7, Calbindin-D28k) (Figure 6, top and middle panels). This phenomenon was always absent at 30 days, where the cells in endothelial structures expressing von Willebrand Factor never expressed epithelial CK8.18 and CK7 and vice versa (Figure 6, bottom panels).

Characterization of nephrosphere cells

We investigated whether the cells into the NS had already entered a specific differentiation pathway, which would indicate if they were already committed at the moment of seeding on the scaffold. The expression of renal embryonic, epithelial, proximal and distal tubular, and endothelial markers have been studied. NS cells were positive for renal embryonic marker Pax2, demonstrating the renal origin of sphere cells, as we previously described[21]. These NS cells co-expressed proximal tubular marker N-Cadherin and distal tubular marker E-Cadherin, as shown by the yellow signal (Figure 7A). Instead, these two markers, specific for different tubular portions, were never expressed together in the tubular structures generated by the NS cells when cultured on scaffolds with basal medium (Supplemental figure S3A), mimicking the adult renal tissue and the differentiated tubular primary cell cultures[30-33]. Although, by immunofluorescence on the spheres, most of the cells within the NS expressed the distal marker CK7 (Figure 7A) whilst proximal marker CD10 was almost non-detectable (data not shown), FACS analysis highlighted the co-expression of these two markers in NS cells. In fact, approximately 7% were $CK7^{+}/CD10^{+}$. Moreover, FACS analysis also confirmed the co-expression of other different proximal (CD13) and distal (PROM2) tubular markers: approximately 9% of the cells were $CD13^{+}/PROM2^{+}$. Of note, we could also observe

approximately 40% of $CD13^+/CD10^-$ cells and approximately 5% of $CD13^-/CD10^+$ cells, two phenotypes absent in mature proximal tubular cells that are supposed to co-express both these two proximal markers (Figure 7B). Although 11% of cells were $CD13^+/CD10^+$ (Figure 7B), approximately 75% of them co-expressed also the distal CK7 marker (Supplemental figure S3C). Interestingly, in the whole sphere some cells seemed to co-express both epithelial CK8.18 and endothelial vWf markers, as immunofluorescence on cytospinned cells dissociated from the NS confirmed (Figure 7A, arrows). All this data indicated that cells of different phenotypes were present in the spheres and the cells were not yet committed to a specific differentiation lineage before seeding on decellularized scaffolds.

Discussion

The advancement in stem cell research has contributed to knowledge regarding the possibility of developing and regenerating organs or tissues from a single cell. Significant progress has been made in the production and optimization of decellularization protocols, facilitating the complete removal of resident cells and preservation of ECM complexity to obtain kidney scaffolds. Advantageous sources of decellularized scaffolds can be kidneys of pigs[3, 6, 8-10], of non-human primates[11,12] and cadaveric human kidneys[3] unsuitable for transplantation[13-15]. However, these scaffolds

are yet to be tested for their compatibility for transplantation in humans. One of the challenges is now the identification of the ideal cell types that can be successfully used in a recellularization process in human renal scaffolds. Multipotent human renal stem/progenitor cells, that could potentially be the right candidates for repopulation attempts, have never been tested on decellularized scaffolds. Although it has been reported by lineage tracing experiments that, at least in mice, lineage-restricted progenitors exist[34] in this paper we have shown the capacity of NS cells, that coexpress markers of different lineages, to repopulate different nephron portions of decellularized human renal scaffolds comprising cortex, medulla and papilla. NS cells cultured on scaffolds with basal medium, without specific growth factors, were able to generate proximal and distal tubular structures as well as endothelial-like structures expressing the specific differentiation markers. Furthermore, they were able to attach and proliferate in the peripheral areas of glomerular space but not in the inner glomerular endothelium or epithelium. We directly seeded NS cells on decellularized slices in a static system and the capillary matrix structure inside the glomerulus may represent a physic obstacle for cell integration. The lack of glomerular endothelium can also explain the absence of visceral epithelium in the glomerulus. In fact, it is described[35] that after establishment of the vasculature, endothelial cells appear

responsible of a signaling inducing the final maturation of podocytes.

Although repopulating vascular spaces, NS cells when cultured with epithelial medium were only able to generate epithelia expressing proximal or distal tubular markers but not endothelial markers. On the contrary, NS cells cultured with endothelial medium mainly generated endothelial-like structures that did not express epithelial tubular markers. This data indicated that NS cells were able to respond to differentiation stimuli present in epithelial (EFG and HGF) and endothelial (VEGF) media that, likely, cooperate with the ECM signals amplifying the differentiation stimuli, and inducing only a specific differentiation lineage. Interestingly, when growth factors or external stimuli were not present in the medium (basal medium) NS cells were forced to differentiate, likely, responding to stimuli retained in the ECM that may sustain cellular viability and proliferation. Our findings were in agreement with published observations describing that decellularized scaffolds, in addition to ECM composition, preserve growth factors such as VEGF, HGF, CTGF, PDGF, insulin-like growth factor and TGFβ[5,6,36]. Moreover, the basement membrane and the underlying ECM have also been recently described to provide signals capable of influencing polarization and differentiation of human renal progenitors[37].

One of the critical points in the recellularization process is the reconstitution of the vascular tree that, until now, has been obtained using HUVEC cells[3] or human iPS-derived endothelial cells[6,20]. The recently published paper of Du et al.[20] is of particular interest because it describes the importance of the parenchymal and endothelial cells to be genetically identical for the establishment of the fundamental cell-cell interactions that contribute to the final kidney function. The only other examples of progressive expression of renal lineage markers and endothelial markers have been obtained with murine or human embryonic stem cells in rat or monkey decellularized scaffolds, respectively, although a complete differentiation process was not observed[4,19]. Here, we have described, for the first time, the capability of an adult human renal stem/progenitor-like cell population, obtained from clonal NS of individual subjects[21], to spontaneously differentiate into parenchymal and endothelial cell populations. Another group, using cells from non clonal spheroids obtained from kidney tissue were also able to produce tubular structures on chorioallontoic membrane (CAM), but these cells were not tested on decellularized kidney scaffolds[38]. Of note, in our repopulated scaffolds at 15 and 23 days of culture we can still observe co-expressions of markers of different lineages, typical of undifferentiated status as seen in the NS grown in sphere-forming conditions[21] and in cells before seeding. At 30 days of culture

these coexpressions were no more noted, as in adult renal tissue and this underline the time dependent role of ECM in cell differentiation. In conclusion, the capacity of NS cells to recreate tubular epithelial and endothelial structures in human renal decellularized scaffolds, together with their previously described differentiation capacity in 2D and 3D in vitro cultures, and in vivo under the murine renal capsule[21], make these cells promising for kidney recellularization and regenerative studies. The data obtained here can provide a foundation for experimental investigations focused on the study of parenchymal and endothelial cell-cell interactions in models of whole kidney reconstruction in order to prospectively create completely functional nephrons that are capable of filtration and reabsorption.

Acknowledgments

We thank Andrew Smith and Maureen Quinn for English revision, and Maddalena Bolognesi for technical support with Hamamatsu Nanozoomer S60 scanner.

Figure Legends

Figure 1. Decellularization of human renal tissue slices and preservation of kidney matrix architecture. Photographs of the kidney slices at every step of the decellularization protocol **(A)**. Haematoxylin and eosin staining of a section of human renal tissue before (left) and after (right) decellularization. Red arrow: vessel; blue arrow: glomerulus; green arrow: tubular space **(B)**. Azan Trichrome staining of a section of human renal tissue before (left) and after (right) decellularization **(C)**. Alcian/Pas staining of section of human renal tissue before (left) and after (right) decellularization **(D)**. Original magnification 100X. Scale bars, 200 μm. DNA quantification comparison between native kidney tissue and decellularized scaffolds. Mean ± SD of three independent experiments. *** $p<0.001$ **(E)**.

Figure 2. ECM protein evaluation. Representative immunofluorescence images of Collagen IV, Fibronectin and Laminin (red) in human renal tissue sections before (left) and after (right) decellularization **(A)**. Blue: DAPI. Original magnification: 400x. Quantitative analysis of ECM proteins based on immunofluorescence staining **(B)**. Mean ± SD of three different fields for each sample (three independent experiments).

Figure 3. Three-dimensional staining of scaffolds repopulated with NS cells. Representative images of DAPI (blue) and Falloidin (red) immunofluorescence staining of the scaffolds at 4, 7, 15 and 30 days after seeding NS cells. Chosen Z stack sections (left) and 3D reconstruction (right). Total thickness of the different structures shown at the indicated time points were: 4 days: 70.73 µm; 7 days: 73.5; 15 days: 48 µm; 30 days: 46 µm. Original magnification 400x. Scale bars, 50 µm.

Figure 4. Histological characterization of the scaffold repopulated with NS cells. 10 independent experiments were performed. Representative hematoxylin and eosin staining of scaffold sections 30 days after seeding NS cells in presence of: basal medium **(A)**, endothelial medium **(B)**, epithelial medium **(C)**. Scale bars, 100 µm, except the right panel in **(B)**, that is 50 µm. Inserts: 3x digital magnification respect to the original field. Percentage of immunofluorescent Ki-67 positive nuclei respect to the total number of nuclei stained with DAPI. Section scaffolds evaluated at 15, 23 and 30 days after seeding the NS cells in presence of the indicated media. Mean ± SEM. *$p<0.05$; **$p<0.01$ **(D)**. Representative IF analysis of the FFPE scaffolds repopulated with NS in basal medium at 15, 23 and 30 days with Ki-67 antibody. Scale bars, 100 µm (**E**).

Figure 5. Characterization of the scaffolds repopulated with NS cells in presence of basal **(A)**, endothelial **(B)**, and epithelial medium **(C)** at 30 days. Representative IF analysis of the FFPE scaffolds with the indicated antibodies able to recognise specific tubular or vascular phenotypes. 10 independent experiments were performed. The different antibody combinations are able to identify: in **(A)** proximal tubules (left), distal tubules (middle) and endothelium (right); in **(B)** mostly endothelium (arrowheads) and a few epithelial cells (arrows); in **(C)** distal tubular epithelial cells. Sequential immunostaining has been performed in the representative left and middle panels of **(A)**, right panels of **(B)** and both left and right panels of **(C**). Scale bars, 50 µm, except the left panel in **(B),** that is 100 µm. CK: Cytokeratin; vWf: von Willebrand Factor; Blue:DAPI.

Figure 6. Representative sequential immunofluorescence staining of the FFPE scaffold repopulated with NS in basal medium at 15, 23 and 30 days with the indicated antibodies. Yellow/orange signal in the bottom right panel indicates the coexpression of the distal markers Calbindin-D28k and Cytokeratin 7. Light blue: DAPI. Scale bars: 50 µm.

Figure 7. Immunophenotypical characterization of nephrospheres cultured in sphere-forming conditions. IF analysis of NS with the indicated antibodies **(A)**. For PAX2 panel the DAPI signal is in the insert. The arrows indicate the NS cells that co-express CK8/18 and vWf. Yellow: colocalization of red and green signals of E-Cadherin and N-Cadherin. Blue: DAPI. Results are representative of at least three independent experiments. Original magnification 400x. Scale bars, 50 µm. FACS analysis of NS cells with the indicated antibodies **(B)**. Mean ± SD of positive cells is reported and is referred to at least three independent experiments. CK: Cytokeratin; vWf: von Willebrand Factor; ECAD: E-Cadherin; NCAD: N-Cadherin; PROM2: Prominin2.

Supplemental figure legends

Supplemental figure S1. ECM protein evaluation **(A)**. Representative immunohistochemical images of Collagen IV, Fibronectin and Laminin in human renal tissue sections before (left) and after (right) decellularization. Scale bars, 200 µm. **(B)**. Representative immunofluorescence staining of Laminin on FFPE decellularized kidney scaffold indicating different Laminin pattern in the vascular (arrowhead) and tubular (arrow) basement membrane. **(C).** Representative immunofluorescence analysis of the FFPE repopulated scaffold with the indicated antibodies. Arrowhead in the top

panels indicates the vWf^+ structure also presenting a more intense signal of Laminin while the arrows indicate epithelial structures. Lower panels indicate a big vessel expressing vWf and Laminin in its particular pattern. Scale bar: 100 µm. Insert: 2x digital magnification respect to the original field. Blue: DAPI.

Supplemental figure S2. Representative IF analysis of the FFPE scaffolds repopulated with NS in basal medium at 15, 23 and 30 days with Cleaved Caspase 3 antibody. Scale bars, 100 µm. Inserts: 4x digital magnification respect to the original field. Blue: DAPI. On the bottom right of each panel, percentage of immunofluorescent Cleaved Caspase 3 positive cells respect to the total number of nuclei stained with DAPI. Mean ±SEM.

Supplemental figure S3. (A) E-Cadherin and N-Cadherin expression in the structures generated by NS cells cultured on scaffolds with basal medium Representative images of sequential immunostaining of the same slide with the two antibodies. Blue: DAPI. Scale bars, 50 µm**. (B)** Representative images of sequential immunostaining of the same slide with the indicated antibodies. Blue: DAPI (when present). Scale bars, 50 µm. **(C)** FACS analysis of NS cells with the indicated antibodies. The gate on the dot plot on the left represents $CD10^+/CD13^+$ cells, which are further

analyzed in the dot plot on the right, showing $CK7^+$ cells. Mean ± SD of positive cells is reported and is referred to at least three independent experiments.

Figure 1

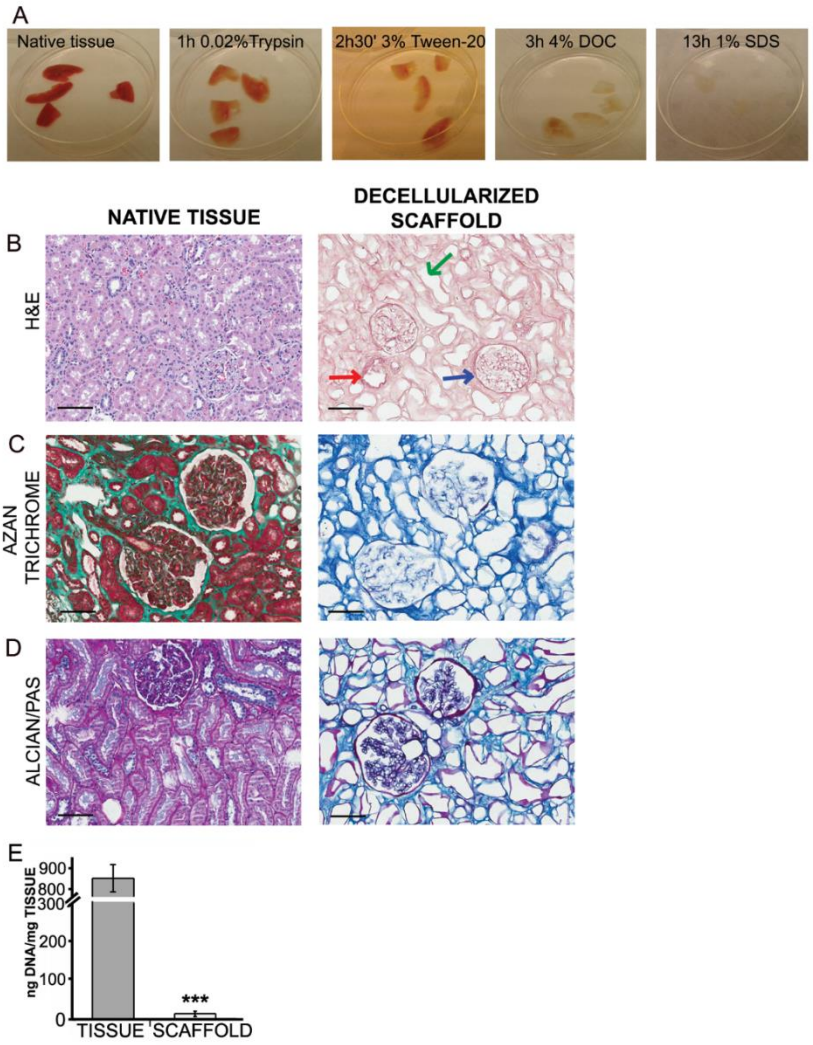
A
Native tissue
1h 0.02%Trypsin
2h30' 3% Tween-20
3h 4% DOC
13h 1% SDS
NATIVE TISSUE
DECELLULARIZED SCAFFOLD
B
H&E
C
AZAN TRICHROME
D
ALCIAN/PAS
E
ng DNA/mg TISSUE
900
800
300
200
100
0
***
TISSUE
SCAFFOLD

Figure 2

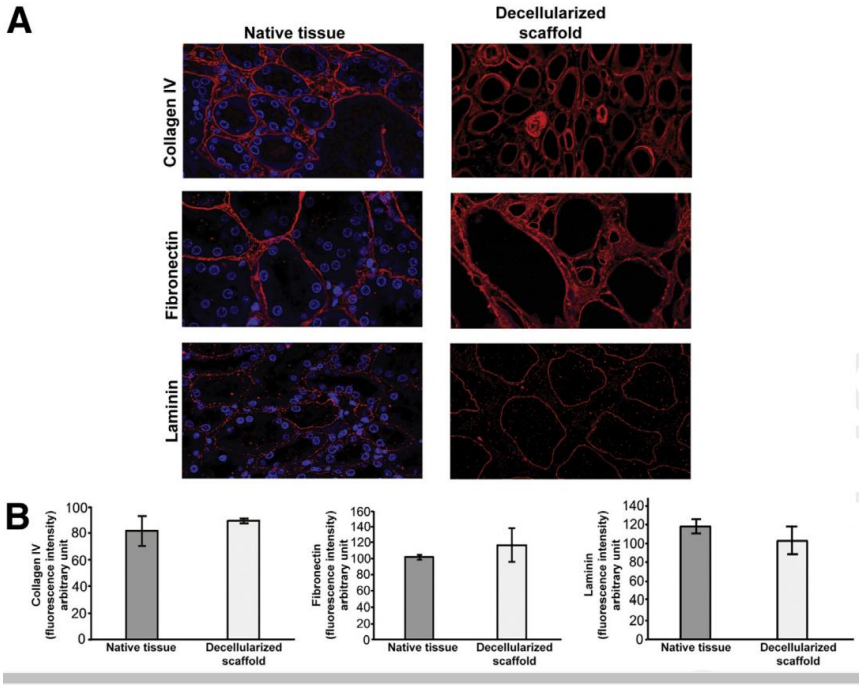
A
Native tissue
Decellularized scaffold
Collagen IV
Fibronectin
Laminin
B
Collagen IV (fluorescence intensity) arbitrary unit
Fibronectin (fluorescence intensity) arbitrary unit
Laminin (fluorescence intensity) arbitrary unit
Native tissue
Decellularized scaffold

Figure 3

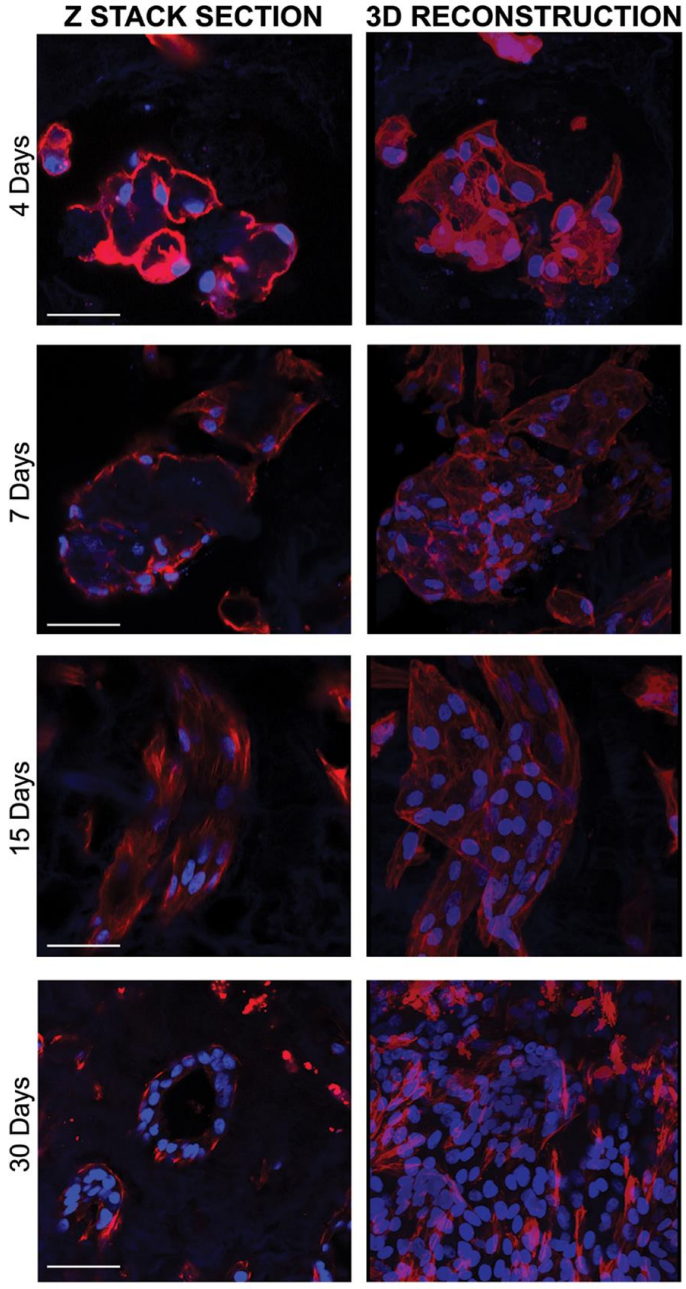
Z STACK SECTION
3D RECONSTRUCTION
4 Days
7 Days
15 Days
30 Days

Figure 4

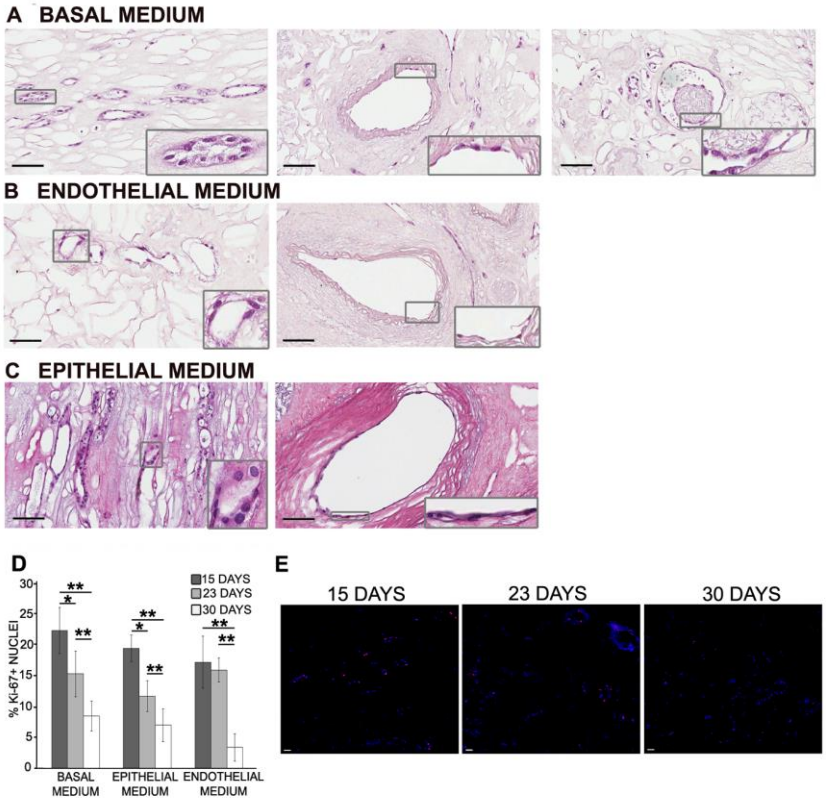
A BASAL MEDIUM
B ENDOTHELIAL MEDIUM
C EPITHELIAL MEDIUM
D
% KI-67+ NUCLEI
15 DAYS
23 DAYS
30 DAYS
BASAL MEDIUM
EPITHELIAL MEDIUM
ENDOTHELIAL MEDIUM
E
15 DAYS
23 DAYS
30 DAYS

Figure 5

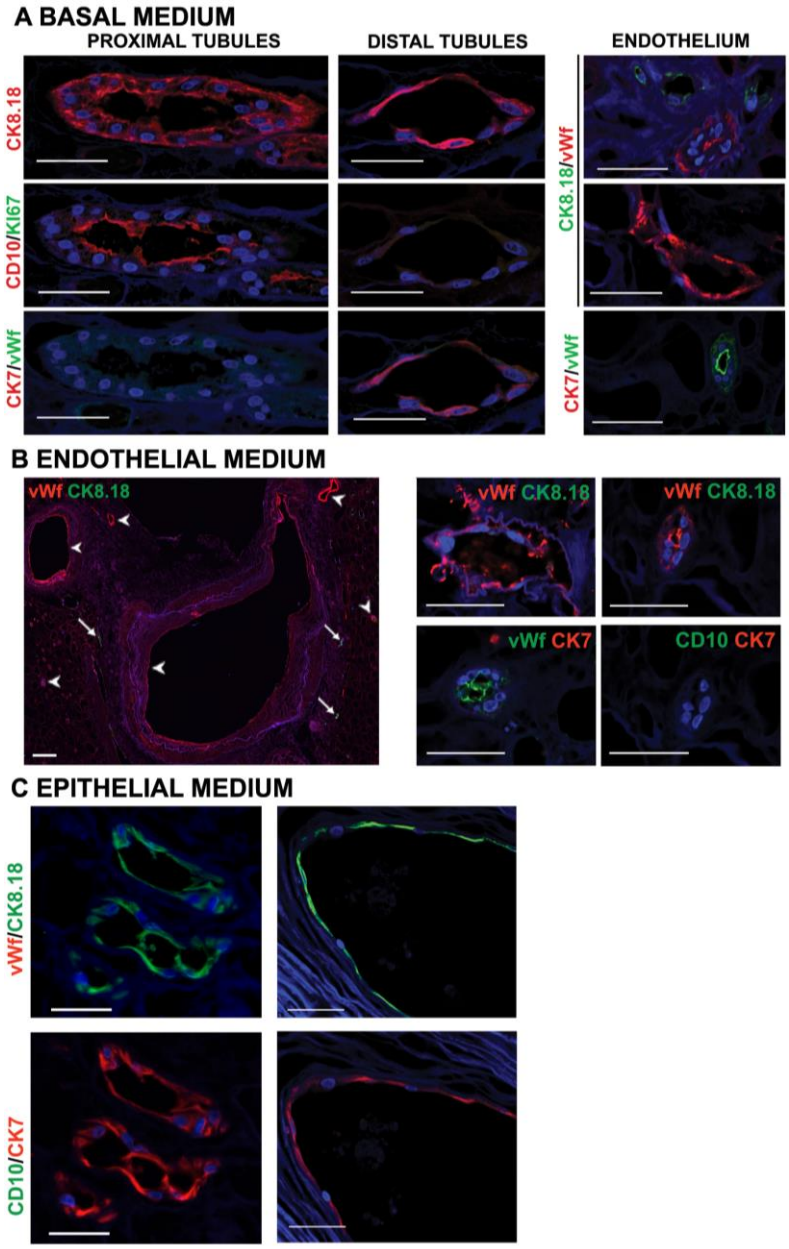
A BASAL MEDIUM
PROXIMAL TUBULES
DISTAL TUBULES
ENDOTHELIUM
CK8.18
CD10/KI67
CK7/vWf
CK8.18/vWf
CK7/vWf
B ENDOTHELIAL MEDIUM
vWf CK8.18
vWf CK8.18
vWf CK8.18
vWf CK7
CD10 CK7
C EPITHELIAL MEDIUM
vWf/CK8.18
CD10/CK7

Figure 6

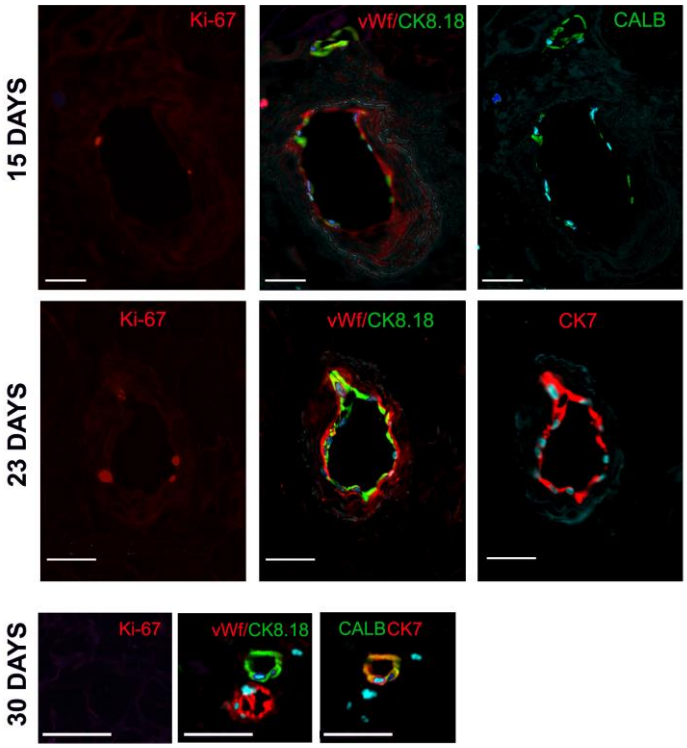
15 DAYS
Ki-67
vWf/CK8.18
CALB
23 DAYS
Ki-67
vWf/CK8.18
CK7
30 DAYS
Ki-67
vWf/CK8.18
CALBCK7

Figure 7

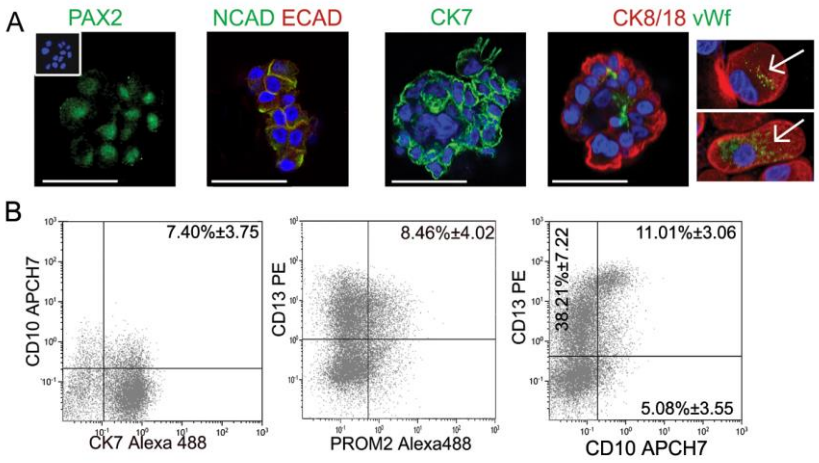
A
PAX2
NCAD ECAD
CK7
CK8/18 vWf
B
7.40%±3.75
CD10 APCH7
CK7 Alexa 488
8.46%±4.02
CD13 PE
PROM2 Alexa488
11.01%±3.06
38.21%±7.22
5.08%±3.55
CD13 PE
CD10 APCH7

Supplemental figure S1

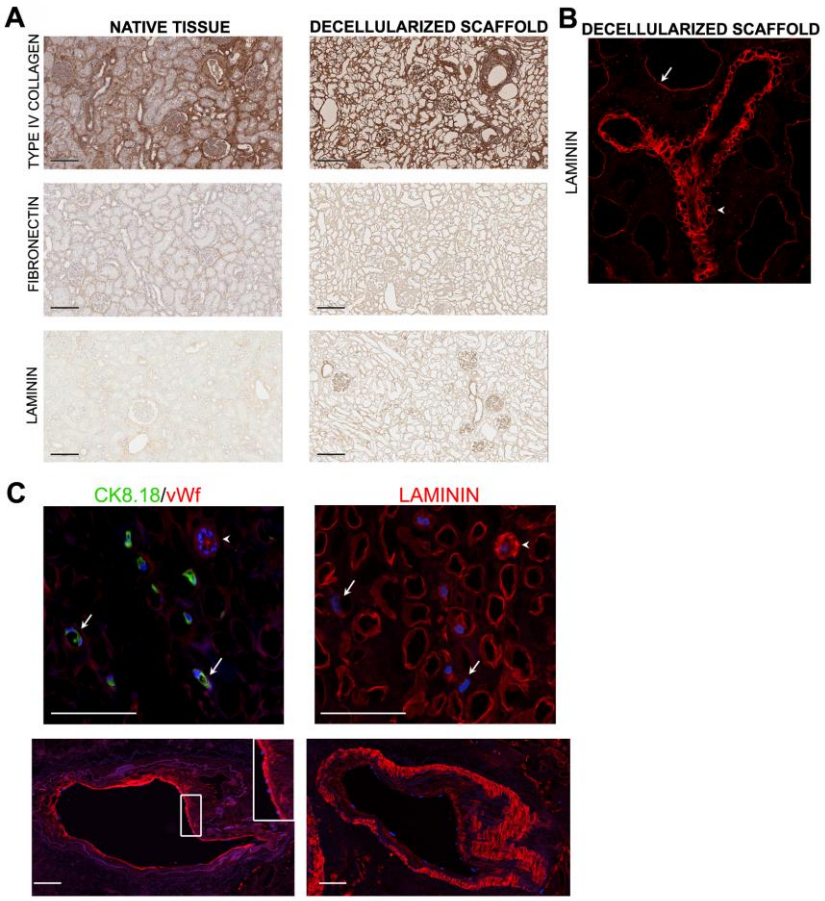

Supplemental figure S2

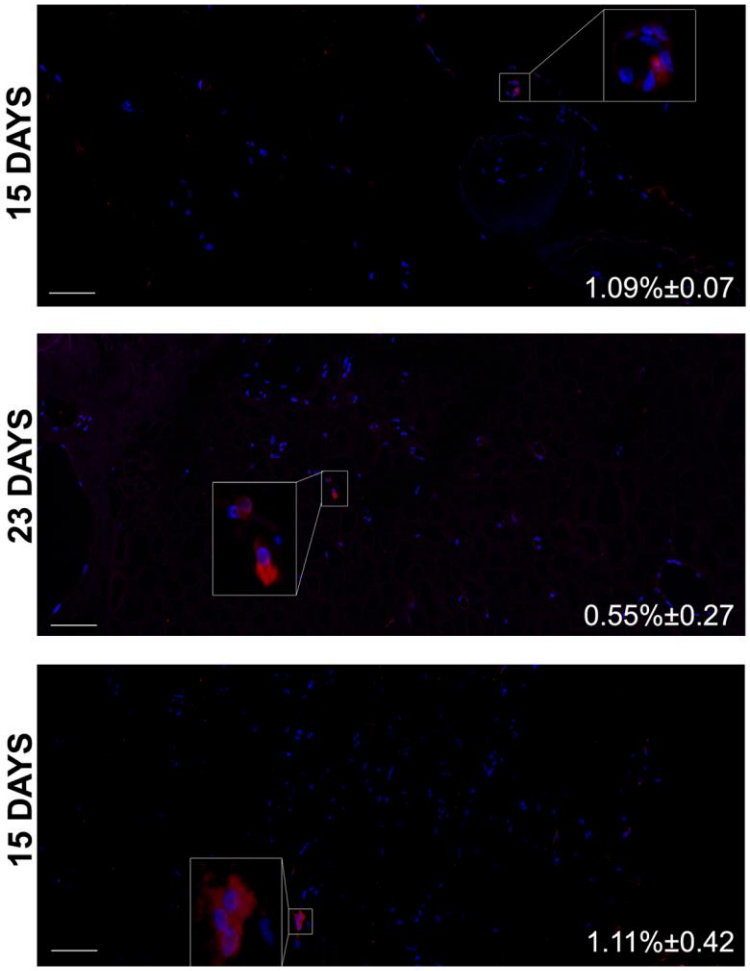

Supplemental figure S3

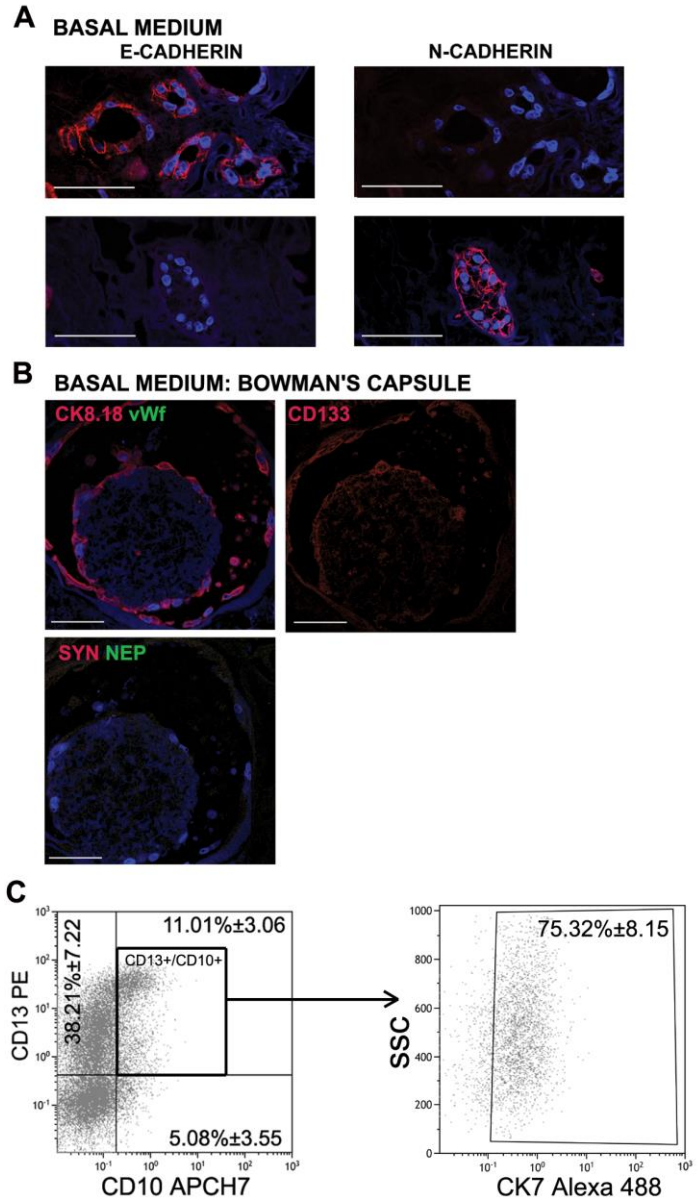

References

1. Jha V, Garcia-Garcia G, Iseki K, Li Z, Naicker S, Plattner B, Saran R, Wang AY, Yang CW: Chronic kidney disease: global dimension and perspectives. Lancet 2013, 382: 260-272.
2. Bussolati B, Camussi G: Therapeutic use of human renal progenitor cells for kidney regeneration. Nat Rev Nephrol 2015, 11: 695-706
3. Song JJ, Guyette JP, Gilpin SE, Gonzalez G, Vacanti JP, Ott HC: Regeneration and experimental orthotopic transplantation of a bioengineered kidney. Nat Med 2013, 19: 646-651
4. Bonandrini B, Figliuzzi M, Papadimou E, Morigi M, Perico N, Casiraghi F, Sangalli F, Conti S, Benigni A, Remuzzi A, Remuzzi G: Recellularization of well-preserved acellular kidney scaffold using embryonic stem cells. Tissue Eng Part A 2014, 20: 1486-1498
5. Peloso A, Ferrario J, Maiga B, Benzoni I, Bianco C, Citro A, Currao M, Malara A, Gaspari A, Balduini A, Abelli M, Piemonti L, Dionigi P, Orlando G, Maestri M: Creation and implantation of acellular rat renal ECM-based scaffolds. Organogenesis 2015, 11: 58-74
6. Caralt M, Uzarski JS, Iacob S, Obergfell KP, Berg N, Bijonowski BM, Kiefer KM, Ward HH, Wandinger-Ness A, Miller WM, Zhang ZJ, Abecassis MM, Wertheim JA: Optimization and critical evaluation of decellularization

strategies to develop renal extracellular matrix scaffolds as biological templates for organ engineering and transplantation. Am J Transplant 2015, 15: 64-75

7. O'Neill JD, Freytes DO, Anandappa AJ, Oliver JA, Vunjak-Novakovic GV: The regulation of growth and metabolism of kidney stem cells with regional specificity using extracellular matrix derived from kidney. Biomaterials 2013, 34: 9830-9841
8. Orlando G, Farney AC, Iskandar SS, Mirmalek-Sani SH, Sullivan DC, Moran E, AbouShwareb T, De Coppi P, Wood KJ, Stratta RJ, Atala A, Yoo JJ, Soker S: Production and implantation of renal extracellular matrix scaffolds from porcine kidneys as a platform for renal bioengineering investigations. Ann Surg 2012, 256: 363-370
9. Wang Y, Bao J, Wu Q, Zhou Y, Li Y, Wu X, Shi Y, Li L, Bu H: Method for perfusion decellularization of porcine whole liver and kidney for use as a scaffold for clinical-scale bioengineering engrafts. Xenotransplantation 2015, 22: 48-61
10. Sullivan DC, Mirmalek-Sani SH, Deegan DB, Baptista PM, Aboushwareb T, Atala A, Yoo JJ: Decellularization methods of porcine kidneys for whole organ engineering using a high-throughput system. Biomaterials 2012, 33: 7756-7764
11. Nakayama KH, Batchelder CA, Lee CI, Tarantal AF: Decellularized rhesus monkey kidney as a three-

dimensional scaffold for renal tissue engineering. Tissue Eng Part A 2010, 16: 2207-2216

12. Nakayama KH, Batchelder CA, Lee CI, Tarantal AF: Renal tissue engineering with decellularized rhesus monkey kidneys: age-related differences. Tissue Eng Part A 2011, 17: 2891-2901

13. Orlando G, Booth C, Wang Z, Totonelli G, Ross CL, Moran E, Salvatori M, Maghsoudlou P, Turmaine M, Delario G, Al-Shraideh Y, Farooq U, Farney AC, Rogers J, Iskandar SS, Burns A, Marini FC, De Coppi P, Stratta RJ, Soker S: Discarded human kidneys as a source of ECM scaffold for kidney regeneration technologies. Biomaterials 2013, 34: 5915-5925

14. Peloso A, Petrosyan A, Da Sacco S, Booth C, Zambon JP, O'Brien T, Aardema C, Robertson J, De Filippo RE, Soker S, Stratta RJ, Perin L, Orlando G: Renal Extracellular Matrix Scaffolds From Discarded Kidneys Maintain Glomerular Morphometry and Vascular Resilience and Retains Critical Growth Factors. Transplantation 2015, 99: 1807-1816

15. Katari R, Peloso A, Zambon JP, Soker S, Stratta RJ, Atala A, Orlando G: Renal bioengineering with scaffolds generated from human kidneys. Nephron Exp Nephrol 2014, 126: 119

16. Ross EA, Williams MJ, Hamazaki T, Terada N, Clapp WL, Adin C, Ellison GW, Jorgensen M, Batich CD:

Embryonic stem cells proliferate and differentiate when seeded into kidney scaffolds.
J Am Soc Nephrol 2009, 20: 2338-2347

17. Ross EA, Abrahamson DR, St John P, Clapp WL, Williams MJ, Terada N, Hamazaki T, Ellison GW, Batich CD: Mouse stem cells seeded into decellularized rat kidney scaffolds endothelialize and remodel basement membranes. Organogenesis 2012, 8: 49-55

18. Guan Y, Liu S, Sun C, Cheng G, Kong F, Luan Y, Xie X, Zhao S, Zhang D, Wang J, Li K, Liu Y: The effective bioengineering method of implantation decellularized renal extracellular matrix scaffolds. Oncotarget 2015, 6: 36126-36138

19. Batchelder CA, Martinez ML, Tarantal AF Natural scaffolds for renal differentiation of human embryonic stem cells for kidney tissue engineering. PLoS One 2015, 10: e0143849

20. Du C, Narayanan K, Leong MF, Ibrahim MS, Chua YP, Khoo VMH, Wan ACA: Functional kidney bioengineering with pluripotent stem-cell-dervived renal progenitor cells and decellularized kidney scaffolds. Adv Healthcare Mater 2016, 5: 2080-2091

21. Bombelli S, Zipeto MA, Torsello B, Bovo G, Di Stefano V, Bugarin C, Zordan P, Viganò P, Cattoretti G, Strada G, Bianchi C, Perego RA: PKH^{high} cells within clonal human

nephrospheres provide a purified adult renal stem cell population. Stem Cell Res 2013, 11: 1163-1177

22. Bianchi C, Bombelli S, Raimondo F, Torsello B, Angeloni V, Ferrero S, Di Stefano V, Chinello C, Cifola I, Invernizzi L, Brambilla P, Magni F, Pitto M, Zanetti G, Mocarelli P, Perego RA: Primary cell cultures from human renal cortex and renal-cell carcinoma evidence a differential expression of two spliced isoforms of Annexin A3. Am J Pathol 2010, 176: 1660-1670

23. Di Stefano V, Torsello B, Bianchi C, Cifola I, Mangano E, Bovo G, Cassina V, De Marco S, Corti R, Meregalli C, Bombelli S, Viganò P, Battaglia C, Strada G, Perego RA: Major Action of Endogenous Lysyl Oxidase in Clear Cell Renal Cell Carcinoma Progression and Collagen Stiffness Revealed by Primary Cell Cultures. Am J Pathol 2016, 186: 2473-85

24. Bacci S, Pieri L, Buccoliero AM, Bonelli A, Taddei G, Romagnoli P: Smooth muscle cells, dendritic cells and mast cells are sources of TNFalpha and nitric oxide in human carotid artery atherosclerosis. Thromb Res 2008, 122: 657-667

25. Scalia CR, Gendusa R, Cattoretti G: A 2-Step Laemmli and Antigen Retrieval Method Improves Immunodetection. Appl Immunohistochem Mol Morphol 2016, 24: 436-446

26. Gendusa R, Scalia CR, Buscone S, Cattoretti G: Elution of High-affinity (>10-9 KD) Antibodies from Tissue

Sections: Clues to the Molecular Mechanism and Use in Sequential Immunostaining. J Histochem Cytochem 2014, 62: 519-531

27. Boi G, Scalia CR, Gendusa R, Ronchi S, Cattoretti G: Disaccharides Protect Antigens from Drying-Induced Damage in Routinely Processed Tissue Sections. J Histochem Cytochem 2016, 64: 18-31

28. Skinnider BF, Folpe AL, Hennigar RA, Lim SD, Cohen C, Tamboli P, Young A, de Peralta-Venturina M, Amin MB: Distribution of cytokeratins and vimentin in adult renal neoplasms and normal renal tissue: potential utility of a cytokeratin antibody panel in the differential diagnosis of renal tumors. Am J Surg Pathol 2005, 29: 747-754

29. Sagrinati C, Netti GS, Mazzinghi B, Lazzeri E, Liotta F, Frosali F, Ronconi E, Meini C, Gacci M, Squecco R, Carini M, Gesualdo L, Francini F, Maggi E, Annunziato F, Lasagni L, Serio M, Romagnani S, Romagnani P: Isolation and characterization of multipotent progenitor cells from the Bowman's capsule of adult human kidneys. J Am Soc Nephrol 2006, 17: 2443-56

30. Nouwen EJ, Dauwe S, van der Biest I, De Broe ME: Stage- and segment-specific expression of cell-adhesion molecules N-CAM, A-CAM, and L-CAM in the kidney. Kidney Int 1993, 44, 147-158

31. Prozialeck WC, Lamar PC, Appelt DM: Differential expression of E-cadherin, N-cadherin and beta-catenin in

proximal and distal segments of the rat nephron. BMC Physiol 2004, 4: 10

32. Keller C, Kroening S, Zuehlke J, Kunath F, Krueger B, Goppelt-Struebe M: Distinct mesenchymal alterations in N-cadherin and E-cadherin positive primary renal epithelial cells. PLoS One 2012, 7: e43584

33. Torsello B, Bianchi C, Meregalli C, Di Stefano V, Invernizzi L, Bovo G, Brivio R, Strada G, Bombelli S, Perego RA: Arg tyrosine kinase modulates TGF-β1 production in human renal tubular cells under high glucose conditions. J Cell Sci 2016, 29: 2925-2936

34. Rinkevich Y, Montoro DT, Contreras-Trujillo H, Harari-Steinberg O, Newman AM, Tsai JM, Lim X, Van-Amerongen R, Bowman A, Januszyk M, Pleniceanu O, Nusse R, Longaker MT, Weissman IL, Dekel B: In vivo clonal analysis reveals lineage-restricted progenitor characteristics in mammalian kidney development, maintenance, and regeneration. Cell Rep 2014, 7: 1270-1283

35. Pavenstädt H, Kriz W, Kretzler M: Cell biology of the glomerular podocyte. Physiol Rev 2003, 83: 253-307.

36. Yu YL, Shao YK, Ding YQ, Lin KZ, Chen B, Zhang HZ, Zhao LN, Wang ZB, Zhang JS, Tang ML, Mei J: Decellularized kidney scaffold-mediated renal regeneration. Biomaterials 2014, 35: 6822-6828

37. Sciancalepore AG, Portone A, Moffa M, Persano L, De Luca M, Paiano A, Sallustio F, Schena FP, Bucci C, Pisignano D: Micropatterning control of tubular commitment in human adult renal stem cells. Biomaterials 2016, 94: 57-69

38. Buzhor E, Harari-Steinberg O, Omer D, Metsuyanim S, Jacob-Hirsch J, Noiman T, Dotan Z, Goldstein RS, Dekel B: Kidney spheroids recapitulate tubular organoids leading to enhanced tubulogenic potency of human kidney-derived cells. Tissue Eng Part A 2011, 17: 2305-19

Chapter 3

Study Of Multipotent Renal Pkh^{high} Stem-Like Cells, Isolated From Human Nephrospheres: Regenerative Abilities And Transcriptomic Profile

Chiara Meregalli[1] et al.

[1]School of Medicine and Surgery, Milano-Bicocca University, Via Cadore 48, 20900 Monza, Italy

Manuscript in peparation

Abstract

The mechanism underlying the recovery of renal cell injury is still a matter of debate that concerns the involvement of fully differentiated cells, or the existence of quiescent scattered multipotent stem cells. By sphere forming assay and sorting, our group isolated a population of PKH26 most fluorescent cells with characteristics of adult renal stem-like cells (PKH^{high} cells). We previously assessed the ability of PKH^{high} cells to differentiate in vitro along epithelial, podocytic and endothelial lineages. We also demonstrated that PKH^{high} population is heterogeneous in composition and within nephrospheres the cells with stem capacities are $PKH^{high}/CD133^{+}/CD24^{-}$ (RSC).

We recently published that our nephrosphere cells, comprising PKH^{high} cells and their $PKH^{low/neg}$ progeny, are able to repopulate human decellularized renal scaffolds.

With this research, we now aim:

I) to prove the regenerative capabilities of PKH^{high} stem-like cells, even in absence of their $PKH^{low/neg}$ progeny.

II) to find the molecular signature of RSC that among PKH^{high} cells are those with the wider stem capacities.

To reach these aims, we cultured isolated PKH^{high} cells on acellular scaffolds for 30 days and the cells of the repopulated structures were characterized by sequential immunofluorescence using specific markers of differentiation. Some structures indicated a specific lineage

differentiation into proximal and distal tubular epithelium and endothelium. Only few structures coexpressed some or all markers tested, indicating still immature phenotypes.

For the disclosure of RSC molecular signature, transcriptomic analysis of RSC, of their $PKH^{low/neg}$ progeny and of terminally differentiated primary cell cultures (PCC) was performed and differentially expressed genes (DEG) were evidenced. Bioinformatic Gene Set Enrichment Analysis suggested a renal immature status of our RSC, but different from embryonic stem cells. Crossing DEG lists potential markers were obtained and some of them were selected and validated.

In conclusion, we highlighted the proximal and distal tubular epithelial and endothelial differentiative and regenerative abilities of PKH^{high} cells. Moreover, we showed that PKH^{high} cells, completely lacking any endothelial marker, were able to give rise to endothelial-like structures. The occasional coexpression of epithelial and endothelial markers in repopulated structures may indicate a transitional early status toward cell differentiation. The eventual role of the $PKH^{low/neg}$ progeny of PKH^{high} cells in speeding up the complete PKH^{high} differentiation will be clarified.

Finally, the obtained RSC signature would open the possibility for the direct isolation of adult renal stem-like cells from normal kidney tissue.

Introduction

Chronic kidney disease is one of the leading causes of mortality and morbidity, estimated to affect approximately 10% of adult population in Europe (Jager, ERA-EDTA, 2016), and therefore considered a global public health problem. It can progress toward end-stage renal disease, with the unavoidable outcome of dialysis and renal transplantation.

Currently, the evident shortage of transplantable kidneys has driven researches towards bioengineering strategies for renal tissue regeneration, since there is a serious need to overcome these issues.

In recent years, tissue engineering research focused its attention on scaffolds of natural extracellular matrix (ECM), obtained by removing cellular components from the native organs by a decellularization process (Yamanaka and Yokoo, 2015; Poornejad, 2016).

Many attempts of renal decellularization and recellularization have been performed in different species and with different cell types (Ross, 2009; Bonandrini, 2014; Caralt, 2015; Peloso, 2015; Sullivan, 2012; Orlando, 2012; Nakayama, 2010; Song, 2013; Orlando, 2013; Katari, 2014; Du, 2106). An attractive cell type for recellularization seems to be represented by adult renal stem cells, which could play a direct role in the regeneration. This last point poses the problem a univocal definition of a population of adult renal

stem-like cells that is still lacking (Bussolati and Camussi, 2015), due to the absence of unique markers.

Our group identified and demonstrated the ability of PKH^{high} human renal stem-like cells, obtained from clonal nephrospheres (NS), to self-renew and differentiate in 2D culture in tubular and podocytic lineages as well as in endothelial cells (Bombelli, 2013). We also know that the 70% of PKH^{high} cells have $PKH^{high}/CD133^{+}/CD24^{-}$ phenotype that is associated with the *in vitro* self-renewal and mulipotecy capacity toward proximal and distal tubular, podocytic and endothelial lineages. These cells were defined as renal stem-like cell (RSC) population (Bombelli, 2013). Recently, we showed, for the first time, that nephrosphere cell population is able to give rise to tubular and endothelial structures, when cultured on acellular human renal matrix (Bombelli, 2017). Based on these premises, we now aim to demonstrate that PKH^{high} cells alone are able to give rise to both lineages of differentiation.

We also aim to find the molecular signature of $PKH^{high}/CD133^{+}/CD24^{-}$ subpopulation to better understand what phenotype may be hidden behind the PKH^{high} status and to find out possible additional markers. This could allow the identification and the direct isolation from normal kidney tissue of adult renal stem-like cells.

Materials and Methods

Tissues

Normal kidney tissues were obtained from patients undergone nephrectomy because of renal tumours. The normal tissue derived from a healthy region of the kidney, opposite to the tumour and exceeding the diagnostic request. Nephrosphere (NS) cultures were established from fresh renal tissue samples.

Frozen pieces of renal tissue, comprising cortex, medulla, and papilla, were stored at -80°C until use.

Nephrosphere cultures

Single cell suspension from renal tissue was obtained from tissue samples as previously described (Bombelli, 2013). After mechanical dissociation and enzymatic digestion, the suspension was forced through a 250 µm cell strainer and then passed through a pipette syringe to obtain a single cell suspension. Red blood cells were removed by hemolysis with 0.8% NH4Cl solution for 5 minutes 4°C. Bulk epithelial cells passed through an adhesion step in Stem Cell (SC) medium containing DMEM-F12 (Lonza), supplemented with B27 (Invitrogen), ITS supplement (5 µg/ml Insulin, 5 µg/ml Transferrin, 5 ng/ml sodium selenite), 36 ng/ml Hydrocortisone, 40 pg/ml Triiodothyronine (all from Sigma Aldrich), 20 ng/ml EGF, 20 ng/ml bFGF (Cell Signalling). The adherence passage permitted the loss of hematopoietic cells

and fibroblasts (Pece, 2010) and thus the selection of the bulk epithelial population. Trypsinized cells were stained with PKH26 lipophilic dye (Sigma Aldrich) according to the manufacturer's instruction and plated (10,000 cells/mL) in Stem Cell medium on poly-Hema (Sigma Aldrich), coated dishes in non-adherent conditions. After 10 to 12 days NS were collected and dissociated enzymatically for 5 minutes 37°C in TrypLE Express (Life Technologies) and then mechanically by repetitive pipette syringing for FACS sorting or propagation of culture. Renal differentiated primary cell cultures were used as control and were obtained as described (Bianchi, 2010).

Decellularization

Scaffold decellularization was performed as previously described (Bombelli, 2017). Frozen renal tissues were cut into approximately 2 mm thick slices maintaining all kidney regions. Slices were washed with 2x PBS supplemented with penicillin and streptomicin (P/S) for 15 minutes, followed by one hour of 0.02% Trypsin, two hours of 2% Tween-20, three hours of 4% sodium deoxycholate, and 1% SDS (all from Euroclone) overnight treatment. Following each step, slices were washed with 2x PBS for 15 minutes. Every step was performed under agitation. At the end, slices were washed with 2x PBS containing P/S for four hours and then with 1x PBS containing P/S for other four hours.

FACS analysis and cell sorting

FACS analysis was performed on primary and secondary nephrospheres using MoFLO Astrios cell sorter and Kaluza 1.3 software (both from Beckman Coulter). FACS staining was performed as described (Di Stefano, 2016). Acquisition was stopped when 20,000 events were collected in the population gate. Cell sorting was performed on single dissociated nephrosphere cells or single cells obtained after tissue dissociation. An average of sorting rate of 1000-1500 events per second at a sorting pressure of 60 psi with a 70 µm nozzle was maintained. For the sorting on single cells after kidney tissue dissociation, the following gating strategy was adopted. Using PI as a vitality marker, dead cells were gated out. Among live cells, the residual $CD45^+$ hematopoietic cells, and $CD31^+$ endothelial cells were excluded. On a CD133 versus CD24 plot, the four studied populations were sorted.

The following primary antibodies were used: rabbit monoclonal anti-Cytokeratin 7 (clone EPR1619Y, Abcam; 1:20), mouse monoclonal PE-conjugated anti-CD13 (clone WM15, Biolegend; 1:10), mouse monoclonal APCH7-conjugated anti-CD10 (clone HI10a, Becton Dickinson; 1:20), mouse monoclonal APC-conjugated anti-CD133/1 (clone AC133, Miltenyi Biotec; 1:5), mouse monoclonal FITC-conjugated anti-CD24 (clone ML5, Biolegend; 1:20), mouse

monoclonal PerCP-eFluor™ 710-conjugated anti-CD24 (clone SN3 A5-2H10, eBioecence™; 1:20), mouse monoclonal FITC-conjugated CD31 (clone WM-59, Invitrogen 1:20), mouse monoclonal PE-conjugated CD45 (clone HI30, eBioecence™; 1:20), mouse monoclonal anti-CA125 (clone M11, DAKO; 1:100). When needed, secondary antibodies anti rabbit Alexa Fluor® 488 and anti mouse Alexa Fluor® 680 (both Molecular Probes; 1:100) were used.

Immunofluorescence on cells after cytospin

10,000 PKH sorted cells or dissociated secondary nephrospheres or cells sorted from tissues were cytospinned for 15 min 800g. Immunofluorescence staining was performed as previously described (Bianchi, 2010).

The primary antibodies used are the following: mouse monoclonal anti-Cytokeratin 8.18 (clone 5D3, Thermo Fisher Scientific; 1:50), rabbit polyclonal anti-von Willebrand factor (DAKO; 1:2000); rabbit polyclonal anti-IRF8 (Sigma Aldrich; 1:100); rabbit polyclonal anti-fibrillin2 (FBN2) (Sigma Aldrich; 1:5); mouse monoclonal anti-CA125 (clone M11, DAKO; 1:100); mouse monoclonal anti-CD133/1 (clone AC133, Miltenyi Biotec; 1:5). As secondary antibodies anti mouse Alexa Fluor®488, anti rabbit Alexa Fluor®594, anti rabbit Alexa Fluor®488, Anti mouse Alexa Fluor®680 (molecular Probes, 1:100) were used. Slides were mounted with

ProLong Gold Antifade with DAPI (Molecular Probes) for nuclear counterstaining.
Immunofluorescence images were obtained at 400x or 630x magnification using a Zeiss LSM710 confocal microscope and Zen2009 software (Zeiss).

PKH^{high} cell culture on decellularized scaffolds

15,000 alive PKH^{high} cells obtained from FACS sorting of NS were seeded on decellularized renal scaffolds and cultured with basal medium containing DMEM low glucose supplemented with 10% FBS, 1% L-glutammine, 1% P/S, 1% amphotericin (all from Euroclone) in 96-well poly-Hema coated plates. The cells were allowed to attach to the ECM scaffold for five days only adding medium, then medium was changed regularly every week.
The culture was stopped at 30 days and sections were formalin-fixed for at least 16 hours and paraffin embedded for histological analysis.

Histologic characterization

The cultured decellularized scaffolds were FFPE, sectioned (2 μm thick), and H&E-stained for cellular repopulation assessment and evaluation of morphological features of the formed structures.
Sequential immunofluorescence stainings were performed as described (Scalia, 2016 and Gendusa, 2014) on FFPE

sections using the following antibodies: monoclonal mouse anti-aquaporin1 (AQP1), proximal tubular marker (clone B11, Santa Cruz; 1:50); rabbit monoclonal anti-Cytokeratin 7 (CK7), distal tubular marker (clone EPR1619Y, Abcam; 1:200); rabbit polyclonal anti-CD13, proximal tubular marker (Santa Cruz; 1:50); mouse monoclonal anti-Cytokeratin 8.18 (CK 8.18), epithelial generical marker (clone 5D3, Thermo Fisher Scientific; 1:50); rabbit polyclonal anti von Willebrand factor (vWf) endothelial marker (DAKO; 1:2000);

Sections were subjected to a pre-conditioning treatment for antigen relaxing by incubation in a 0.5% SDS, 50 mM 2-Mercaptoethanol (MERCK) modified Laemmli buffer at 95 °C for 10 minutes. After antigen retrieval with 10 mM EDTA in Trisbuffer pH8, 8 minutes at 800 Watt and 20 minutes at 600 Watt, slides were incubated with the primary antibodies overnight in humidity chamber at 4 °C followed by anti rabbit Alexa Fluor® 594 and anti mouse Alexa Fluor® 680 secondary antibodies (Molecular Probes). Primary and secondary antibodies were diluted in TBS containing 2% BSA and 10% lactose. Sections were mounted with DAPI 5,45µM in glycerol 60%, PBS pH7.5 supplemented with sucrose 6M (Bolognesi, 2017) for nuclear counterstaining.

Whole section images were acquired using the Hamamatsu Nanozoomer S60 scanner (Nikon) equipped with NDP.view2 software. FFPE sections (2 µm thick) of native renal tissue were processed as described above and used as positive

controls. For sequential staining, after the first staining the sections were subjected to antibody elution by incubation in a shaking water bath at 56 °C for 30 minutes in a 2% SDS, 114 mM 2-Mercaptoethanol, 60 mM Tris-HCl pH6.8 solution (Gendusa, 2014).

Transcriptomic and bioinformatic analysis

RNA was extracted by Arcturus® PicoPure® RNA Isolation kit (Life Technologies) according to the manifacturer's instructions from sorted $PKH^{high}/CD133^{+}/CD24^{-}$ RSC, $PKH^{low/neg}$ progenitors and from primary cultures as a control. In collaboration with the Integrative Biology Unit of INGM, we performed a transcriptomic analysis (Illumina HumanHT-12 v4 Expression BeadChip) by comparing RSC with their progenitors (LN) and with terminally differentiated renal tubular primary cell cultures (PCC). Lists of differentially expressed genes (DEG) between cell types were obtained by t-test, considering a pval ≤ 0.05 and a fold change (FC) ≥ 1.5. Only the common DEG genes between the two comparisons are considered for futher analysis for the choice of marker.

Statistical analysis between our data and gene sets available online and in literature was performed through Gene Set Enrichment Analysis tool (GSEA Broad Institute). GSEA is a statistical methodology evaluating whether a given gene set is significantly enriched in a list of gene markers (in our case RSC gene marker list). Our markers are ranked by their

correlation with the phenotype of interest. The software calculates an enrichment score (ES) for the ranked gene list, increasing the value if the marker is present in the compared gene set, while decreasing it, if the marker is not in the gene set used. The metric used for the analysis is the log2 Ratio of Classes, with 1,000 gene set permutations for significance testing.

As gene sets to compare we chose:

-BENPORATH_ES_1 (M1871) for embryonic stem cells (from Ben-Porath, 2008),

-PECE_MAMMARY_STEM_CELL_UP (M2534) for adult human mammary stem cells (from Pece, 2010),

-LIM_MAMMARY_STEM_CELL_UP (M2573) for adult human and mouse mammary stem cells (from Lim, 2010),

-for adult renal progenitors Sallustio, 2010,

-SYSTEM_DEVELOPMENT (M11617),

-GO_WNT_SIGNALING_PATHWAY (M11722),

-REACTOME_CELL_CYCLE (M543)

- c5.all.v6.0symbols (comprising molecular function (MF), cellular component (CC) or biological process (BP) terms for unbiased analysis, which allows to give a general insight into the analysis without specifically address it.

For all analysis we used 1000 as number of permutations and Signal2Noise as metric for ranking genes. We considered significant only results with at lest a p-value ≤ 0.05.

Statistical analysis

The unpaired two-tail Student's t-test was used to analyze statistical differences and $p < 0.05$ was considered significant.

Results

PKH^{high} cell culture on human decellularized scaffolds

As shown by our recent data, we set a working four-step detergent-based procedure to decellularize human renal scaffolds and we characterized them in terms of integrity and extracellular matrix protein composition (Bombelli, 2017). With this procedure, we obtained intact kidney scaffolds, in terms of structure and ECM composition, making them a valuable support for cell seeding.

In the current research, the cells seeded were PKH^{high} cells obtained by FACS sorting from NS cultured for 10 days (Fig.1A). PKH^{high} cells represent the PKH26 most fluorescent cells, gated as about 0.8-1% of the total NS population. This percentage corresponds to the usual sphere forming efficiency observed (Bombelli, 2013). We seeded 15,000 sorted cells on decellularized scaffolds placed in poly-Hema coated 96 well plates. Both the poly-Hema coating and the cell number are optimized in order to avoid cell attachment to plastic and cell scattering in the well. A higher cell number would not result in a better recellularization but, on the

contrary, would enhance cells remaining in the well without attaching the scaffold.

After 30 days of culture on scaffold in presence of a basal medium, without any additional grow factor that could drive cell differentiation toward a specific lineage, PKH^{high} cells were able to attach to different portions of the scaffold. Moreover, H&E showed the presence of simple cuboidal epithelial-like cells, typical of the renal tubular portion (Fig.1B) as well as simple squamous epithelial-like cells located on the big vessel basement membrane (Fig. 1C).

Characterization of cells in repopulated structures

To investigate whether PKH^{high} cells differentiated into specific nephron phenotypes, the repopulated structures were characterized by sequential immunofluorescence staining using epithelial (CK8.18), proximal (AQP1 or CD13) and distal (CK7) tubular and endothelial (vWf) markers. Thanks to this approach, described by Cattoretti's group (Scalia, 2016 and Gendusa, 2014), we were able to evaluate several markers on the same repopulated structure.

PKH^{high} cells after 30 days of culture on decellularized scaffolds mostly generated epithelial proximal or distal tubules or endothelium (Fig.2). Tubular structures expressed CK8.18 and, proximal CD13/AQP1 or distal CK7 tubular markers in a mutual exclusive way, indicating a specific lineage differentiation (Fig.2, left and middle panels).

Endothelial vWf was not detectable in the structures expressing tubular markers (Fig.2, left and middle panels). Instead, some of the structures expressed endothelial vWf, while lacking the expression of epithelial and tubular markers (Fig.2, right panels).

Of note, few structures had cells that coexpressed different markers, suggesting a still immature cell phenotype (Fig.3). In fact, some of them coexpressed epithelial and specific tubular segment markers (CK8.18 and CK7) and endothelial (vWf) markers (Fig.3, left panels). Few other cells coexpressed all the differentiation markers tested, the distal and proximal tubular CK7 and AQP1, the epithelial CK8,18 together with the endothelial vWF (Fig.3, right panel).

Characterization of PKH^{high} cells before seeding

To analyse whether PKH^{high} cells are already characterized by a cell commitment toward a specific renal or endothelial lineage, we valued their phenotype before seeding on decellularized scaffold.

Comparing PKH^{high} cells to their PKH^{low} and PKH^{neg} cell progenies, we found that PKH^{high} cells showed an enrichment (52.33% ± 6.60) in cells that coexpressed the proximal CD10 and distal CK7 tubular markers (Fig.4A, upper panel), suggesting an immature phenotype respect to PKH^{low} (19.67% ± 4.63) and PKH^{neg} (4.19% ± 1.74) cells, but also respect to whole NS cells (12.03% ± 5.31). Moreover, it is

important to highlight that in PKH^{high} cells no expression (0%) of endothelial CD31 marker (Fig.4A, lower panel) was detectable. On the contrary, in their PKH^{low} (0.56% ± 0.36) and PKH^{neg} (1.55% ± 1.36) cell progeny CD31 was expressed and seemed to enrich in relation to progenitor proliferation/differentiation associated with PKH26 dye decrement. Together with the total absence of CD31 endothelial marker in PKH^{high} cells, we showed on cytospinned PKH^{high} cells the positivity of all cells to the generic epithelial marker CK8.18 and the total negativity to the other endothelial marker (von Willebrand factor, vWF) (Fig.4B, left panel). Instead, we could observe the presence of an endothelial phenotype (vWF^{+}) in $PKH^{low/neg}$ cells (Fig4B, white arrow in right panel).

Therefore, we speculated the existence of a differentiation gradient within the NS starting from PKH^{high} cells, which are the sphere forming cells, toward different lineage commitment evidenced in PKH^{low} and PKH^{neg} progenitor cells.

Cell commitment toward endothelium

To confirm that the presence of $CD31^{+}$ cells in NS derives from $CD31^{-}$ PKH^{high} cells, we sorted from NS the PKH^{high} cells, completely $CD31^{-}$, and plated them to form new secondary NS (Fig.5A). After 10 days of culture, we analysed these new secondary NS cells both by FACS analysis and by

immunofluorescence on cytospinned dissociated NS cells. FACS analysis revealed a CD31 re-expression, demonstrating that $PKH^{high}/CD31^{-}$ cells were able to generate $CD31^{+}$ progenitors, probably due to a lineage commitment within NS. In particular, in secondary NS the PKH^{high} sphere forming cells maintained again their $CD31^{-}$ phenotype (0%), while CD31 expression was detectable in PKH^{low} (1.29%) and PKH^{neg} (2.51%) subpopulations (Fig.5B). Also in secondary NS, as in primary ones, we noticed an enrichment in $CD31^{+}$ cells along proliferation/differentiation from the quiescent PKH^{high} cells to the proliferating PKH^{low} and PKH^{neg} cells. Furthermore, by immunofluorescence (Fig.5C) we confirmed the expression of the endothelial marker vWF in some cells of secondary NS obtained from $PKH^{high}/CD31^{-}/vWF^{-}$ cells. These data supported the observation that PKH^{high} cells were able to give rise to endothelial cells.

Transcriptomic analysis and biocomparing

Within PKH^{high} cell population the cells able of self-renewal and multilineage differentiation are $PKH^{high}/CD133^{+}/CD24^{-}$ (RSC), representing about 70% of total PKH^{high} cells (Bombelli, 2013). To understand and reveal the phenotype behind PKH^{high} status, we performed transcriptomic analysis comparing RSC with their $PKH^{low/neg}$ progenitors (LN) and with terminally differentiated renal tubular primary cell cultures (PCC). Lists of differentially expressed genes (DEG)

(119 upregulated and 148 downregulated in RSC vs LN comparison and 476 upregulated and 233 downregulated in RSC vs PCC comparison) (Fig.6A) were obtained. The two DEG lists were crossed to find out the most significant upregulated genes in RSC (Fig. 6B). Only upregulated RSC common DEG were considered for further analysis.

We then proceeded trough statistical analysis and bio-comparing, exploiting Gene Set Enrichment Analysis (GSEA) as a tool to verify potential enrichments in our RSC phenotype in comparison to LN and PCC, matching our trancriptomic analysis with gene sets from databases. Firstly, performing a GSEA, we found that RSC phenotype negatively correlated with embryonic stem cell profile (Benporath, 2008) (Fig.7A, first and second upper panels). Moreover, we tested the correlation between RSC and another type of adult stem cells, the mammary stem cells, isolated exploiting the same sphere forming assay and PKH26 staining (Pece, 2010). We evidenced a positive correlation between the two respect to LN (Fig.7B, first upper panel), confirming the adult stem nature of our RSC. Of note, the same positive correlation was maintained comparing with another mammary stem cell profile, shared by human and mouse (Lim, 2010) (Fig.7B, second upper panel).

We also performed GSEA analysis to correlate our RSC transcriptomic profile with $CD133^{+}/CD24^{+}$ adult renal progenitors described in Sallustio, 2010. Interestingly we

reported a positive correlation suggesting a similarity between the two cell types. This fact was expected since they are both $CD133^{+}$ adult cells of renal origin. Of interest, the positive correlation with RSC was registered only for their comparison with PCC (Fig.7B, last upper panel), indicating that Sallustio's progenitors are transcriptionally more similar to RSC than to PCC. Instead, when RSC were compared to LN, Sallustio's progenitors resulted more similar to LN than to RSC, although not significantly (data not shown). This data indicates that RSC and Sallustio's progenitors are two distinct cell types and, these last are similar to our LN rather than to RSC.

By using GSEA analysis we were also able to further confirm the stem characteristics of RSC respect to the differentiated PCC. In fact, we could notice the positive correlation with the gene sets 'system development' (Fig7B, first lower panel) and 'wnt signalling pathway' (Fig.7B, second lower panel), typical of stem cells. In addition, we also registered a negative correlation of RSC respect to the LN progenitors and differentiated PCC with cell cycle dataset from Reactome (Fig.7A, last upper and first lower panels), since quiescence is a typical feature of stemness.

Finally, an unbiased analysis (c5.all.v6.0symobls), performed to give a general insight on our RSC, revealed a positive correlation of RSC respect to LN progenitors with the 'transport vesicle' dataset (Fig.7B, last lower panel),

indicating an active role of RSC in microenvironment signals. In addition, we registered a negative correlation with ‘DNA replication’ of RSC respect to LN (Fig.7A, second lower panel) and with ‘ribosome biogenesis’ respect to PCC (Fig.7A, last lower panel). Both these findings are in accordance with RSC quiescence.

Marker selection and validation

Among the genes that define the RSC molecular signature, we selected 3 candidates to be validated in view of their use as specific markers. The choice was based on their fold change values in RSC respect to LN progenitors and differentiated PCC and on their very rare expression in the adult renal tissue. Ultimately, our choice fell on: IRF8, a transcription factor, FBN2, a structural protein, and MUC16 that is CA125, a well known transmembrane marker. They were upregulated DEG and their fold change values were respectively: 2.78, 2.52 and 1.90 for RSC vs LN comparison, and 2.64, 2.42 and 3.54 for RSC vs PCC one.

Moreover, all three markers resulted from the intersection among upregulated DEG in RSC versus LN progenitors and in RSC versus differentiated PCC.

By sequential immunofluorescence, we validated these three markers at protein level on cytospinned PKH^{high} sorted cells and we confirmed the existence of cells, which co-express all the three markers (Fig.8A, left panels). In particular, in the

same cell IRF8 showed a nuclear distribution, FBN2 a cytoplasmic positivity, and CA125 a surface signal. Moreover, we showed that cells positive for all three markers, were also positive for CD133 staining (Fig. 8B). Comparing the expression of these three markers with $PKH^{low/neg}$ cells (Fig.8A, middle panel) and PCC (Fig.8A, right panel), IRF8 and FBN2 did not show any signal, while CA125 was expressed to some extent. For this reason, we decided to quantify CA125 expression in the three mentioned populations, revealing an enrichment in $CA125^{+}$ cells in PKH^{high} cells and a progressive significant decrease in $PKH^{low/neg}$ and PCC cells (Fig.8C).

Summarizing, we identified three additional markers, which could be useful to detect renal stem like cells in adult human kidney tissue.

Tissue analysis

Starting from these results, we directly FACS sorted from renal tissue the four different subpopulations, based on CD133 and CD24 expression, excluding $CD45^{+}$ hematopoietic cells, $CD31^{+}$ endothelial cells and dead cells.

By immunofluorescence after cytospin on sorted subpopulations, we evaluated the expression of CA125, FBN2 and IRF8 markers (Fig. 9A). Of note, we were not able to detect IRF8 expression with this approach.

CA125 expression was found to be enriched in $CD133^+/CD24^-$ population (31.7%) respect to all other subpopulations (Fig.9B). Instead, FBN2 expression was particularly frequent in $CD133^+/CD24^+$ subpopulation (36.96%) (Fig.9B), but it has to be considered its peculiar distribution. In fact, in all the other subpopulations FBN2 presented its typical cytoplasmic distribution and only in $CD133^+/CD24^+$ cells it assumed a stippled membranous distribution like secreted proteins (Fig.9A), suggesting the possible acquisition of a different function respect to all the other phenotypes.

In general, it is important to notice that $CA125^+/FBN2^+$ double positive cells are enriched in $CD133^+/CD24^-$ subpopulation (12.2%) from renal adult tissue (Fig.9B).

We succeeded in demonstrating for the first time the renal cell expression of FBN2 and CA125 markers and the identification in adult renal tissue of a $CD133^+/CD24^-/CA125^+/FBN2^+$ population that can be further studied to evaluate eventual stem properties.

Discussion

In this work, we aim to demonstrate the capacity of PKH^{high} cells to repopulate different nephron portions of decellularized human renal scaffolds, without being lineage-restricted before repopulation attempt. We evidenced that PKH^{high} cells that give rise to NS, are able to repopulate tubular and vascular segments of renal scaffold differentiating respectively in epithelial and endothelial lineages. In particular, PKH^{high} cells, not expressing CD31 endothelial marker, are able to form NS containing $CD31^{+}$ cells. We also observed in PKH^{high} cells an enrichment in cells coexpressing proximal and distal tubular markers. This coexpression decreased in the progeny of PKH^{high} cells, the $PKH^{low/neg}$ cells. These data may indicate a differentiation gradient within NS, in which $PKH^{low/neg}$ progeny represents the way toward differentiation into more mature proximal and distal tubular and endothelial cells. This differentiation gradient was described also in mammospheres (Pece, 2010). The differentiation into an endothelial lineage was quite unexpected, however, these data confirmed those previously shown with whole NS cells (Bombelli, 2017). Actually, we have not a definitive explanation for these observations that we repetetly obtained with PKH^{high} cells lacking not only endothelial, but also mesenchymal and hematopoietic markers (data not shown). This result led us to think about the embryological origin of vascular progenitors. In fact, both

vascular progenitors and renal vesicle originate from the intermediate mesoderm (Little, 2012). Moreover, the same lineage differentiation had been already reported in literature during formation of 3-D kidney organoids from iPSC reprogrammed into intermediate mesoderm (Takasato, 2015), supporting our explanation. Our data could be thus supported by a common embryological origin of renal vasculature and renal vesicle. Of course, our hypothesis does not clarify how PKH^{high} cells, supposed to be adult stem-like cells, can enter the endothelial or epithelial lineages. This issue should be addressed, and it might open interesting translational perspectives for our PKH^{high} cells.

Our result also showed that some structures generated by PKH^{high} cells on decellularized scaffolds presented cells coexpession markers specific of different lineages of differentiation, and this could be probably due to a still immature cell phenotype. To explain this phenomenon, we hypothesized that 30 days of culture are not enough for all PKH^{high} cells to terminally differentiate.

The second hypothesis is that lack of signals from the niche decelerated their final maturation. In fact, we know that 30 days of culture on decellularized scaffolds enables whole NS cells, composed by PKH^{high} cells together with their $PKH^{low/neg}$ progeny, to terminally differentiate into proximal and distal tubular and endothelial lineages (Bombelli, 2017). Similarly, we previously demonstrated that PKH^{high} cells can generate

structures, only when transplanted in vivo under nude mice capsule with their $PKH^{low/neg}$ progeny (Bombelli, 2013). Therefore, our herein results made us argue that PKH^{high} alone could respond to stimuli retained in the ECM, which may sustain cellular viability, proliferation and differentiation (Sciancalepore et al, 2016), but the lack of $PKH^{low/neg}$ progeny may slow down terminal differentiation. In fact, it is known that stem cell progeny can provide important and diversified feedback mechanisms to regulate their stem cell parents and participate in the creation of a unique microenvironment to host the stem cells and drive a complete differentiation (Hsu and Fuchs, 2012).

Among the PKH^{high} cells, the ones with $CD133^{+}/CD24^{-}$ phenotype are those with the wider stem properties, comprising the endothelial differentiation, and represent the 70% of the entire PKH^{high} population (Bombelli, 2013). In our repopulation results with whole PKH^{high} cells, very likely $PKH^{high}/CD133^{+}/CD24^{-}$ cells play a significant role, but this has to be confirmed by further experiments.

To better clarify what phenotype is hidden behind the functional PKH^{high} status of our renal stem-like cells, we performed a transcriptomic analysis on $PKH^{high}/CD133^{+}/CD24^{-}$ cells, obtaining a molecular signature.

Compairing our transcriptomic data by a metanalysis we were able to support the adult stem-like nature of our cells and their typical characteristics of quiescence.

Moreover, we evidenced IRF8, FBN2 and CA125 products as possible candidate specific markers for our RSC.

IRF8 is a transcription factor of the IFN regulatory factor family, also known as IFN consensus sequence-binding protein. It represented an attractive candidate since its ability to be a regulator of cell differentiation is largely recognized for hematopoietic progenitors (Wang, 2014 and Paschall, 2015).

FBN2 is a fibrillar protein, able to be transported out of cells into the extracellular matrix. Here, fibrillin-2 binds to other microfibrils, becoming part of elastic fibres. It seemed a good candidate to be marker of stem cells in kidney, since it was suggested to play a role in directing the assembly of elastic fibres during embryonic development, being expressed only in renal tubules during early development, while in late development it is found both in tubules and in glomeruli (Quondamatteo, 2002). FBN2 has been recently found upregulated in human foetal $Six2^{+}/Cited1^{+}$ nephron progenitors (Da Sacco, 2017)

MUC16, also called CA125, is a transmembrane glycoprotein belonging to mucin family. It is thought to provide a protective, lubricating barrier against particles and infectious agents at mucosal surfaces and it is commonly used as a

biomarker for ovarian cancer. It was surprising to find this gene among those upregulated in RSC, since CA125 expression was not detected in kidney during development (Wang, 2008). This evidence, together with the characteristic of CA125 to be responsible for tumorigenic, metastatic and drug-resistant properties in pancreatic cancer cells (Das, 2015), made CA125 an attractive gene to test as a marker for stemness.

In conclusion, validating these three gene products on our PKH^{high} cells, we were able to find cells with a $PKH^{high}/CD133^{+}/IRF8^{+}/FBN2^{+}/CA125^{+}$ phenotype, that were never described before and that could match the stem-like properties of our RSC.

With these new markers, attempts of identification and localization on adult renal tissue of cells with the phenotype described above are ongoing. The preliminary promising results obtained suggest the possibility to isolate these cells with the membrane surface proteins, to give a more detailed insight into the issue of an adult renal stem cell existence.

Finally, our transcriptomic analysis could also pave the way to search for transcription factors that are typical of this cell type and could in future allow the identification of a cocktail of genes useful for future attempts of cell reprogramming towards adult renal stem-like cells.

Figure Legends:

Figure 1:

Repopulation of human decellularized scaffolds with PKH^{high} cells. (A): Representative sorting plot. PKH^{high} cells were FACS separated from $PKH^{low/neg}$ cells based on PKH26 fluorescence.

Representative hematoxylin and eosin staining of tubular-like structures (B) and vascular-like structure (C) 30 days after seeding PKH^{high} cells. Inserts: 2X digital magnification respect to the original field.

Figure 2:

Characterization of scaffolds repopulated with PKH^{high} cells. Representative sequential immunofluorescence staining of FFPE scaffolds with the indicated antibodies, able to recognise specific tubular or vascular phenotypes. The different antibody combinations are able to identify proximal tubules (left), distal tubules (middle), and endothelium (right). AQP1: aquaporin 1, proximal tubular marker; CK8.18: Cytokeratin 8.18, epithelial marker; CK7: Cytokeratin 7, distal tubular marker; vWF: von Willebrand Factor, endothelial marker.

Figure 3:

Characterization of human renal scaffolds repopulated with PKH^{high} cells. Representative sequential immunofluorescence staining of FFPE scaffolds with the indicated markers. The different marker combinations highlight immature phenotypes. AQP1: aquaporin 1; CK8.18: Cytokeratin 8.18; CK7: Cytokeratin 7; vWF: von Willebrand Factor. Blue: DAPI.

Figure 4:

(A) Immunophenotypical FACS characterization of whole dissociated nephrospheres (NS) and of PKH^{neg}, PKH^{low} and PKH^{high} subpopulations before seeding on decellularized scaffolds. The used markers are indicated. Mean ± SD of positive cells is reported and is referred to 3 independent experiments. CK7: Cytokeratin 7. (B): Immunofluorescence on cytospinned PKH^{high} and $PKH^{low/neg}$ cells. White arrow indicates vWf positive cell among $PKH^{low/neg}$ cells. vWF: von Willebrand Factor; CK8.18: Cytokeratin 8.18. Blue: DAPI. Scale bars: 50 µm.

Figure 5:

$CD31^{+}$ cell derivation in NS. (A) $PKH^{high}/CD31^{-}$ cells sorted from primary NS were plated in sphere-forming conditions for 10 days to obtain secondary NS. (B) FACS analysis of CD31 endothelial marker on PKH^{neg}, PKH^{low} and PKH^{high}

subpopulations from secondary NS. (C) Representative IF on cytospinned secondary NS dissociated to single cells. vWF: von Willebrand Factor. Blue: DAPI. Scale bar: 50µm.

Figure 6:

Representation of transcriptomic analysis of renal stem-like cells (SC), progenitors (LN) and differentiated primary cultures (PCC); (A) Heat map of differentially expressed genes (DEG) both significantly upregulated (UP) or downregulated (DOWN) by t-test. SC vs LN in the upper panel, and SC vs PCC in the lower panel. (B): Crossing between DEG upregulated in SC vs LN comparison and DEG upregulated in SC vs PCC comparison. 48 common upregulated genes are listed. In red the chosen markers to test.

Figure 7:

Correlation profiles from GSEA analysis. (A) Negative correlations between RSC (SC) and the indicated population (LN progenitors or differentiated PCC). Tested data sets indicated on the top of each correlation profile. (B) Positive correlations between RSC (SC) and the indicated population (LN or PCC). Tested data sets indicated on the top of each correlation profile. Correlations were considered significant with at least a nominal p-value ≤ 0.05.

Figure 8:

Marker validation on sorted PKH^{high}, $PKH^{low/neg}$ cells and on PCC. (A) Separated acquired channels of immunofluorescence stainings merged in and (B). (B) Sequential immunofluorescence staining with specific antibodies. IRF8: Interferon regulatory factor 8; FBN2: Fibrillin 2; CA125: Cancer Antigen 125, also known as mucin16. Blue: DAPI. (C) Quantification of CA125 expression in PKH^{high}, $PKH^{low/neg}$ cells and PCC calculated as the percentage of CA125 positive cells respect to the total number of nuclei stained with DAPI. *p< 0,05; **p<0,01; data expressed as mean ± ES.

Figure 9:

Marker validation on human adult renal tissue. (A) Representative IF staining with CA125 and FBN2 markers on cytospinned $CD133^{+}/CD24^{+}$, $CD133^{+}/CD24^{-}$, $CD133^{-}/CD24^{+}$, $CD133^{-}/CD24^{-}$ subpopulation, directly sorted from renal tissue. Blue: DAPI. Scale bars 25µm.

(B) Quantification of CA125 and FBN2 expression. The percentage of single or double positive cells respect to the total number of nuclei stained with DAPI in the four subpopulations indicated in (A) is reported. IRF8: Interferon regulatory factor 8; FBN2: Fibrillin 2; CA125: Cancer Antigen 125, also known as mucin16.

Figure 1

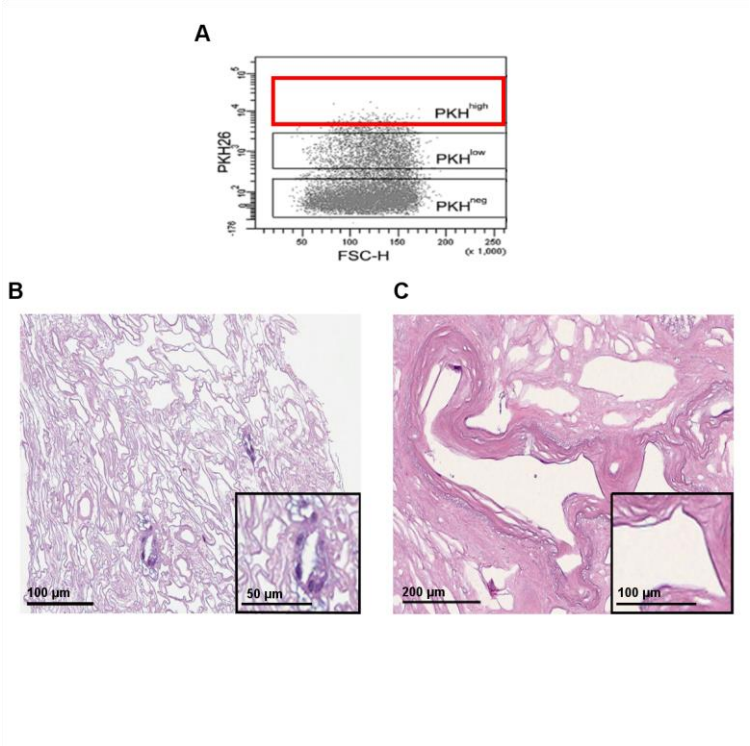
A
PKH26
PKH^high
PKH^low
PKH^neg
FSC-H
(x 1,000)
B
100 µm
50 µm
C
200 µm
100 µm

Figure 2

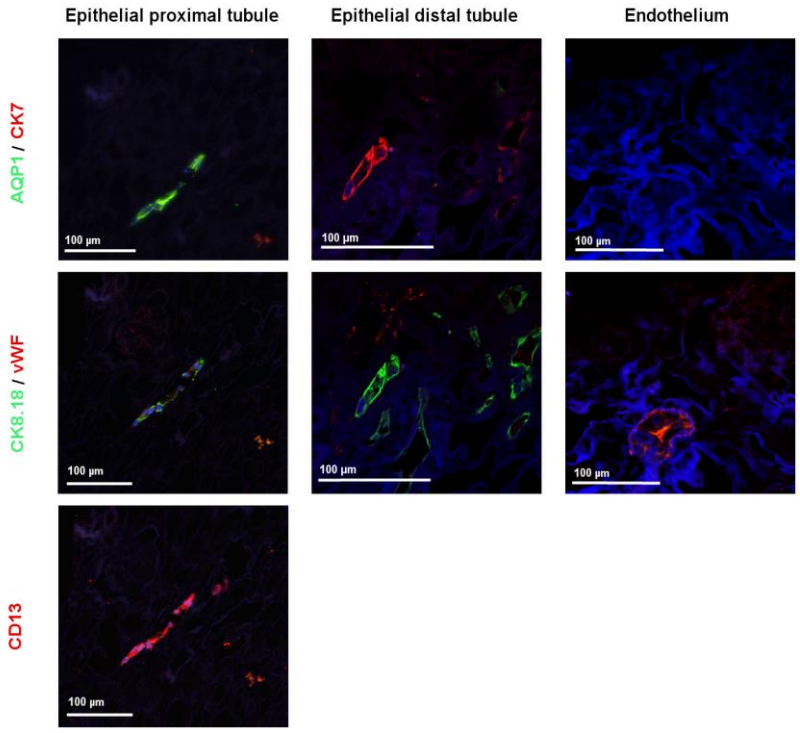
Epithelial proximal tubule
Epithelial distal tubule
Endothelium
AQP1 / CK7
CK8.18 / vWF
CD13
100 µm

Figure 3

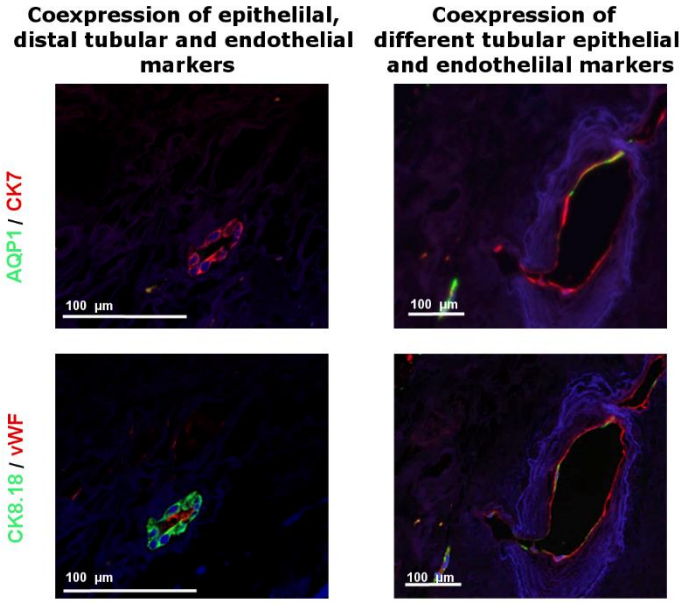
Coexpression of epithelilal, distal tubular and endothelial markers
Coexpression of different tubular epithelial and endothelilal markers
AQP1 / CK7
CK8.18 / vWF
100 µm
100 µm
100 µm
100 µm

Figure 4

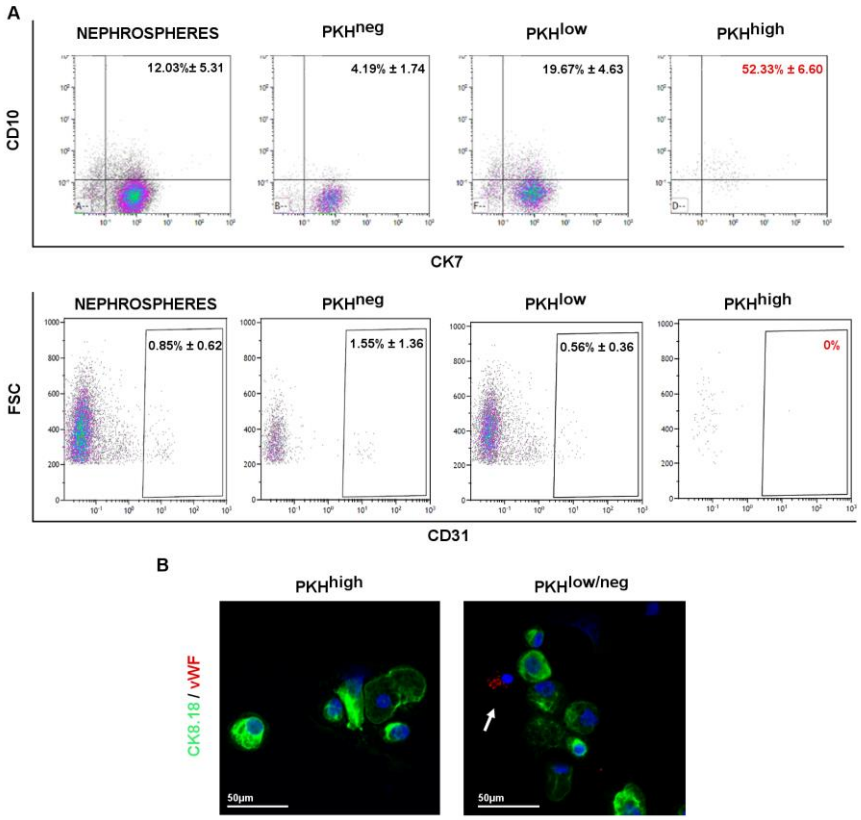
A
NEPHROSPHERES
PKHneg
PKHlow
PKHhigh
12.03%± 5.31
4.19% ± 1.74
19.67% ± 4.63
52.33% ± 6.60
CD10
CK7
NEPHROSPHERES
PKHneg
PKHlow
PKHhigh
0.85% ± 0.62
1.55% ± 1.36
0.56% ± 0.36
0%
FSC
CD31
B
PKHhigh
PKHlow/neg
CK8.18 / vWF
50µm
50µm

Figure 5

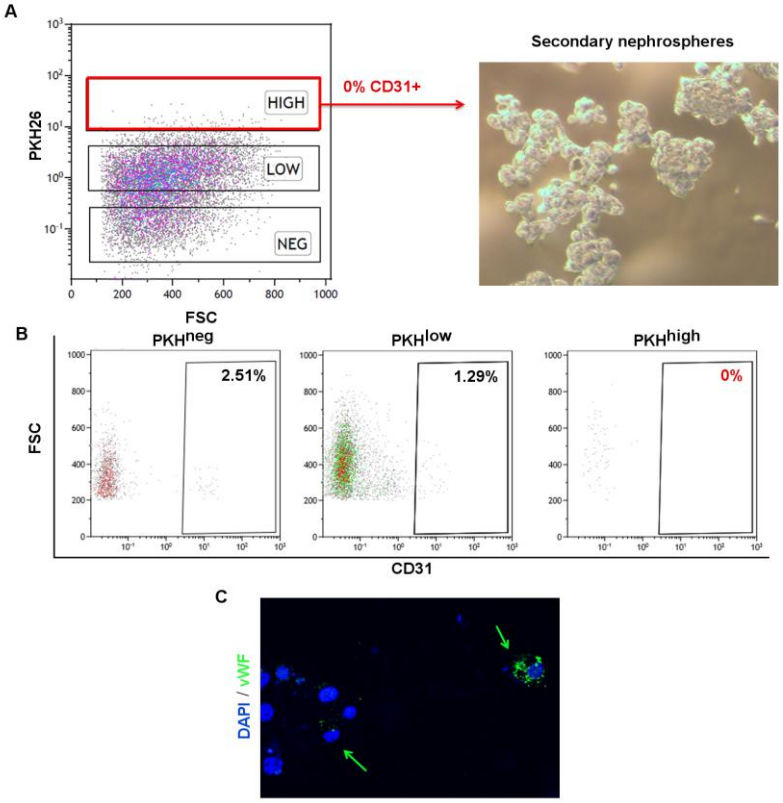
A
PKH26
HIGH
LOW
NEG
FSC
0% CD31+
Secondary nephrospheres
B
PKHneg
PKHlow
PKHhigh
2.51%
1.29%
0%
FSC
CD31
C
DAPI / vWF

Figure 6

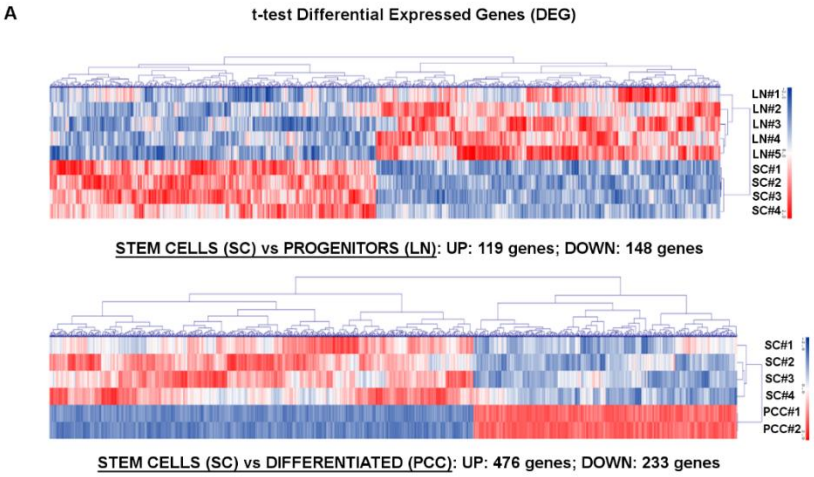

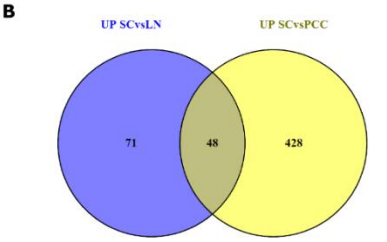

48 common elements in "UP SCvsLN" and "UP SCvsPCC":

AGT	HTRA1	PDLIM3
PROS1	PSAP	PARM1
KRT17	SPARC	SLC47A1
C1QB	TIMP1	TMEM176A
IL1B	GPR137B	MUC16
PTGDS	AKR1C3	BHLHB3
FCRLB	STOM	RASSF4
FAM150B	DPEP1	HAVCR2
TCN1	CCL20	PIK3IP1
CA12	VNN1	CCL28
CFB	GPC6	MYOM3
CRYAB	SULT1C4	ZNF533
CTSB	HHLA2	C1QC
FBN2	BAMBI	TMEM171
IRF8	TMEM176B	NAPSB
LAMP2	HSPB8	LOC642299

Figure 7

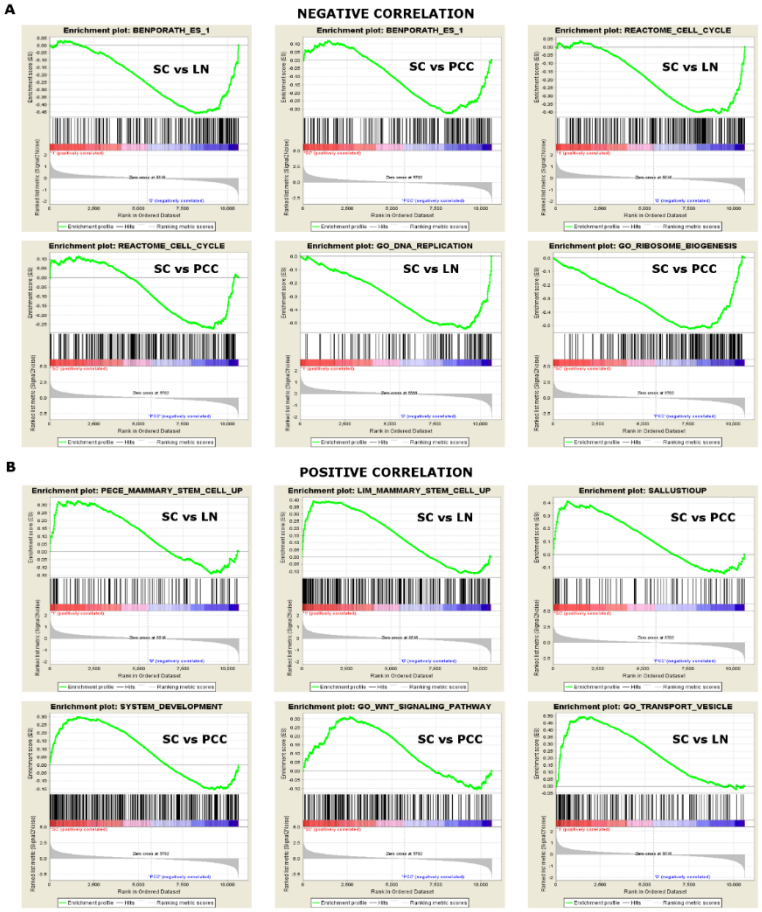
A
NEGATIVE CORRELATION
Enrichment plot: BENPORATH_ES_1
SC vs LN
Enrichment plot: BENPORATH_ES_1
SC vs PCC
Enrichment plot: REACTOME_CELL_CYCLE
SC vs LN
Enrichment plot: REACTOME_CELL_CYCLE
SC vs PCC
Enrichment plot: GO_DNA_REPLICATION
SC vs LN
Enrichment plot: GO_RIBOSOME_BIOGENESIS
SC vs PCC
B
POSITIVE CORRELATION
Enrichment plot: PECE_MAMMARY_STEM_CELL_UP
SC vs LN
Enrichment plot: LIM_MAMMARY_STEM_CELL_UP
SC vs LN
Enrichment plot: SALLUSTIOUP
SC vs PCC
Enrichment plot: SYSTEM_DEVELOPMENT
SC vs PCC
Enrichment plot: GO_WNT_SIGNALING_PATHWAY
SC vs PCC
Enrichment plot: GO_TRANSPORT_VESICLE
SC vs LN

Figure 8

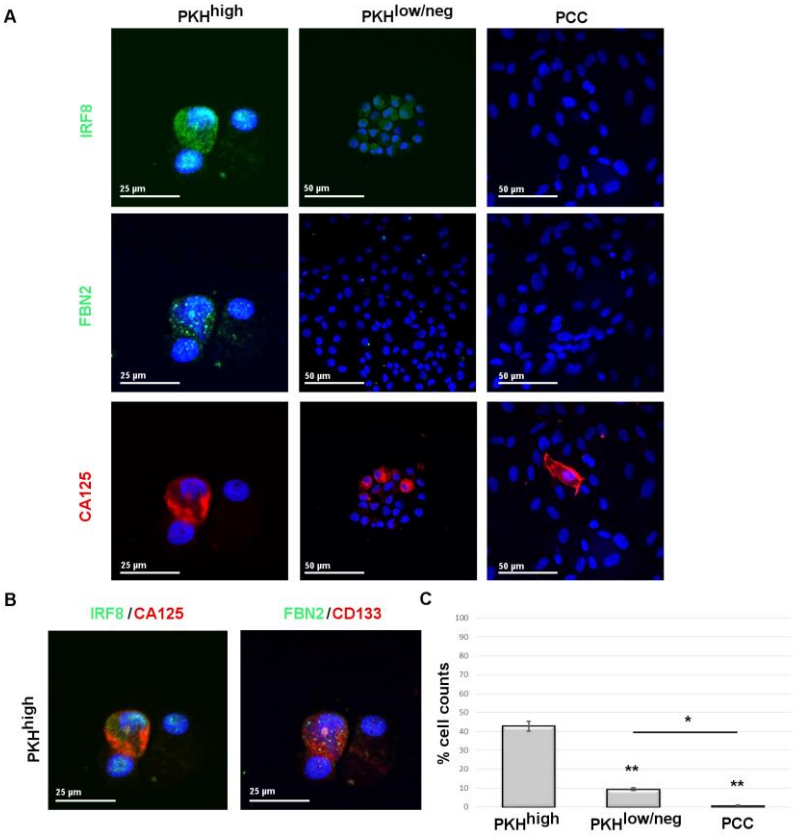
A
PKHhigh
PKHlow/neg
PCC
IRF8
FBN2
CA125
25 µm
50 µm
B
IRF8 /CA125
FBN2 /CD133
PKHhigh
C
% cell counts
PKHhigh
PKHlow/neg
PCC
*
**
**

Figure 9

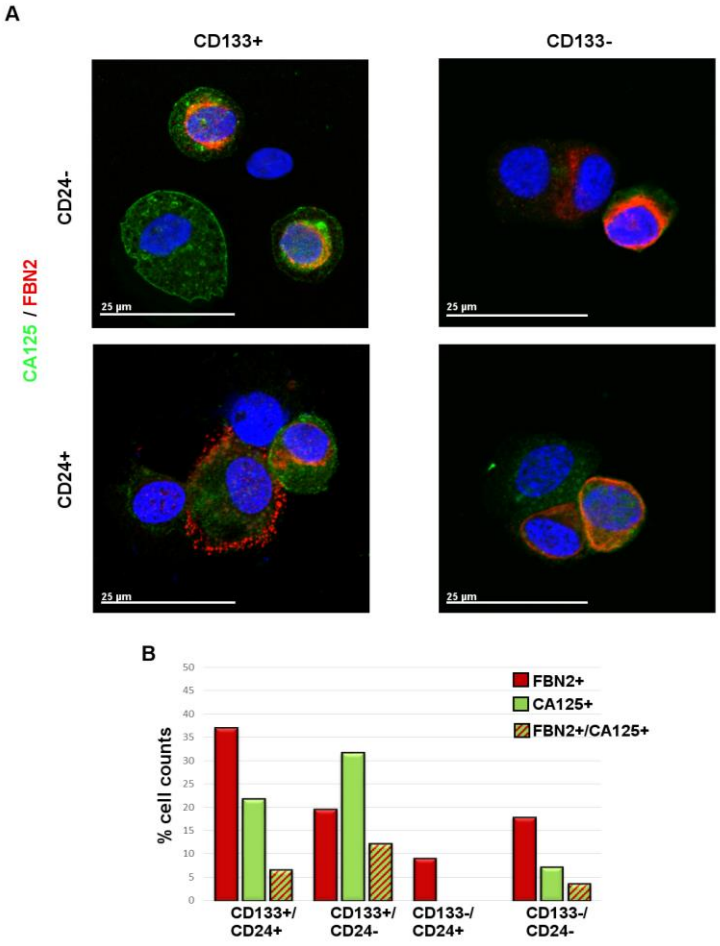
A
CD133+
CD133-
CD24-
CD24+
CA125 / FBN2
25 µm
B
% cell counts
FBN2+
CA125+
FBN2+/CA125+
CD133+/ CD24+
CD133+/ CD24-
CD133-/ CD24+
CD133-/ CD24-

References

Ben-Porath I, Thomson MW, Carey VJ, Ge R, Bell GW, Regev A, Weinberg RA: “An embryonic stem cell-like gene expression signature in poorly differentiated aggressive human tumors.” *Nat Genet. 2008 May;40(5):499-507.*

Bianchi C, Bombelli S, Raimondo F, Torsello B, Angeloni V, Ferrero S, Di Stefano V, Chinello C, Cifola I, Invernizzi L, Brambilla P, Magni F, Pitto M, Zanetti G, Mocarelli P, Perego RA: “Primary cell cultures from human renal cortex and renal-cell carcinoma evidence a differential expression of two spliced isoforms of Annexin A3.” *Am J Pathol. 2010 Apr;176(4):1660-70.*

Bombelli S, Zipeto MA, Torsello B, Bovo G, Di Stefano V, Bugarin C, Zordan P, Viganò P, Cattoretti G, Strada G, Bianchi C, Perego RA: “PKH^{high} cells within clonal human nephrospheres provide a purified adult renal stem cell population.” *Stem Cell Res 2013, 11: 1163-1177.*

Bombelli S, Meregalli C, Scalia C, Bovo G, Torsello B, De Marco S, Cadamuro M, Viganò P, Strada G, Cattoretti G, Bianchi C, Perego RA: “Nephrosphere-Derived Cells are Induced to Multilineage Differentiation when Cultured on Human Decellularized Kidney Scaffolds.” *Am J Pathol. 2017 Oct 14. doi: 10.1016/j.ajpath.2017.09.012*

Bonandrini B, Figliuzzi M, Papadimou E, Morigi M, Perico N, Casiraghi F, Sangalli F, Conti S, Benigni A, Remuzzi A, Remuzzi G: “Recellularization of well-preserved acellular kidney scaffold using embryonic stem cells.” *Tissue Eng Part A 2014, 20: 1486-1498.*

Bussolati B, Camussi G: “Therapeutic use of human renal progenitor cells for kidney regeneration*.” Nat Rev Nephrol. 2015 Dec;11(12):695-706.*

Caralt M, Uzarski JS, Iacob S, Obergfell KP, Berg N, Bijonowski BM, Kiefer KM, Ward HH, Wandinger-Ness A, Miller WM, Zhang ZJ, Abecassis MM, Wertheim JA: “Optimization and critical evaluation of decellularization strategies to develop renal extracellular matrix scaffolds as biological templates for organ engineering and transplantation*.” Am J Transplant 2015, 15: 64-75.*

Da Sacco S, Thornton ME, Petrosyan A, Lavarreda-Pearce M, Sedrakyan S, Grubbs BH, De Filippo RE, Perin L: “Direct Isolation and Characterization of Human Nephron Progenitors.” *Stem Cells Transl Med. 2017 Feb;6(2):419-433.*

Das S, Rachagani S, Torres-Gonzalez MP, Lakshmanan I, Majhi PD, Smith LM, Wagner KU, Batra SK: “Carboxyl-terminal domain of MUC16 imparts tumorigenic and metastatic functions through nuclear translocation of JAK2 to pancreatic cancer cells.” *Oncotarget. 2015 Mar 20;6(8):5772-87.*

Di Stefano V, Torsello B, Bianchi C, Cifola I, Mangano E, Bovo G, Cassina V, De Marco S, Corti R, Meregalli C, Bombelli S, Viganò P, Battaglia C, Strada G, Perego RA: “Major Action of Endogenous Lysyl Oxidase in Clear Cell Renal Cell Carcinoma Progression and Collagen Stiffness Revealed by Primary Cell Cultures.” *Am J Pathol. 2016 Sep;186(9):2473-85.*

Du C, Narayanan K, Leong MF, Ibrahim MS, Chua YP, Khoo VMH, Wan ACA: “Functional kidney bioengineering with pluripotent stem-cell-dervived renal progenitor cells and decellularized kidney scaffolds.” *Adv Healthcare Mater 2016, 5: 2080-2091.*

Gendusa R, Scalia CR, Buscone S, Cattoretti G: “Elution of High-affinity (>10-9 KD) Antibodies from Tissue Sections: Clues to the Molecular Mechanism and Use in Sequential Immunostaining.” *J Histochem Cytochem. 2014 Jul;62(7):519-31.*

Hsu YC, Fuchs E: “A family business: stem cell progeny join the niche to regulate homeostasis.” *Nat Rev Mol Cell Biol. 2012 Jan 23;13(2):103-14.*

Jager K: “Prevalence of Chronic Kidney Disease varies a lot across Europe!” *4 January 2016; News-European Renal Associacion- European Dialysis and Transplant Associacion.*

Katari R, Peloso A, Zambon JP, Soker S, Stratta RJ, Atala A, Orlando G: “Renal bioengineering with scaffolds generated from human kidneys.” *Nephron Exp Nephrol 2014, 126: 119.*

Lim E, Wu D, Pal B, Bouras T, Asselin-Labat ML, Vaillant F, Yagita H, Lindeman GJ, Smyth GK, Visvader JE: “Transcriptome analyses of mouse and human mammary cell subpopulations reveal multiple conserved genes and pathways.” *Breast Cancer Res. 2010;12(2):R21*.

Little MH, McMahon AP: “Mammalian kidney development: principles, progress, and projections.” *Cold Spring Harb Perspect Biol. 2012 May 1;4(5).*

Nakayama KH, Batchelder CA, Lee CI, Tarantal AF: “Decellularized rhesus monkey kidney as a three-dimensional scaffold for renal tissue engineering.” *Tissue Eng Part A 2010, 16: 2207-2216.*

Orlando G, Farney AC, Iskandar SS, Mirmalek-Sani SH, Sullivan DC, Moran E, AbouShwareb T, De Coppi P, Wood KJ, Stratta RJ, Atala A, Yoo JJ, Soker S: “Production and implantation of renal extracellular matrix scaffolds from porcine kidneys as a platform for renal bioengineering investigations.” *Ann Surg. 2012 Aug;256(2):363-70.*

Orlando G, Booth C, Wang Z, Totonelli G, Ross CL, Moran E, Salvatori M, Maghsoudlou P, Turmaine M, Delario G, Al-Shraideh Y, Farooq U, Farney AC, Rogers J, Iskandar SS, Burns A, Marini FC, De Coppi P, Stratta RJ, Soker S: “Discarded human kidneys as a source of ECM scaffold for kidney regeneration technologies.” *Biomaterials 2013, 34: 5915-5925.*

Paschall AV, Zhang R, Qi CF, Bardhan K, Peng L, Lu G, Yang J, Merad M, McGaha T, Zhou G, Mellor A, Abrams SI, Morse HC, Ozato K, Xiong H, Liu K: ”IFN regulatory factor 8 represses GM-CSF expression in T cells to affect myeloid cell lineage differentiation.” *J Immunol. 2015 Mar 1;194(5):2369-79.*

Pece S, Tosoni D, Confalonieri S, Mazzarol G, Vecchi M, Ronzoni S, Bernard L, Viale G, Pelicci PG, Di Fiore PP: “Biological and molecular heterogeneity of breast cancers correlates with their cancer stem cell content.” *Cell. 2010 Jan 8;140(1):62-73.*

Peloso A, Ferrario J, Maiga B, Benzoni I, Bianco C, Citro A, Currao M, Malara A, Gaspari A, Balduini A, Abelli M, Piemonti L, Dionigi P, Orlando G, Maestri M: “Creation and implantation of acellular rat renal ECM-based scaffolds.” *Organogenesis. 2015;11(2):58-74.*

Poornejad N, Schaumann LB, Buckmiller EM, Roeder BL, Cook AD: “Current Cell-Based Strategies for Whole Kidney Regeneration.” *Tissue Eng Part B Rev. 2016 Oct;22(5):358-370.*

Quondamatteo F, Reinhardt DP, Charbonneau NL, Pophal G, Sakai LY, Herken R: “Fibrillin-1 and fibrillin-2 in human embryonic and early fetal development.” *Matrix Biol. 2002 Dec;21(8):637-46.*

Ross EA, Williams MJ, Hamazaki T, Terada N, Clapp WL, Adin C, Ellison GW, Jorgensen M, Batich CD: “Embryonic stem cells proliferate and differentiate when seeded into kidney scaffolds.” *J Am Soc Nephrol 2009, 20: 2338-2347.*

Sallustio F, De Benedictis L, Castellano G, Zaza G, Loverre A, Costantino V, Grandaliano G, Schena FP: “TLR2 plays a role in the activation of human resident renal stem/progenitor cells.” *FASEB J. 2010 Feb;24(2):514-25.*

Scalia CR, Gendusa R, Cattoretti G: “A 2-Step Laemmli and Antigen Retrieval Method Improves Immunodetection.*” Appl Immunohistochem Mol Morphol. 2016 Jul;24(6):436-46.*

Sciancalepore AG, Portone A, Moffa M, Persano L, De Luca M, Paiano A, Sallustio F, Schena FP, Bucci C, Pisignano D: “Micropatterning control of tubular commitment in human adult renal stem cells.” *Biomaterials. 2016 Jul;94:57-69.*

Song JJ, Guyette JP, Gilpin SE, Gonzalez G, Vacanti JP, Ott HC: “Regeneration and experimental orthotopic transplantation of a bioengineered kidney*.” Nat Med 2013, 19: 646-651.*

Sullivan DC, Mirmalek-Sani SH, Deegan DB, Baptista PM, Aboushwareb T, Atala A, Yoo JJ: “Decellularization methods of porcine kidneys for whole organ engineering using a high-throughput system.” *Biomaterials 2012, 33: 7756-7764.*

Takasato M, Er PX, Chiu HS, Maier B, Baillie GJ, Ferguson C, Parton RG, Wolvetang EJ, Roost MS, Chuva de Sousa Lopes SM, Little MH: “Kidney organoids from human iPS cells contain multiple lineages and model human nephrogenesis.” *Nature. 2015 Oct 22;526(7574):564-8.*

Wang Y, Cheon DJ, Lu Z, Cunningham SL, Chen CM, Luo RZ, Xing D, Orsulic S, Bast RC Jr, Behringer RR: “MUC16 expression during embryogenesis, in adult tissues, and ovarian cancer in the mouse.” *Differentiation. 2008 Dec;76(10):1081-92.*

Wang H, Yan M, Sun J, Jain S, Yoshimi R, Abolfath SM, Ozato K, Coleman WG Jr, Ng AP, Metcalf D, DiRago L, Nutt SL, Morse HC: “A reporter mouse reveals lineage-specific and heterogeneous expression of IRF8 during lymphoid and myeloid cell differentiation.” *J Immunol. 2014 Aug 15;193(4):1766-77.*

Yamanaka S, Yokoo T: “Current Bioengineering Methods for Whole Kidney Regeneration*.” Stem Cells Int. 2015;2015:724047.*

Chapter 4

Summary, Conclusions and Future Perpectives

Summary

Chronic kidney disease is one of the leading causes of morbidity, estimated to affect 11-13% of the population worldwide (Hill, 2016). It can progress toward end-stage renal disease and the only treatment option is dialysis and, consequently, renal transplantation. To date an emerging shortage of transplantable kidneys has been registered, addressing researches towards the integration among stem cell research, regenerative medicine and tissue engineering. Kidney regeneration is particularly difficult because of the anatomical complexity of the organ. As a tool for renal reconstitution, to date a valuable alternative seems to be the recellularization of decellularized scaffolds (Poornejad, 2016). Many attempts of decellularization and recellularization have been performed in different species and with different cell types (Ross, 2009; Bonandrini, 2014; Caralt, 2015; Peloso, 2015; Sullivan, 2012; Orlando, 2012; Nakayama, 2010; Song, 2013; Orlando, 2013; Katari, 2014; Du, 2016), even if the ultimate cell type, able to reconstitute various portions of renal architecture, is still not so well understood. To this aim, one of the suitable possibilities could be adult renal stem cells, but their existence (reviewed in Bussolati and Camussi, 2015) and possible role in tissue recovery after renal cell injury is still a matter of debate (Lombardi, 2016).

In this scenario, our group contributed to the debate obtaining nephrospheres (NS) from adult human renal tissue (Bombelli, 2013), that I had the opportunity to handle during my PhD years. Moreover, we set the method to efficiently decellularize slices of human renal scaffolds and we tried and succeeded in exploiting NS cells to repopulate them both in tubular and in vascular components, as described in chapter 2 (Bombelli, 2017).

Of note, cells with stem properties were previously identified as a subpopulation within the NS, being the PKH26 most fluorescent cells (PKH^{high}cells) (Bombelli, 2013). Evaluating the expression of the two markers CD133 and CD24, our group also demonstrated that PKH^{high} cell population is heterogeneous, and within the NS the cells able to self-renew and to differentiate along different lineages had $PKH^{high}/CD133^{+}/CD24^{-}$ phenotype (RSC) (Bombelli, 2013).

In this thesis I also aimed to prove the abilities of PKH^{high} cells alone to attach and differentiate on decellularized scaffolds, as discussed in chapter 3. This work showed, for the first time, that PKH^{high} cells were able to repopulate both tubular and vascular segments of renal scaffold differentiating in epithelial and endothelial lineages.

Since the definition of an adult renal cell with stem properties still lacks, I also aimed to find the molecular signature of RSC subpopulation to better disclose the phenotype hidden behind PKH^{high} functional status and to find possible

additional markers that could allow their identification on tissue, as described in chapter 3. Transcriptomic analysis of RSC and their $PKH^{low/neg}$ progeny was performed and differentially expressed genes (DEG) were evidenced. Bioinformatic Gene Set Enrichment Analysis suggested a renal early status of differentiation of our RSC, different from embryonic stem cells. Finally, to obtain RSC signature, DEG were crossed and IRF8, FBN2 and CA125 gene products were selected as potential markers and validated on PKH^{high} sorted cells.

The subsequent step was the identification of cells expessing these markers on adult renal tissue. We set up the digestion method of renal tissue to obtain viable single cells for FACS marker analysis, and we identified for the first time the presence of a $CD133^{+}/CD24^{-}/FBN2^{+}/CA125^{+}$ subpopulation in adult renal tissue (chapter 3).

Conclusion and application to translational medicine

In conclusion, my PhD work deals with two main big open issues: kidney regeneration and human adult stem cell identification.

During this work, it has been showed the ability of NS cells, comprising PKH^{high} cells and their $PKH^{low/neg}$ progeny, to recellularize a decellularized renal scaffold. I partecipated to the experiments addressed to the optimization of

decellularization protocols and to the repopulation and differentiation experiments as described in chapter 2.

Then I was primarly involved in the work described in chapter 3.

The work was focused on a specific subpopulation of NS cells, the PKH^{high} cells, constituted for the 70% by the $PKH^{high}/CD133^{+}/CD24^{-}$ cell phenotype that has the wider stem-like capacities. I performed the experiments reported in which it has been shown that PKH^{high} cells alone, without their $PKH^{low/neg}$ progeny, are able to recellularize the acellular renal scaffold and to differentiate into specific tubular epithelial segments and endothelial lineage.

Moreover, as described in chapter 3, I gave a deeper insight into the transcriptional profile of $PKH^{high}/CD133^{+}/CD24^{-}$ cells (RSC) and demonstrated the coexpression of IRF8, FBN2, and CA125 markers, never described before in kidney cells. Furthermore, some of these markers have been found to be positively coexpressed directly on kidney tissue.

From a translational point of view, whole NS cells and PKH^{high} stem-like cells could be defined as promising for kidney recellularization and regenerative studies.

Moreover, the new validated markers could help the localization of adult renal stem-like cells on tissue and their transcriptomic profile could pave the way for future studies on other markers and transcription factors.

However, the bioengineering of kidney still hides various challenge to overcome before clinical applicability, but the identification and the more detailed description of a reliable cell type to carry out the recellularization process lay the first foundation to improve this research field.

Future perspectives

Having demonstrated the abilities of NS cells and PKH^{high} stem-like cells to repopulate acellular kidneys, as a future perspective we expect to better understand the role of the crosstalk between PKH^{high} cells and PKH$^{low/neg}$ cell progeny to create a specific microenvironment for terminal cell differentiation during recellulariuzation. This hypothesis is suggested by the fact that some structures generated by PKH^{high} cells alone showed a still immature phenotype, while, at the same time point of culture, structures generated by whole NS cells succeeded in terminally differentiating. The knowledge about this crosstalk might also clarify how our PKH^{high} cells enter into the endothelial lineage.

In addition, we are planning to trace PKH^{high} and $PKH^{low/neg}$ when cultured together on the acellular scaffolds to understand the relative contribution in cell differentiation and repopulation.

Concerning the new markers identified, we now aim to prove their usefulness for the isolation of cells with stem properties from adult renal tissue. New experiments of single cell sorting are ongoing, based on CD133, CD24 and, additionally on the new identified cell surface marker, CA125. First attempts confirmed immunofluorescence data in terms of marker expression. Our next focus will be the confirmation of stemness of the cell population, evaluated as self-renewal capability, that is the ability to enrich the sphere forming formation respect to the bulk epithelial population, and multilineage differentiative capabilities.

Finally, the transcriptomic description of RSC we provided in this work could ideally disclose the opportunity to individuate possible lists of transcription factors for future attempts of cell reprogramming toward adult renal stem-like cells.

References

Bombelli S, Zipeto MA, Torsello B, Bovo G, Di Stefano V, Bugarin C, Zordan P, Viganò P, Cattoretti G, Strada G, Bianchi C, Perego RA: "PKH^{high} cells within clonal human nephrospheres provide a purified adult renal stem cell population." *Stem Cell Res 2013, 11: 1163-1177.*

Bombelli S, Meregalli C, Scalia C, Bovo G, Torsello B, De Marco S, Cadamuro M, Viganò P, Strada G, Cattoretti G, Bianchi C, Perego RA: "Nephrosphere-Derived Cells are Induced to Multilineage Differentiation when Cultured on Human Decellularized Kidney Scaffolds." *Am J Pathol. 2017 Oct 14. doi: 10.1016/j.ajpath.2017.09.012.*

Bonandrini B, Figliuzzi M, Papadimou E, Morigi M, Perico N, Casiraghi F, Sangalli F, Conti S, Benigni A, Remuzzi A, Remuzzi G: "Recellularization of well-preserved acellular kidney scaffold using embryonic stem cells." *Tissue Eng Part A 2014, 20: 1486-1498.*

Bussolati B, Camussi G: "Therapeutic use of human renal progenitor cells for kidney regeneration*." Nat Rev Nephrol. 2015 Dec;11(12):695-706.*

Caralt M, Uzarski JS, Iacob S, Obergfell KP, Berg N, Bijonowski BM, Kiefer KM, Ward HH, Wandinger-Ness A, Miller WM, Zhang ZJ, Abecassis MM, Wertheim JA: “Optimization and critical evaluation of decellularization strategies to develop renal extracellular matrix scaffolds as biological templates for organ engineering and transplantation*.” Am J Transplant 2015, 15: 64-75.*

Du C, Narayanan K, Leong MF, Ibrahim MS, Chua YP, Khoo VMH, Wan ACA: “Functional kidney bioengineering with pluripotent stem-cell-dervived renal progenitor cells and decellularized kidney scaffolds.” *Adv Healthcare Mater 2016, 5: 2080-2091.*

Hill NR, Fatoba ST, Oke JL, Hirst JA, O'Callaghan CA, Lasserson DS, Hobbs FD: “2016 Global Prevalence of Chronic Kidney Disease - A Systematic Review and Meta-Analysis.” *PLoS One 11:e0158765, 2016*.

Katari R, Peloso A, Zambon JP, Soker S, Stratta RJ, Atala A, Orlando G: “Renal bioengineering with scaffolds generated from human kidneys.” *Nephron Exp Nephrol 2014, 126: 119.*

Lombardi D, Becherucci F, Romagnani P: “How much can the tubule regenerate and who does it? An open question.” *Nephrol Dial Transplant. 2016 Aug;31(8):1243-50.*

Nakayama KH, Batchelder CA, Lee CI, Tarantal AF: “Decellularized rhesus monkey kidney as a three-dimensional scaffold for renal tissue engineering.” *Tissue Eng Part A 2010, 16: 2207-2216.*

Orlando G, Farney AC, Iskandar SS, Mirmalek-Sani SH, Sullivan DC, Moran E, AbouShwareb T, De Coppi P, Wood KJ, Stratta RJ, Atala A, Yoo JJ, Soker S: “Production and implantation of renal extracellular matrix scaffolds from porcine kidneys as a platform for renal bioengineering investigations.” *Ann Surg. 2012 Aug;256(2):363-70.*

Orlando G, Booth C, Wang Z, Totonelli G, Ross CL, Moran E, Salvatori M, Maghsoudlou P, Turmaine M, Delario G, Al-Shraideh Y, Farooq U, Farney AC, Rogers J, Iskandar SS, Burns A, Marini FC, De Coppi P, Stratta RJ, Soker S: “Discarded human kidneys as a source of ECM scaffold for kidney regeneration technologies.” *Biomaterials 2013, 34: 5915-5925.*

Peloso A, Ferrario J, Maiga B, Benzoni I, Bianco C, Citro A, Currao M, Malara A, Gaspari A, Balduini A, Abelli M, Piemonti L, Dionigi P, Orlando G, Maestri M: “Creation and implantation of acellular rat renal ECM-based scaffolds.” *Organogenesis. 2015;11(2):58-74.*

Poornejad N, Schaumann LB, Buckmiller EM, Roeder BL, Cook AD: “Current Cell-Based Strategies for Whole Kidney Regeneration.” *Tissue Eng Part B Rev. 2016 Oct;22(5):358-370.*

Ross EA, Williams MJ, Hamazaki T, Terada N, Clapp WL, Adin C, Ellison GW, Jorgensen M, Batich CD: “Embryonic stem cells proliferate and differentiate when seeded into kidney scaffolds.” *J Am Soc Nephrol 2009, 20: 2338-2347.*

Song JJ, Guyette JP, Gilpin SE, Gonzalez G, Vacanti JP, Ott HC: “Regeneration and experimental orthotopic transplantation of a bioengineered kidney*.” Nat Med 2013, 19: 646-651.*

Sullivan DC, Mirmalek-Sani SH, Deegan DB, Baptista PM, Aboushwareb T, Atala A, Yoo JJ: “Decellularization methods of porcine kidneys for whole organ engineering using a high-throughput system.” *Biomaterials 2012, 33: 7756-7764.*

Publications

Bombelli S, **Meregalli C**, Scalia C, Bovo G, Torsello B, De Marco S, Cadamuro M, Viganò P, Strada G, Cattoretti G, Bianchi C, Perego RA:
Nephrosphere-Derived Cells are Induced to Multilineage Differentiation when Cultured on Human Decellularized Kidney Scaffolds.
Am J Pathol. 2017 Oct 14. doi: 10.1016/j.ajpath.2017.09.012.

Bianchi C, **Meregalli C**, Bombelli S, Di Stefano V, Salerno F, Torsello B, De Marco S, Bovo G, Cifola I, Mangano E, Battaglia C, Strada G, Lucarelli G, Weiss RH, Perego RA: The glucose and lipid metabolism reprogramming is grade-dependent in clear cell Renal Cell Carcinoma primary cultures and is targetable to modulate cell viability and proliferation. *Oncotarget. 2017 accepted for publication.*

Di Stefano V, Torsello B, Bianchi C, Cifola I, Mangano E, Bovo G, Cassina V, De Marco S, Corti R, **Meregalli C**, Bombelli S, Viganò P, Battaglia C, Strada G, Perego RA: Major Action of Endogenous Lysyl Oxidase in Clear Cell Renal Cell Carcinoma Progression and Collagen Stiffness Revealed by Primary Cell Cultures. *Am J Pathol. 2016 Sep;186(9):2473-85.*

Torsello B*, Bianchi C*, **Meregalli C**, Di Stefano V, Invernizzi L, De Marco S, Bovo G, Brivio R, Strada G, Bombelli S, Perego RA: Arg tyrosine kinase modulates TGF-β1 production in human renal tubular cells under high-glucose conditions. *J Cell Sci. 2016 Aug 1;129(15):2925-36.*

Conference Communications

Meregalli C., Bombelli S., Bovo G., Torsello B., De Marco S., Viganò P., Cattoretti G., Bianchi C., Perego RA. “Evaluation of the capability of PKH^{high} human adult renal stem-like cells to repopulate human decellularized renal scaffolds” 2017, 15-16Sept.-Vascular Pathobiology-Young Scientist Meeting, P53.

Bianchi C, **Meregalli C**, Bombelli S, Torsello B, De Marco S, Salerno F, Cifola I, Mangano E, Battaglia C, Bovo G, Viganò P, Strada G, Perego R: (2017). Grade-dependent lipid storage in ccRCC cells: molecular and functional study performed in primary cell cultures. In Abstracts XXIV Congresso Nazionale AURO.it - PISA 19 - 21 maggio 2017 (pp.68-69).

Meregalli C., Bombelli S., Rossetti G., Ranzani V., Torsello B., De Marco S., Bovo G., Pagani M., Cattoretti G., Strada G., Bianchi C., Perego RA: “Transcriptomic profiling of multipotent renal nephrosphere PKH^{high} cells for the identification of a renal stem signature” HUMANGENE THERAPY, 2016 Nov;27(11), A177-P434.

Meregalli C., Bombelli S., Rossetti G., Ranzani V., Torsello, B., De Marco S., Bovo G., Pagani M., Cattoretti G., Strada G., Bianchi C., Perego RA: “Transcriptomic profileof PKH^{high} multipotent renal cells for the identification of a renal stem signature” THE AMERICAN JOURNAL OF PATHOLOGY, 186(supplement), RMSC1. 2016.

Bianchi, C; **Meregalli, C**; Bombelli, S; Torsello, B; De Marco S; Cifola, I; Mangano, E; Battaglia, C; Bovo, G; Vigano’, P; Strada, G; Perego, R:(2016). Primary cell cultures obtained from clear cell renal cell carcinoma specimens retain the transcriptomic profile and metabolic phenotype of corresponding tissues. In 23° Congresso Nazionale AURO, Roma 22-24 maggio 2016 Abstracts (pp.8-9).

Torsello, B; Di Stefano, V; Bianchi, C; Battaglia, C; Cifola, I; Mangano, E; Bovo, G; Cassina, V; De Marco, S; Corti, R; **Meregalli, C**; Bombelli, S; Vigano’, P; Strada, G; Perego, R: (2016). Endogenous lysyl-oxidase in clear cell renal cell carcinoma promotes tumor progression and collagen stiffness. In Libro Abstracts 89° Congresso Nazionale Società di Urologia, Venezia 15-18 Ottobre 2016 (pp.260-260).

Meregalli C., Bombelli S., Torsello B., Bovo G., Viganò P., Perego R.,Bianchi C., Strada G: “Lipid and glucose metabolism modulation in ccRCC primary cell cultures and cancer stem cells: a new approach for identification of therapeutic targets” 88° National Congress of the Italian Society of Urology, Riccione 10th-13th October 2015. Abstract P93.

Bianchi, C; Bombelli, S; **Meregalli, C;** Torsello, B; Bovo, G; Viganò, P; Strada, G; Perego, RA: (2015). Annexin A4 involvement in lipid storage of clear cell Renal Cell Carcinoma. Intervento presentato a: Congresso Nazionale AURO 24-25-26 maggio, Bologna, Italia.

Bombelli, S; Scalia, C; **Meregalli, C**; Torsello, B; Bovo, G; Cattoretti, G; Viganò, P; Strada, G; Bianchi, C; Perego, RA: (2015). Nephrosphere-derived cells cultured on decellularized kidney scaffolds can differentiate into multiple lineages. Intervento presentato a: NephroTools International Conference 8th - 10th September, Liverpool, UK.

Bianchi C., **Meregalli C.**, Di Stefano V., Cattaneo E., Torsello B., Bombelli S., Bovo G., Viganò P., Strada G., Perego R.A: “Metabolic pathways of clear cell renal cell carcinoma: possible therapeutic targets”87° National Congress of the

Italian Society of Urology, Firenze 27th-30th September 2014.Abstract P166.

Bianchi C., Di Stefano V., Cattaneo E., **Meregalli C**., Torsello B., Bombelli S., Bovo G., Viganò P., Strada G., Perego R.A: “Role of specific metabolic pathways in clear cell Renal Cell Carcinoma (ccRCC)”XXI National Congress of AURO, Roma 4th-6th June 2014. Abstract P181.

Bianchi C., Di Stefano V., Cattaneo E., Torsello B., Bombelli S., **Meregalli C.**, Bovo G., Viganò P., Strada G., Perego R.A: “Effect of specific metabolic pathway inhibition on in vitro viability of ccRCC cells.” 86° National Congress of the Italian Society of Urology, Riccione 5th-8th October 2013. Abstract P65.

Congress proceedings on peer-reviwed journals

Meregalli C., Bombelli S., Rossetti G., Ranzani V., Torsello B., De Marco S., Bovo G., Pagani M., Cattoretti G., Strada G., Bianchi C., Perego RA: "Transcriptomic profiling of multipotent renal nephrosphere PKH^{high} cells for the identification of a renal stem signature" HUMANGENE THERAPY, 2016 Nov;27(11), A177-P434.

Meregalli C., Bombelli S., Rossetti G., Ranzani V., Torsello, B., De Marco S., Bovo G., Pagani M., Cattoretti G., Strada G., Bianchi C., Perego RA: "Transcriptomic profileof PKH^{high} multipotent renal cells for the identification of a renal stem signature" *Am. J. Pathol*., 186(supplement), RMSC1, (2016).

Torsello B., Bianchi C., Bovo G., Cassina V., De Marco S., **Meregalli C.**, Bombelli S., Viganò P., Strada G., Perego R.A: "Endogenous Lysyl oxidase in tumor progession and collagen stiffness: study performed in human clear cell renal cell carcinoma primary cell cultures" *Am. J. Pathol*., 186(supplement), C16, (2016).

Bianchi C., Torsello, B., **Meregalli C**., De Marco S., Bovo G., Brivio R., Strada G., Bombelli S., Perego R: “TGF-b1 production is modulated by Arg tyrosine kinase in high glucose treated human renal tubular cells.” ”*Am. J. Pathol*., 186(supplement), CDIR2, (2016).

Bianchi C., **Meregalli C.**, Di Stefano V., Cattaneo E., Bombelli S., Torsello B., Bovo G., Strada G., Perego R.A: “Lipid storage and Annexin A3 in clear cell renal cell carcinoma”, *Am. J. Pathol*.,, 184 (suppl.) S3, (2014).

Bombelli S., Bovo G., Torsello B., **Meregalli C.**, Di Stefano V., Viganò P., Strada G., Bianchi C., Perego R.A: “Nephrospheres from human kidney contains cells with regenerative abilities” *Am. J. Pathol*., 184 (suppl.) S41, (2014).

Bombelli S., Zipeto M.A., Torsello B., **Meregalli C.**, Di Stefano V., Bovo G., Viganò P., Strada G., Bianchi C., Perego R.A: “Molecular and fuctional characterization of cance stem-like cells isolated from human renal cell carcinoma tissue.” *Am. J. Pathol*., 184 (suppl.) S43, (2014).